

# Floating marine debris along Indonesian coasts

## An atlas of strandings based on Lagrangian modelling



Delphine Dobler  
Elodie Martinez  
Rinny Rahmania  
Budhi Gunadharma Gautama  
A. Riza Farhan

*coordinated by*  
Christophe Maes

2021



# **Floating marine debris along Indonesian coasts**

## An atlas of strandings based on Lagrangian modelling

Delphine Dobler  
Elodie Martinez  
Rinny Rahmania  
Budhi Gunadharma Gautama  
A. Riza Farhan

*coordinated by*  
Christophe Maes

2021

Atlas layout and page setup  
Yanto Wahyantono

Corrections  
Edmond Dounias

Cover photomontage

Maps of average number of particles per grid cell (cf. figures 19 and 27) and photo of stranded plastics on the beach of Batu Namprak, West Java (© Stéphanie Aulong 2021)

Photos

Page 4: Litter discharge in a small river, Cilebut Barat village, West Java (© Suparno Jumar, River Defender)

Page 6: Litter runs off further downstream into larger rivers, Cilebut Barat village, West Java (© Suparno Jumar, River Defender)

Page 10: Floating plastic accumulation in the riverbank of Banten, West Java (© Rinny Rahmania, KKP)

Page 16: Attempt to hold back and collect the floating plastic waste in river, Jakarta (© Jessica Yaputri, Marine Change)

Page 22: Ghost killings: Floating plastic debris increase the morbidity of marine fauna (© Alexis Chappuis, UNSEEN Expeditions)

Page 30: Stranded plastic debris along the beach of a small fishermen village, Papandangan Island, West Sulawesi (© Rinny Rahmania, KKP)

Page 42: Towed rake for the gathering of stranded plastics on the touristic Kuta Beach, Bali (© Christophe Maes, IRD)

Page 86: Community cleanup initiative in Molawe village, Southeastern Sulawesi (© Yann Bigant, Naturevolution)

Page 88: Floating plastic debris are detrimental to tourism business, Lembongan Island, Bali (© Christophe Maes, IRD)

Page 92: A large fraction of plastic waste ends up sinking and settling on the sea floor (© John Van Lent, Making Maluku Free Waste)

The terms of Clauses 2 and 3 of Article L. 122-5 of the Law of 1 July 1992 (Intellectual Property Code) permits only 'copies or reproduction reserved for the use of the person making such copies and not intended for collective use' and analyses and short quotations justified by the work in which they are given and with clear indication of the author and the source. Any partial or total representation or reproduction performed without the author's consent is unlawful.

© IRD, 2021

ISBN 979-10-699-7188-2

# Table of Contents

About the authors	
Acknowledgements	
Prefaces	
Introduction .....	11
Materials .....	17
Surface Current products .....	17
Description .....	17
Energy and current property diagnostics .....	17
Mean Kinetic Energy and Eddy Kinetic Energy .....	17
Divergence .....	20
Surface Kinetic Energy .....	21
River discharges .....	21
Population Density .....	21
Methodology .....	23
Lagrangian analysis .....	23
Spatio-temporal characteristics of the experiment .....	23
Marine debris release scenario .....	23
Horizontal initial position .....	24
Time release .....	25
Particle strandings .....	26
Definition of a numerical stranding .....	26
Definition of stranding subzones .....	27
Results .....	31
Regional dispersion of particles originating from Indonesian rivers .....	31
Spatio-temporal patterns of stranded particles .....	32
Regional patterns .....	32
Spatio-temporal variability .....	33
Connectivity between river mouths and particle stranding subzones .....	37
Impact of physical processes on particle trajectories and strandings .....	38
Detailed strandings for each subzone .....	43
Conclusion .....	87
References .....	89

© Supamo Jumar, River Defender



## About the authors

**Delphine Dobler** is currently working as a research engineer for the French National Research Institute for Sustainable Development (IRD). After a first 11 years' experience in satellites operation in the public and private sectors, she passed a master's degree in physical oceanography in 2018 and has, since then, been working in the oceanography field. She has extensive expertise in physics, mathematics and geoscience data analyses. Under the framework of the "Monitoring and modelling the circulation of marine debris in Indonesia" project, she manages and analyses Lagrangian simulations.

**Elodie Martinez** is a researcher at the French National Research Institute for Sustainable Development (IRD). She is a biogeochemist oceanographer working on ecological issues, mostly in the Pacific Ocean. The drift of marine debris in the ocean has been a recurrent topic in her career over the past 10 years.

**Rinny Rahmania** obtained in 2016 her Ph.D. degree in ecology and biodiversity from the University of Montpellier, France. Since 2006, she has been working for the Marine Research Center, Ministry of Marine Affairs and Fisheries, Republic of Indonesia. Her current research interests include remote sensing, mangrove ecology, marine debris, and coastal zone management.

**Budhi Gunadharma Gautama** is a researcher working since 2008 for the Marine Research Center, Ministry of Marine Affairs and Fisheries Indonesia. He graduated from Bandung Institute of Technology (ITB), with a Bachelor Degree on Ocean Engineering (2001) and a Master on Management and Business Administration (2004). He obtained his Ph.D. Degree in 2017 from IMT Atlantique in France, with a scholarship from the Infrastructure Development of Space Oceanography project under a bilateral cooperation between France and Indonesia. His research focuses on ocean pollution, specially on monitoring, observation and trajectory modelling.

**Aulia Riza Farhan** has nearly 20 years' experience working in marine and fisheries applications both for the Indonesian government and the private sector. He has extensive knowledge with project planning and management, GIS, remote sensing and geospatial applications. He is currently working with the integrated Marine and Fisheries Surveillance Systems project, focusing on the implementation of monitoring, controlling and surveillance of marine environment.

**Christophe Maes** has been conducting his research activities on climate and ocean dynamics for more than 20 years within the French National Research Institute for Sustainable Development (IRD), especially in the subtropical regions and under the context of El Niño Southern Oscillation. Because marine plastics waste represent one of the most pressing environmental issues of our present world, his focus has recently moved towards the global plastic pollution and the means to reduce sources and risks, with a thorough attention on the origins, transport, fate, and incidence of riverine and oceanic plastic debris.

© Suparno Jumar, River Defender



## Acknowledgements

The production of this atlas has been funded by the Agence Française de Développement (AFD) under the framework of a Fund for Technical Expertise and Experience Transfers (FEXTE), which supports technical-cooperation programs and project-preparation studies.

This atlas has received a lot of support from various organisations and individuals. Our gratitudes go to:

- Edmond Dounias, Marine Herrmann, Ariane Koch-Larrouy and Emilie Strady (IRD – French National Research Institute for Sustainable Development)
- Yannis Cuypers and Pascale Bouruet-Aubertot (Université Paris-Sorbonne)
- Director of Marine Research Center, Agency for Marine and Fisheries Research and Human Resources, Ministry of Marine Affairs and Fisheries Republic of Indonesia
- Claire Dufau, Olivia Fauny, Jean-Baptiste Voisin and Sari Wulan Kurnia (CLS – Collecte Localisation Satellites)
- Philippe Gaspar and the Mercator and Copernicus marine user support
- Emmanuel Baudran, Léa Lebechnech, Adeline Souf and Hélène Gobert (AFD – Agence Française de Développement)

We extend our gratitude to the staff of LOPS (Laboratory of Ocean Physics and Satellite Remote Sensing) for fruitful discussions on strandings and Lagrangian simulations, particularly to:

- Bruno Blanke and Nicolas Grima for developing and maintaining the Lagrangian simulation software Ariane
- Thierry Huck, Fanny Chenillat and Clément Weber for their studies of Lagrangian physical processes and strandings at the global scale
- Gwenaëlle Jan and Elise Corre for the regional scale of the Bay of Biscay
- Last but not least, we thank Michèle Joubert for the administrative aspects and Tristan Le Toullec and Ludovic Cosme for their computer technical support

This atlas has benefited from the datasets of the European Union's Copernicus Marine Service Information.

Finally, we wish to warmly thank Stéphanie Aulong, Suparno Jumar (River Defender), Rinny Rahmania (KKP), Jessica Yaputri (Marine Change), Alexis Chappuis (UNSEEN Expeditions), Yann Bigant (Naturevolution), Christophe Maes (IRD), and John Van Lent (Making Maluku Free Waste) for their kind permissions to reproduce their photos in this atlas.

If you wish to cite this atlas, please use the following citation:

Dobler D., Martinez E., Rahmania R., Gautama B.G., Farhan A.R., Maes C. 2021. *Floating marine debris along Indonesian coasts. An atlas of strandings based on Lagrangian modelling.* "Monitoring and modelling the circulation of marine debris in Indonesia" project funded by AFD. Jakarta: IRD, 92 p.

Contact of corresponding author: [christophe.maes@ird.fr](mailto:christophe.maes@ird.fr)

## Preface

Indonesia is the largest archipelago in the world with nearly 13,550 islands and the 6<sup>th</sup> Exclusive Economic Zone.

The country has always designed its development and its international integration on its unique relationship with its surrounding oceans. At the same time, the location of the Indonesian maritime domain, right in the middle of the Coral Triangle, makes Indonesia one of the most important reservoir of marine and coastal biodiversity (coral, fish, mangroves, seagrass, marine mammals...).

Unfortunately, human activities and their incidence on climate change threaten this amazing biodiversity. Plastic pollution is a particularly worrying issue for the country – the second largest producer of plastic after China – as more than 6.5 million people are employed in fisheries and aquaculture sectors.

Hence, the Indonesian government has made sustainable management of marine biodiversity and resources a national priority, and adopted an ambitious national action plan to mitigate marine debris and to reduce plastic debris by 70% before 2025.

In 2019, the Indonesian Government, through the Ministry of Marine Affairs and Fisheries (MMAF), called on AFD's support to improve the monitoring and modelling of marine debris nationwide. The project will provide equipment and research to monitor the distribution and movement of marine debris, particularly in rivers, which carry plastics out to the ocean. What will follow are recommendations for treating and reducing this pollution – and for trying to avoid it in the future.

AFD has provided a 500,000 € grant for this project, which relies on a partnership between MMAF and the French National Research Institute for Sustainable Development (IRD). In addition to helping the Indonesian government to meet its plastic reduction targets, this collaborative research between France and Indonesia will also contribute to the valorization of French expertise in oceanographic research and the commitments of the French State in initiatives such as the Global Plastic Action Partnership.

MMAF and IRD have partnered with the French company Collecte Localisation Satellite (CLS) to implement the project. This pilot program should allow the creation of a marine debris monitoring system at the Indonesian level, generate knowledge and raise awareness about the impact of marine debris, but also provide recommendations for the marine debris collection program and conduct appropriate communication actions. The present atlas is the first deliverable, which maps marine debris stranding along the Indonesian coasts.

This very operational project clearly illustrates the leading role of Indonesia within APEC on plastic pollution reduction, and the great potential for extending the study to a broader regional scale, with a particular focus on reinforced collaborations between Indonesia and less advanced countries of the Southeast Asian region.

We hope that the results of this project will strengthen Indonesia's image as a country actively leading innovative projects to combat global marine pollution and preserve its unique natural marine resources.

Dr. Edmond Dounias  
Representative of IRD for Indonesia and Timor Leste

Dr. Emmanuel Baudran  
Director of AFD Indonesia

## Preface

Like most countries in the world, Indonesia suffers from the hazardous impact of marine debris. The negative ecological and socio-economic impacts of marine debris bring severe threats to the marine and coastal environment and human livelihoods, adversely affecting habitats, species, and ecosystem services; human health and safety; as well as vital economic sectors such as fisheries, tourism, and navigation.

Responding to this problem, President Joko Widodo at the Leaders Retreat, G20 Summit, Hamburg-Germany, Friday, July 7, 2017, stated that Indonesia would reduce waste through 3R (reduce-reuse-recycle) by 30% and set a national target to reduce marine plastic waste by 70% by 2025. To support the achievement of this target, Presidential Regulation No. 83/2018 concerning Marine Debris Management and realized through collaboration between 16 Ministries / Agencies (2016 - 2018) has been passed and enacted. In addition, the government has compiled five strategies to reduce marine debris, with 59 activities comprising the National Action Plan (NAP) to reduce marine debris.

Through the Agency for Marine and Fisheries Research and Human Resources (BRSDM), the Ministry of Marine Affairs and Fisheries has a mandate in the Research and Development strategy to understand marine debris pollution and its impacts. Research of modelling and monitoring of marine debris in Indonesia implements the collaboration between BRSDM and the French National Research Institute for Sustainable Development (IRD) and the Agence Française de Développement (AFD) in 2020. In this joint research, numerical model development and Lagrangian model development for marine waste trajectory, observation, capacity building, and communications are carried out. This atlas on marine debris strandings is one of the results generated from this joint research.

The atlas is expected to complement the various marine debris studies that Indonesian experts have carried out. It provides benefits for the Indonesian government to understand the source of marine debris, the amount of waste load that has been washed into the sea, and its fate. Using information in this atlas, the Government of Indonesia can determine a waste mitigation strategy to reduce marine debris stranded in coastal areas. Mitigation is prioritized to handle waste from its source and capture waste at specific meeting points before the waste is stranded back to the mainland. Furthermore, this atlas is expected to facilitate dialogue on solutions brought together with stakeholders, enhance public awareness, and promote co-responsibility for marine litters in Indonesia, not only improving individuals' perceptions about the problem effectively but also commitment to be part of the solution.

Finally, I thank scientists, researchers and all concerned for their valuable participation in this collaborative project and for their contributions as authors and editors to make this atlas possible. I understand that this atlas is not free from limitations, therefore I certainly hope this atlas can become a catalyst for more sustainable research on marine debris in the future.

Prof. Ir. Sjarief Widjaja, Ph.D.  
Chairman of the Agency for Marine and Fisheries Research and Human Resources  
Ministry of Marine Affairs and Fisheries

© Rinny Rahmania, KKP



# Introduction

Marine plastic debris has become a major human-induced pollution issue of our modern times. This pollution began in the fifties with the rise of the plastic age. The plastic production reached 359 million tonnes in 2018 (Plastics Europe, 2019) and is increasing by roughly 16 million tonnes every year. An important part of this production ends at sea: between 4.8 and 12.7 million tonnes in 2010 according to estimates by Jambeck *et al.* (2015) (see figure 1); between 1.15 and 2.41 million tonnes according to other estimates by Lebreton *et al.* (2017) (see figure 2). These estimates were obtained through the computation of diverse

data regarding waste, waste management, economic status, population density, and hydrology. This pollution is not only a major threat to marine wildlife that can be harmed by ingestion, suffocation, congestion, or false satiety (Germanov *et al.*, 2019; Ryan *et al.*, 2020). Plastic wastes also impact human societies by penetrating the food chain, with deleterious consequences on health. Yet, a great range of economic activities (shipping, fishing, aquaculture, tourism, recreation) are heavily compromised (Jang *et al.*, 2014). The plastic pollution has been identified as one of the seven main concerns during by the 2015 G7 in Berlin (Williamson *et al.*, 2016).

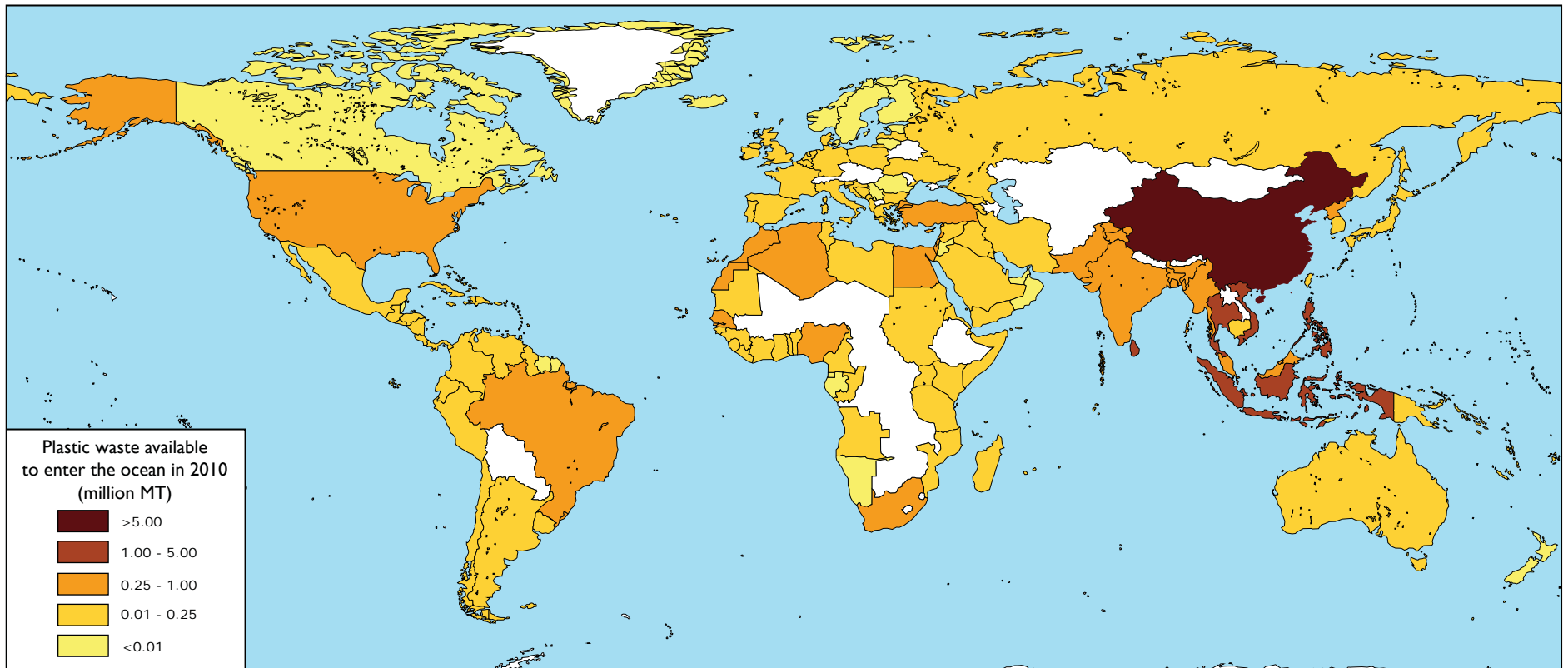


Figure 1: "Global map with each country shaded according to the estimated mass of mismanaged plastic waste [millions of metric tons] generated in 2010 by populations living within 50 km of the coast. We considered 192 countries. Countries not included in the study are shaded white" (excerpt from Jambeck *et al.*, 2015)

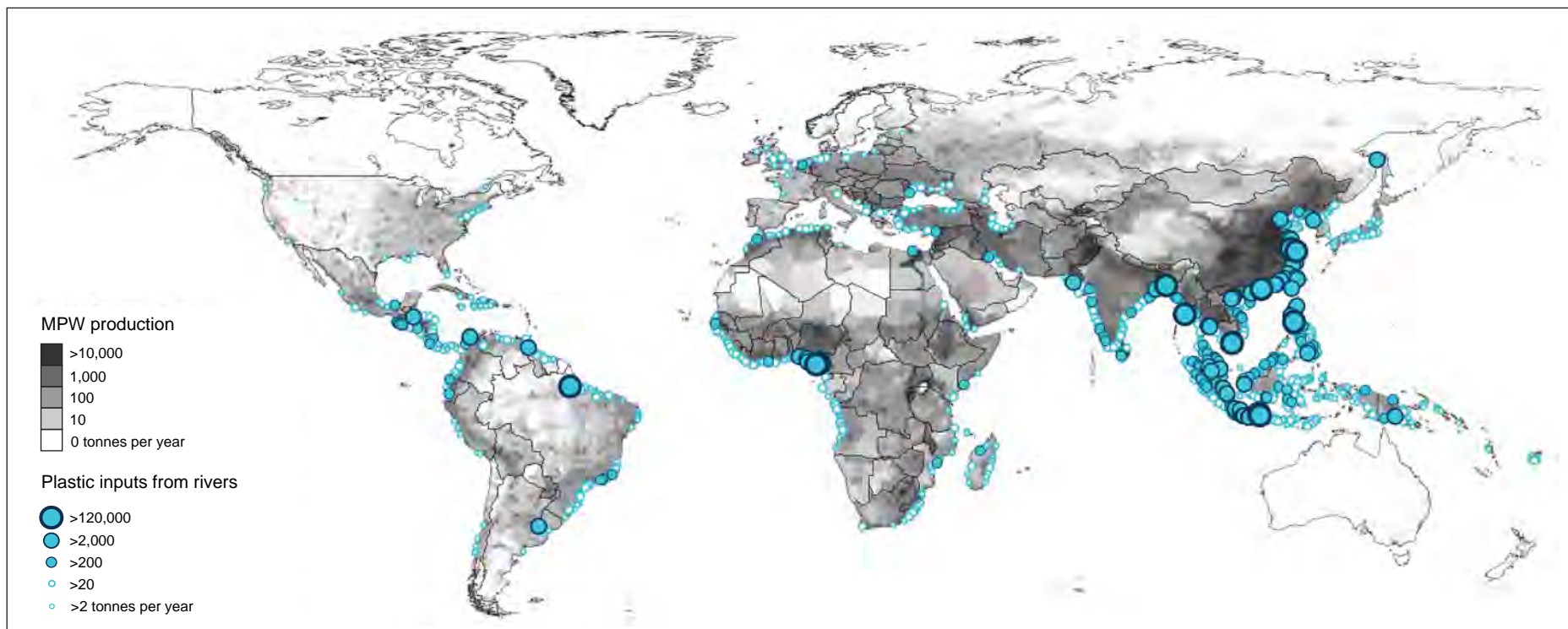


Figure 2: "Mass of river plastic flowing into oceans in tonnes per year. River contributions are derived from individual watershed characteristics such as population density (in inhab/km<sup>2</sup>), mismanaged plastic waste (MPW) production per country (in kg/inhab/day) and monthly average runoff (in mm/d). The model is calibrated against river plastic concentration measurements from Europe, Asia, North and South America." (excerpt from Lebreton et al., 2017)

Plastic pollution at sea is induced by both maritime and inland sources. The contribution of the latter is often estimated to be 80% (UNEP, 2016). Plastic pollution from inland sources mostly enters the ocean through rivers (Lebreton et al., 2017) and a large part is coming from South-East Asian countries (Jambeck et al., 2015; Lebreton et al., 2017). Once at sea, some of these debris travel over large distances to join one of the five main accumulation areas located inside the subtropical gyres (Martinez et al., 2009; Maximenko et al., 2012; van Sebille et al., 2012; Maes et al., 2018; Dobler et al., 2019), some of them are degraded into smaller pieces, can be biofouled and sink, and some of them end up stranded (Maes and Blanke, 2015).

Jambeck et al. (2015) ranked Indonesia as the second most polluting country. Even if this rank should be nuanced, several factors justify that Indonesia is severely impacted by this pollution:

- a high population density, especially on Java Island (figure 3)
- one of the highest level of rainfall in the world (320 mm/yr, figure 4), with an interannual variability linked to the El-Nino Southern Oscillation (ENSO)
- a shoreline particularly jagged with approximately 13,550 islands of different sizes (Andréfouët, 2020), many narrow straits and a total coastline length of more than 81,000 km

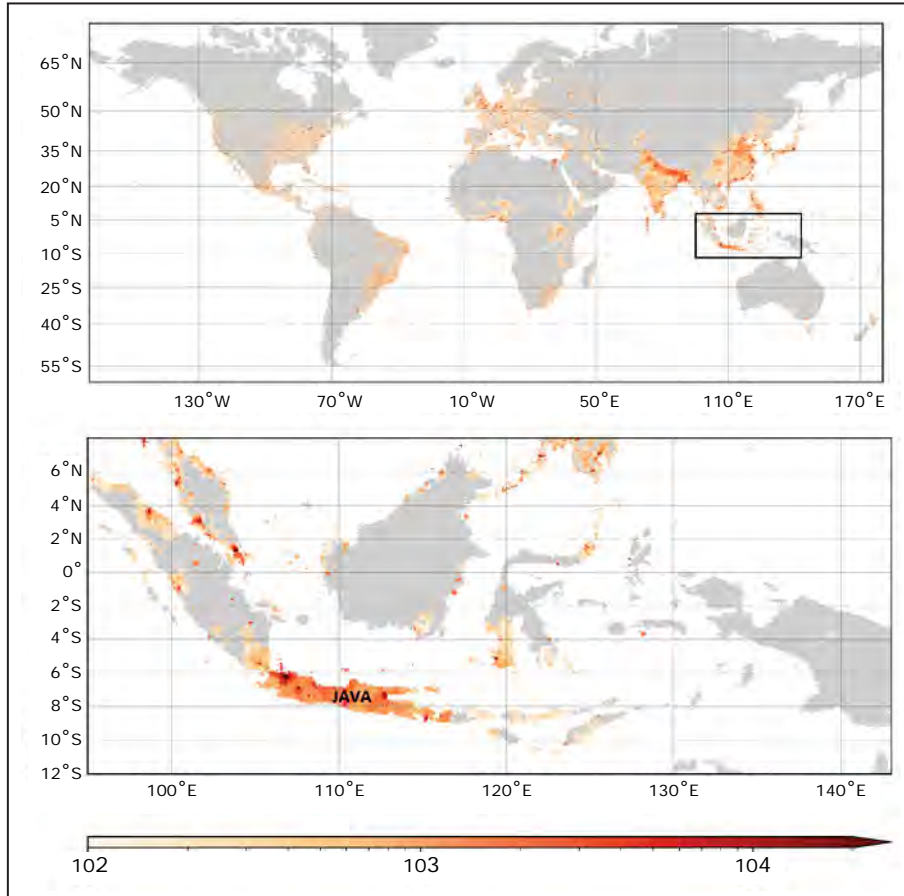


Figure 3: Population density for year 2015 in inhabitant per square kilometer. Upper panel shows population densities for the whole world. Lower panel is a zoom view on Indonesia. Values below 100 inhab/km<sup>2</sup> are shaded in grey. From the NASA Center for International Earth Science Information Network - CIESIN - Columbia University (2018) dataset

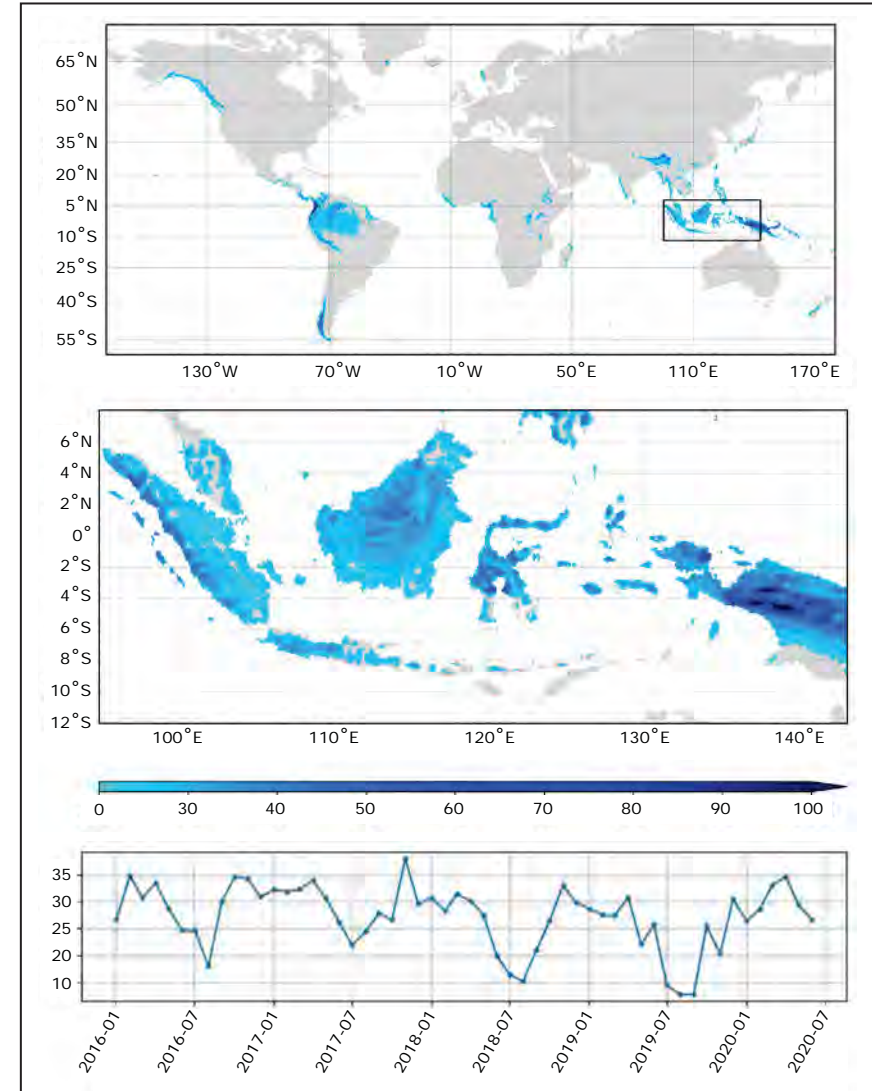


Figure 4: Total rainfall over land in mm/month. Upper panel shows rainfall averaged over 2009-2020. Middle panel is a zoom view on Indonesia. Values below 20 mm/month are shaded in grey. Lower panel shows the rainfall time variability averaged over the Indonesian region as defined in the middle panel. From the GloFAS (2019) dataset

In this context, two Indonesian presidential decrees (No. 97/2017 and No. 83/2018) were adopted in 2017 and 2018 respectively. The first decree addresses home and general waste management whereas the second decree addresses marine debris management. These decrees gave rise to a plan of actions (Ministry of Environment and Forestry, 2020) whose objectives are to reduce by 30% the waste production, to reach 70% of correctly managed waste by 2025 and to improve cleaning actions. The present atlas aims at supporting these initiatives through the modelling and the identification of hotspots of stranded marine debris, for a better decision-making regarding waste management (paragraph 4.3 from Ministry of Environment and Forestry, 2020). More specifically, it also aims at statistically quantifying the fate of the marine plastic pollution coming from Indonesian rivers, their stranding locations along the coasts of Indonesia and of the surrounding countries and the spatio-temporal variability of these strandings.

To understand the trajectories of floating marine debris and the zones of strandings, a Lagrangian numerical experiment was performed. The floating plastic debris were modeled as numerical particles of no size, no shape and neutral density, assuming that stranded debris came mainly from debris drifting in the surface layer of the Ocean. Complex processes of plastic fragmentation and sinking were not considered in this study. These numerical particles were advected by surface currents from an Ocean Global Circulation Model (OGCM). The choice of the Surface Current product was driven by the intense regional dynamics: Indonesia is indeed a pathway between the Pacific and Indian oceans, located along the Equator, with many ocean dynamics such as:

- the monsoon which, for example, reverses oceanic flows from northeastward to southwestward in the South China Sea and from northwestward to southeastward in the Java, Flores and Banda seas (Wyrcki, 1961)
- the tidal currents that may reach very high values locally (up to 1 m/s in some straits)
- ENSO modulation having impacts on both currents (Gordon *et al.*, 2012) and rainfalls influencing river discharges
- the surface Stokes drift, which contributes to the surface drift of floating marine debris
- extreme events, such as typhoons, earthquakes and potentially associated tsunamis

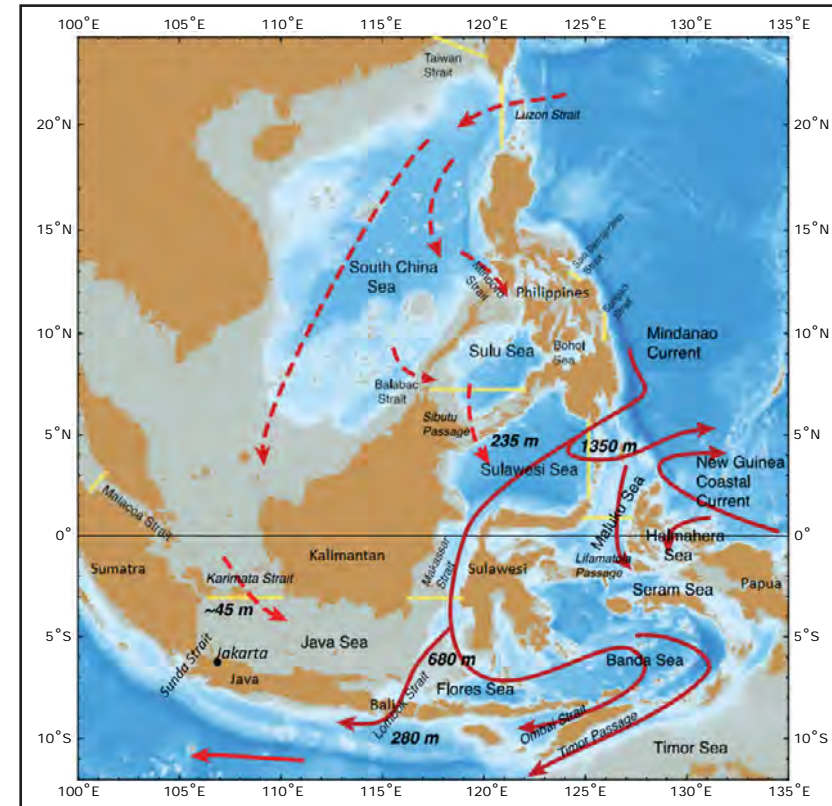


Figure 5: Map of the Indonesian region adapted from Gordon *et al.* (2012): Schematic of the South China Sea throughflow (dashed red arrows) and the Indonesian throughflow (solid red arrows) circulations. Topographic sill depths are given in black italics

The stranding probabilities in the Indonesian region were numerically investigated to provide a probabilistic atlas of stranding time and locations. Moreover, the specific impact of tidal surface currents and surface Stokes drift were assessed.

The first section of this atlas is dedicated to the data materials, the second section presents the methodology, the third section presents general results and the fourth section presents detailed strandings of floating marine debris for each subzone.



© Jessica Yaputri, Marine Change



## Surface Current products

### Description

Surface Merged Ocean Currents (SMOC) product (distributed by the Copernicus Marine Service, <https://resources.marine.copernicus.eu>) was adopted as a means to consider the importance of the tides in the region (up to 1m/s in the straits) and of the Stokes drift effect at global scale (Ardhuin *et al.*, 2009; Dobler *et al.*, 2019). The downloaded data covered the period from the 1<sup>st</sup> of April 2016 to the 31<sup>st</sup> of May 2020. The SMOC product provides three types of surface current datasets interpolated on the same spatio-temporal grid (regular 1/12° spatial grid and hourly outputs):

- surface current outputs from an Ocean Global Circulation Model (OGCM)
- tide-induced surface currents
- surface Stokes drift

The surface current outputs from the OGCM were produced by Mercator Ocean (<https://www.mercator-ocean.fr>). A NEMO 3.1 model was run using a PSYS4V3R1 configuration. The model original grid is a tripolar ORCA 1/12° C-grid with hourly outputs. This model neither includes tides nor waves. The GEBCO8 (30 arc-second resolution) topography product was used above 200 m depth and ETOPO1 (60 arc-second resolution) below 200 m. The model was forced by ECMWF forecast winds, by runoffs from Dai *et al.* (2009) (computed using in-situ gauge data coupled with a land surface model and atmospheric observations to fill in gaps) and assimilated in-situ and remotely sensed data.

The tide-induced surface currents were generated using FES2014 software. This software is distributed by AVISO (<https://www.aviso.altimetry.fr>). All available tidal components were selected (Carrere *et al.*, 2015).

The surface Stokes drift dataset is produced by Meteo France and originally distributed on CMEMS as GLOBAL\_ANALYSIS\_FORECAST\_WAV\_001\_027 product. The Meteo France Wave Model (MFWAM) was run on a regular 1/12° grid with 3 hours-instantaneous outputs. The frequential resolution was 24 directions, 30 frequencies from 0.035 to 0.58 Hz. The model was forced by IFS-ECMWF winds and assimilated significative wave height from altimetry data.

In the atlas hereafter, the addition of these three components will be referred to as "SMOC currents". According to the validation report (QUID internal document from CMEMS), using SMOC currents globally improves by 18.7% the separation distance at three days between simulated particles and drifting buoy

trajectories. This improvement is smaller in regions of high mesoscale activities (e.g. Gulf stream, Kuroshio), and accuracy is difficult to estimate in the Indonesian region because of the lack of circulating drifters.

The main tidal components of the Indonesian region are M2, S2, N2, K2 (approx 12h), K1, O1, J1 (approx 24h), Mm (approx 27 days), Mf (approx 14 days) and M4 (approx 6h) (Tranchant *et al.*, 2016). Thus, hourly outputs are needed to assess the impact of tides on particle trajectories.

### Energy and current property diagnostics

A few energy and current property diagnostics were computed on the regional domain: Mean Kinetic Energy (MKE), Eddy or turbulent Kinetic Energy (EKE) and DIVergence (DIV) with respect to the mean flow of year 2018 and time evolution of Surface Kinetic Energy (SKE) for the four years of simulation. These diagnostics were applied to each component of the SMOC product: OGCM surface currents, tide-induced surface currents, and surface Stokes drift.

### Mean Kinetic Energy and Eddy Kinetic Energy

Maps of MKE and EKE for the OGCM surface currents (figure 6, left panels) are consistent with the expected mean flows and Eddy-rich locations of the region, as can be observed with the drifters from the Global Drifter Program (Todd *et al.*, 2019, figure 7).

Tidal MKE is almost null (figure 6, middle panels), which can be expected from this oscillating component. However tidal EKE can reach high values (more than 500 cm<sup>2</sup>/s<sup>2</sup>) in shallow waters.

On the other hand, surface Stokes drift MKE has features of larger scales with a moderate value range between 50 and 100 cm<sup>2</sup>/s<sup>2</sup> poleward of 10° but its EKE is very weak (figure 6, right panels).

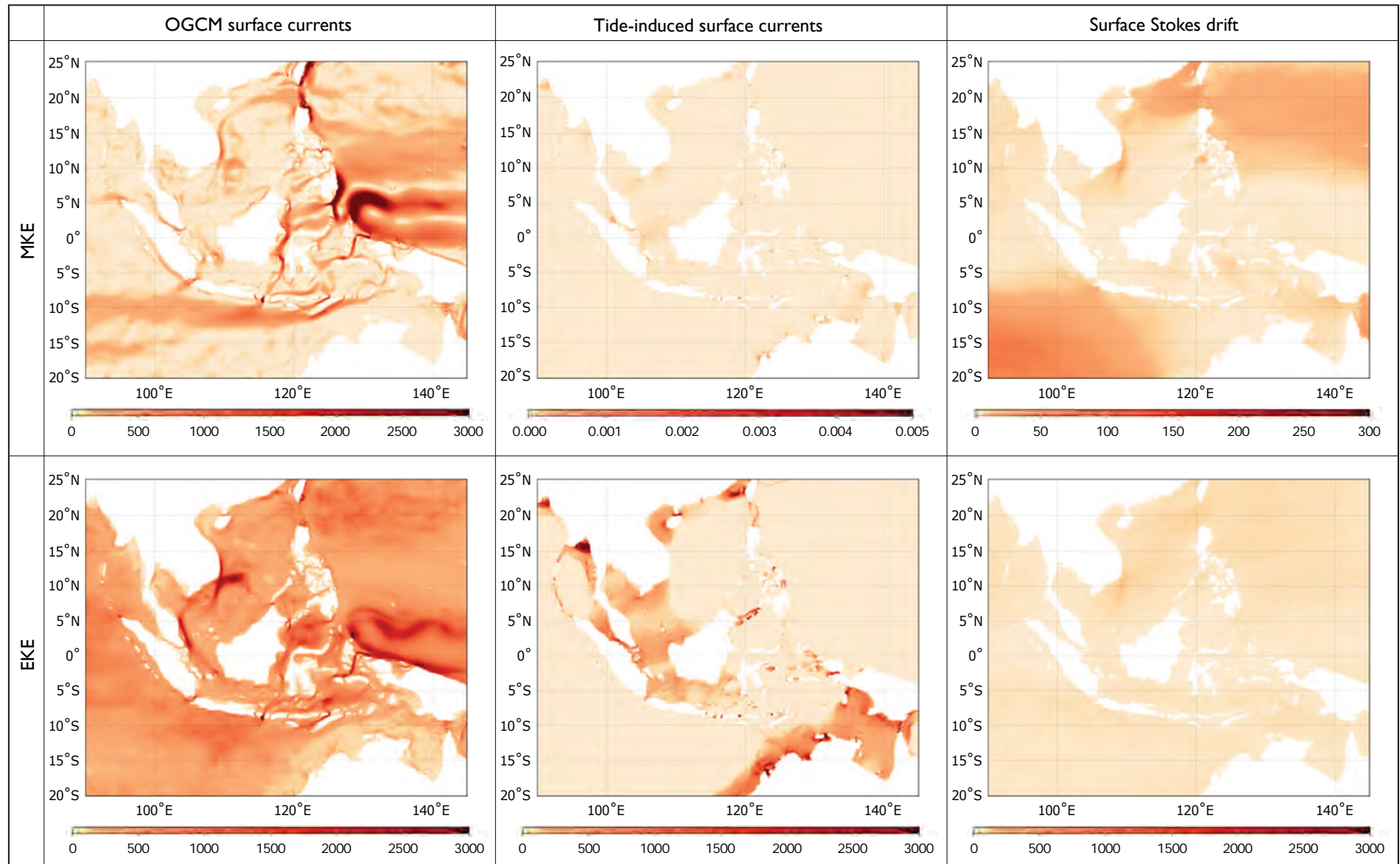


Figure 6: Upper panels: Kinetic Energy of the mean flow (MKE) for 2018 in  $\text{cm}^2/\text{s}^2$ . Lower panels: Eddy Kinetic Energy (EKE) (with respect to the annual mean flow) for 2018 in  $\text{cm}^2/\text{s}^2$  (please notice that different scales are used). From left to right panels: OGCM surface currents, tide-induced surface currents and surface Stokes drift components of the SMOC product

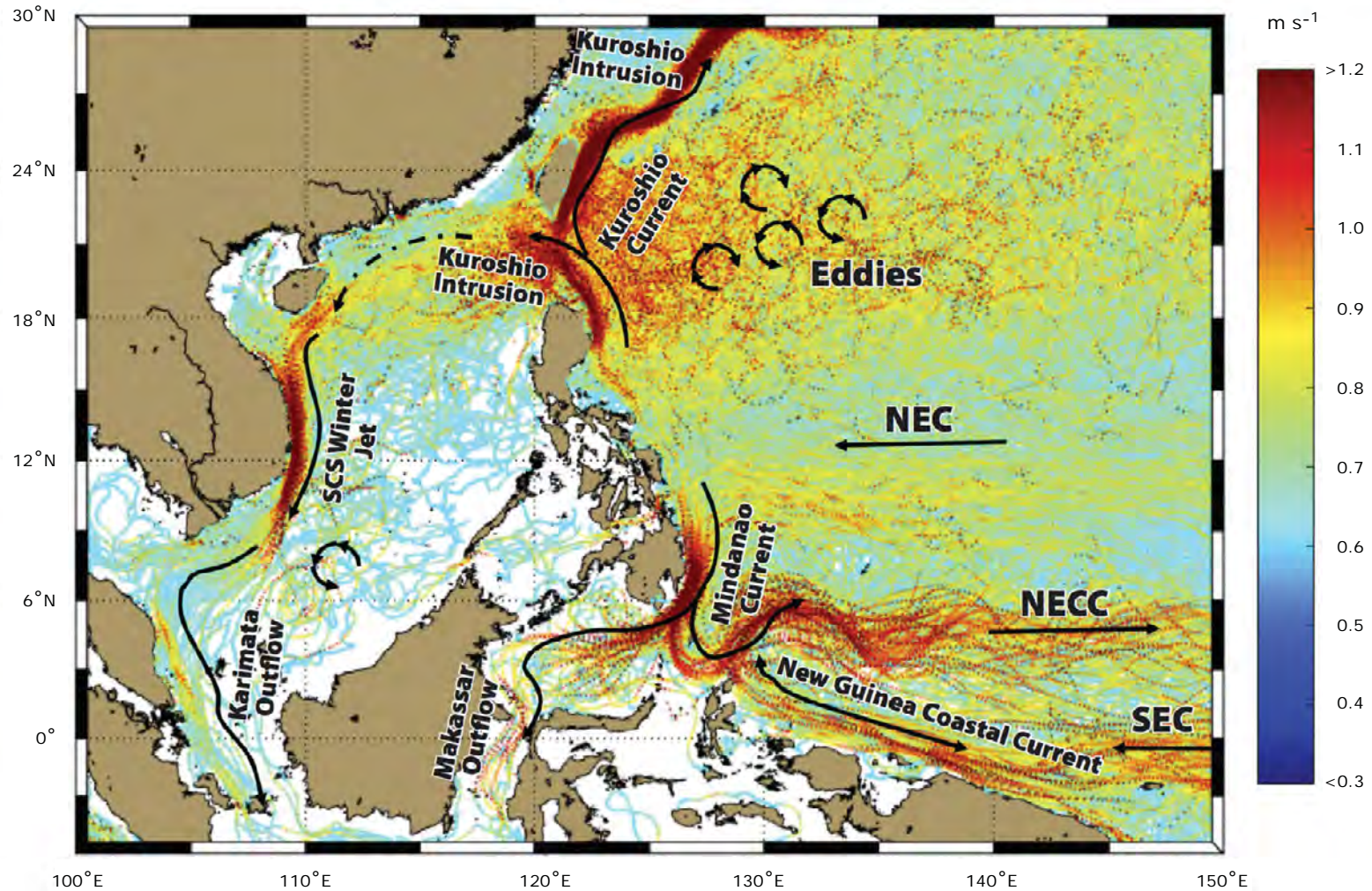


Figure 7: "Trajectories and near-surface velocity estimates from Global Drifter Program drifters in the western Pacific and marginal seas. Over 1.2 million discrete measurements from 1982 to 2014 are included. Paths of various boundary currents are clearly visible, as is the rich Eddy field in the region of the Subtropical Countercurrent around 18-24°N. NEC North Equatorial Current, NECC North Equatorial Counter Current, SEC South Equatorial Current, SCS South China Sea" (excerpt from Todd et al., 2019)

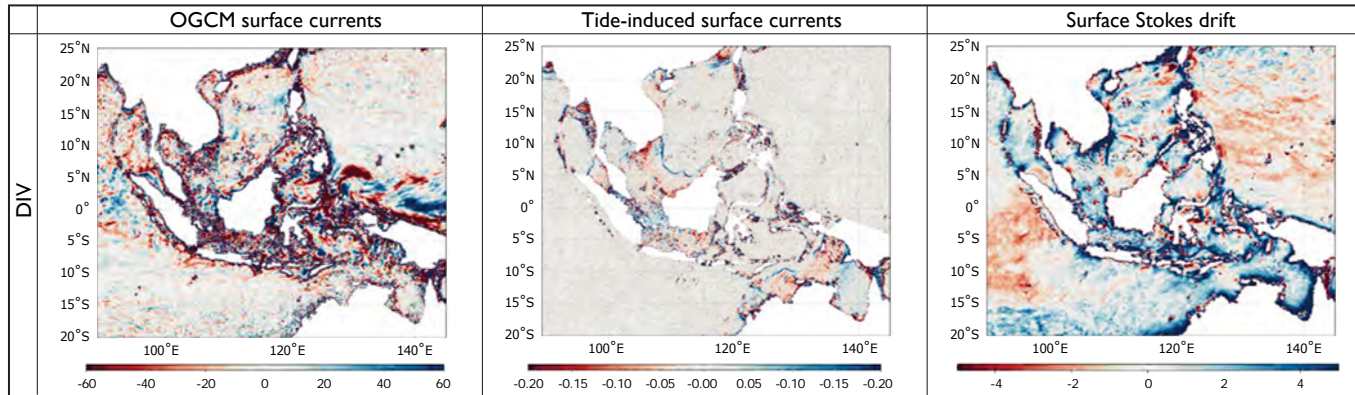


Figure 8: Divergence of the mean flow (DIV) for 2018 in  $10^{-8}\text{s}^{-1}$ . From left to right panels: OGCM surface currents, tide-induced surface currents and surface Stokes drift components of the SMOC product

## Divergence

The divergence of the OGCM surface currents shows different patterns depending on the subregion: the deep waters of the Indian and Pacific oceans as well as the deep waters of the South China Sea are marked with relatively small values, whereas Indonesian internal seas are marked by high values of both convergence (negative values, red shades) and divergence (positive values, blue shades) and with features of smaller scales (figure 8, left panel).

The tidal component shows thin divergent lines (blue lines) at the limit between shallow and deep waters. These lines are clearly visible in the South

China Sea between the coasts of Borneo and Vietnam, in the northern entrance of the Malacca Strait and south of the Timor passage in the Timor Sea (figure 8, middle panel). These thin divergent lines are associated with nearby convergent areas (negative values, red shades) in the adjacent shallow waters.

The surface Stokes drift has features of much larger scale with zones of convergence (negative values, red shades) between  $0^{\circ}\text{S}$  and  $15^{\circ}\text{S}$  on the western part of the domain, and between  $0^{\circ}\text{S}$  and  $15^{\circ}\text{N}$  on the eastern part of the domain (figure 8, right panel). The other regions are mainly divergent (positive values, blue shades).

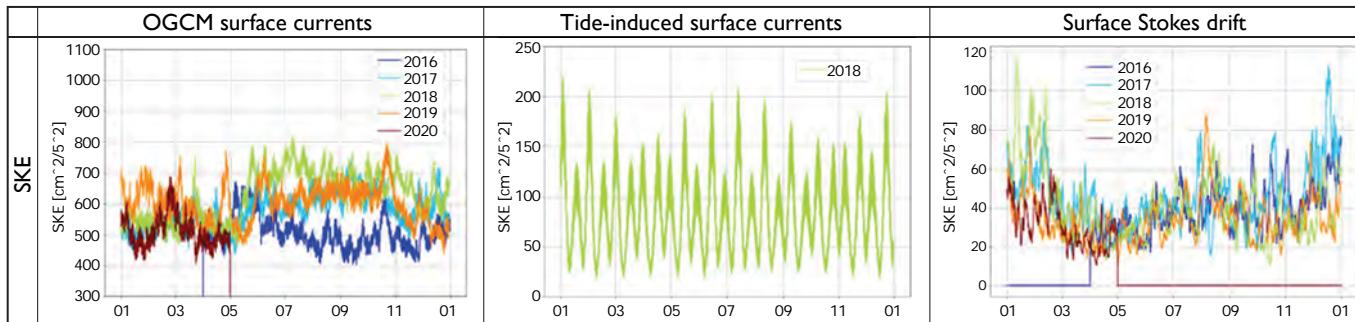


Figure 9: Time series from January to January of the following year of the Surface Kinetic Energy (SKE) spatially averaged over the regional domain in  $\text{cm}^2/\text{s}^2$ . From left to right panels: OGCM surface currents, tide-induced surface currents and surface Stokes drift components of the SMOC product

## Surface Kinetic Energy

The time evolution of the surface kinetic energy shows a seasonal signal for the OGCM surface currents with greater values between May and November, which is linked to the monsoon signal (figure 9, left panel). Some interannual variability can also be observed: The August to December period is less energetic in 2016 than during the other years. This singularity is likely linked to an El-Nino event. Indeed, El-Nino impacts water mass circulation and notably increases the flow of surface water from the South China Sea, through the Sulu Sea and into the northern Makassar Strait. It also reduces the tropical Pacific surface water injection into Makassar Strait (Gordon *et al.*, 2012).

Only one year has been drawn for the tidal component in order to have a better view of the signal oscillation (figure 9, middle panel). Periods larger than 14 days are clearly visible and the daily oscillation is only visible through the line thickness in this plot. There is no clear interannual variability. The surface kinetic energy derived from the surface Stokes drift also shows a seasonal variability with slightly greater values in December and January and smaller values in April and May (figure 9, right panel). However there is no clear interannual variability over the years considered here.

## River discharges

In the numerical experiments, the release of particles follows the river discharge evolution at the river mouths. River discharges are taken from the River discharge and related historical data from the Global Flood Awareness System dataset provided by the Copernicus Emergency Management Service (GloFAS, 2019). This dataset has been generated by a hydrological river routing model using runoff data from a global reanalysis. The model has been validated using measurements performed on stations of 1,801 catchments located around the world (Harrigan *et al.*, 2020). The spatial resolution of the model is  $1/10^\circ$ , and its temporal resolution is 1 day. The highest discharges in the Indonesian region are for rivers located in Borneo, Papua and eastern Sumatra (figure 10, upper panel). The total Indonesian river discharge represents between 50 thousands and 150 thousands of  $m^3/s$  with a strong seasonal signal. This signal is correlated and dephased by approximately a month with the total land precipitation (figure 10, lower panel).

## Population Density

The choice for the location of particle release is partly driven by the population density at river mouths or upstream (see methodology section for a full explanation). The population density was extracted from the NASA Socioeconomic

Data and Applications Center (SEDAC) dataset (Center for International Earth Science Information Network - CIESIN - Columbia University, 2018). This dataset is a human population density estimate (number of persons per square kilometer) based upon counts that are consistent with national censuses and population registers, for the years 2000, 2005, 2010, 2015, and 2020. Values associated to year 2020 were computed by extrapolation. This is the reason why 2015 values were used for this atlas (see figure 3 in the introduction section).

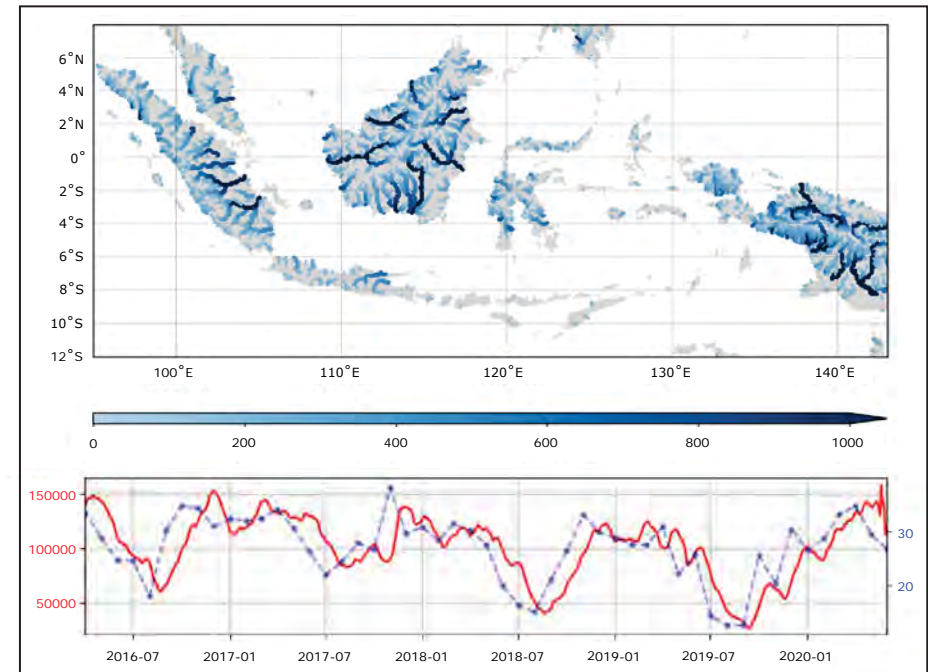


Figure 10: Upper panel: 2018 average of GloFAS discharge in  $m^3/s$ . Values below  $10 m^3/s$  are shaded in grey. Lower panel: Time evolution of discharge in  $m^3/s$  along the Indonesian coast in red (computed as the sum of the values for the Indonesian coastal cells, i.e. the earth cells adjacent to a sea cell with an Indonesian mask), superimposed with the pluviometry in mm/month as shown in figure 4 in dashed blue

© Alexis Chappuis, UNSEEN Expeditions



# Methodology

## Lagrangian analysis

To understand the marine debris pathways and strandings, a Lagrangian point of view was considered (van Sebille *et al.*, 2018). The Lagrangian software Ariane was used to compute the trajectories of numerical particles advected by ocean currents. The strength of the Lagrangian method is in the possibility to store and get access to the full history of the particle trajectory and, in particular, to the connectivity patterns between regions. Another strength is in the possibility to advect particles backward in time and assess where particles can possibly come from.

The Ariane software of Lagrangian advection has been developed, released, and upgraded under CeCill License since 2006 (Blanke and Raynaud, 1997). This Lagrangian tool is used to analyze global ocean currents. It computes 3D trajectories of particles and builds transport diagnostics. Initially, it was developed to evaluate water masses transports. Trajectories are constructed by a 1D-linear formulation from U, V and W transport fields. The 3D non divergence is locally preserved, but velocities are discontinuous in space and time. This scheme has been validated for trajectory estimation. For the present atlas, a special 2D version of Ariane was used, in which particles remain at the same depth by prescribing a null vertical velocity.

## Spatio-temporal characteristics of the experiment

Only Indonesia and its immediate neighbour countries are considered, in a regional domain as defined by  $[90, 145]^{\circ}\text{E} \times [-25, 35]^{\circ}\text{N}$  (figure 11). The spatial domain will be enlarged in future works to assess the fate of the floating marine debris that leave the regional domain into the Indian and Pacific oceans.

The experiments were performed from the 1<sup>st</sup> of April 2016, which corresponds to the beginning of the SMOC product availability, to the 30<sup>th</sup> of April 2020. Seasonal variability can be investigated thanks to the 4 years of simulation. The time series will be extended in future works to assess the inter-annual variability.

## Marine debris release scenario

Where and when marine debris are released in the numerical experiments have to be defined. Marine debris are simulated by fictive numerical particles of no shape, size, or weight. The initial position of a particle is defined by its time and space coordinates. Its trajectory is computed by the Ariane Lagrangian software using the SMOC surface current outputs (see section Materials). A particle is

considered as a point, not submitted to any kind of wind drag (i.e., the windage impact on an emerged part of the marine debris is not studied here). Only floating marine debris were considered (i.e., no positions are initialized below the surface) assuming that stranded debris are mainly coming from surface or very close to surface marine debris. Several considerations and assumptions led to the final particle release scenario and are explained in the following sections.

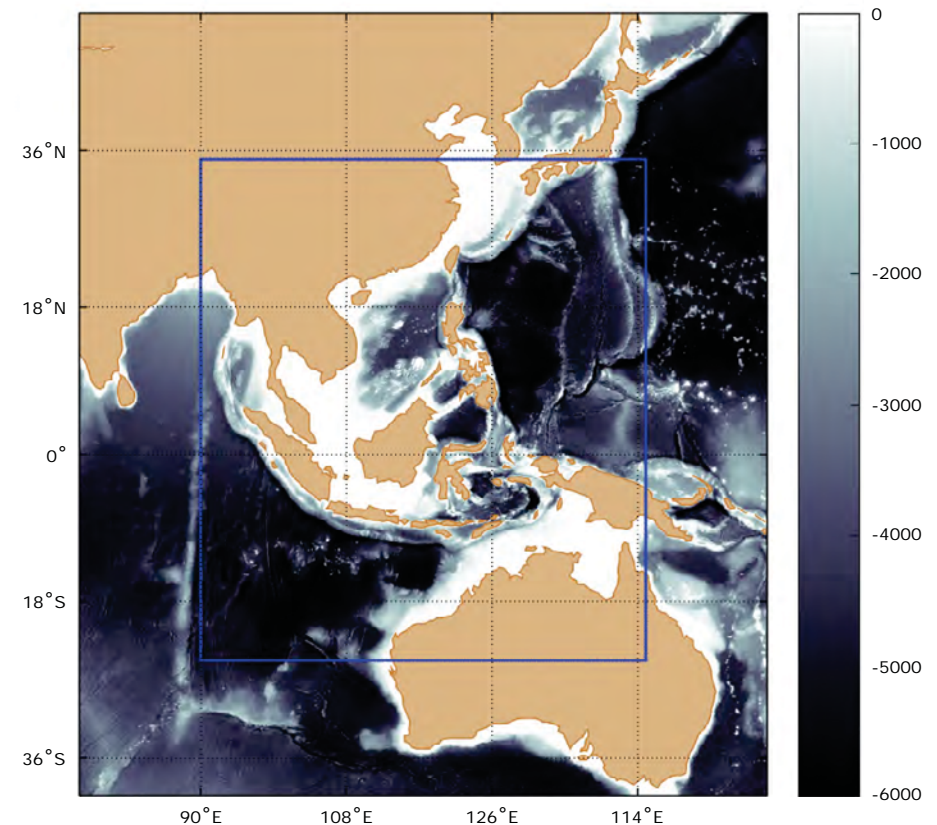


Figure 11: Bathymetry (in meters) of Indonesia and adjacent seas. The blue box defines the boundary of the studied domain

## Horizontal initial position

Particles were positioned at the mouths of a subset of Indonesian rivers, assuming that the main input of marine debris from inland enters the ocean via river mouths (Lebreton *et al.*, 2017). 21 rivers were selected (see table 1 and figure 12) with the following criteria:

- because they are known to be polluted (communication from the Indonesian Ministry of Marine Affairs and Fisheries, or from the Ocean Cleanup project)
- or because there is a high density of population living at the river mouth or upstream
- or because there is a major river discharge even if population density and pollution are small (this is the case for the Digul and Mamberamo rivers in Papua)

River Name	River ID	Longitude [°E]	Latitude [°N]	Mean discharge [m <sup>3</sup> /s]	Pop Density [inhab/km <sup>2</sup> ]
CISADANE	0	106.632768	-6.014785	250	19,970
CILIWUNG	1	106.828585	-6.118554	250	19,970
CITARUM	2	107.33093	-5.97122	648	22,158*
SEMARANG	3	110.394308	-6.945955	134	4,589
SURABAYA	4	112.844718	-7.304786	612	8,582
SOLO	5	112.55665	-6.87701	962	1,086
TELUK BENOA	6	115.229959	-8.755988	131	7,161
JOGJA	7	110.204309	-7.982368	279	7,205
PELABUHAN RATU	8	106.50322	-6.963589	241	868
BATANG KANDIS	9	100.34998	-0.93157	112	1,590
DELI	10	98.70478	3.78461	312	7,427
BATANG HARI	11	104.20258	-1.06836	2,819	4,068*
MUSI	12	104.9225	-2.343611	3,066	5,999*
KAPUAS	13	109.10711	-0.165324	7,803	1,947
BARITO	14	114.50226	-3.50246	576	6,037
TALLO	15	119.448473	-5.097552	70.9	9,633
MAHAKAM	16	117.46206	-0.66603	5,953	1,423*
KAYAN	17	117.62	2.98	2,261	1,000
AMBON	18	128.103	-3.73	13.4	1,498
DIGUL	19	138.64197	-6.86235	189	6.1
MAMBERAMO	20	137.90108	-1.46669	12,852	0.84

Table 1: Characteristics of the 21 selected rivers along with their mouth location, the corresponding average river discharge over 2016-2020 from the GloFAS dataset and population density in 2015 from the SEDAC dataset. Population density are either provided at river mouth or upstream depending on the main city location. Upstream cases are indicated with an asterisk

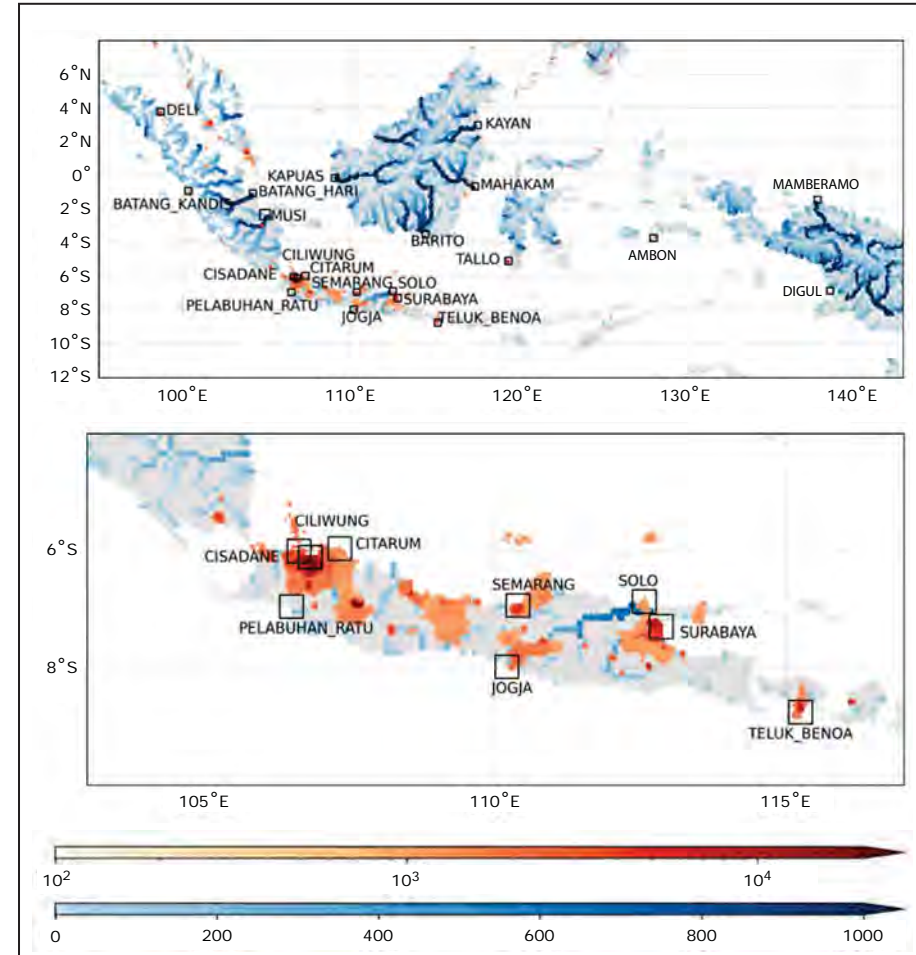


Figure 12: River mouths selected as marine debris sources. Points in shades of blue are river discharges from GloFAS product (2019 average). Values are displayed when above 10 m<sup>3</sup>/s and are saturated at 1,000 m<sup>3</sup>/s. Shades of orange correspond to population per square meter from the Nasa SEDAC product for 2015. Values are displayed when above 1,000 inhab/km<sup>2</sup>. Upper panel shows all selected rivers. Lower panel zooms on Java and Bali rivers

Particles were randomly released within a 30-kilometer radius from the river mouths (figure 13). This choice was driven by the observed mean plume extension in the surface sea salinity fields of the Ocean General Circulation Model.

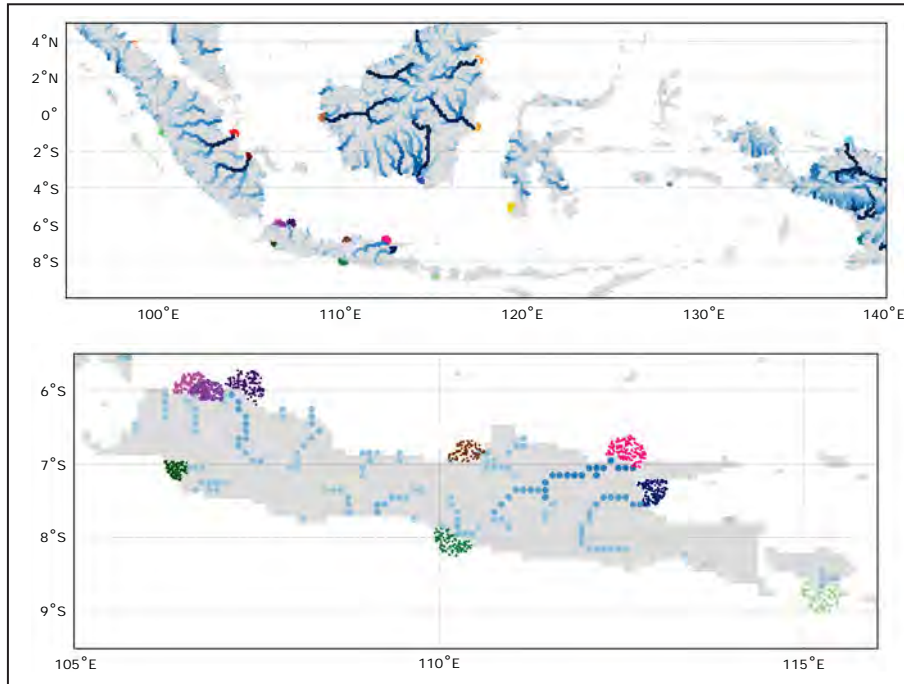


Figure 13: Released particles: Dots represent the position of the particles released the first day of the simulation. The colors differentiate the riverine origin. Lower panel is a zoom view on the Java Island

### Time release

Particles were released following the time evolution of the river discharge at river mouths. Indeed, a correlation exists between high discharge and high level of inland waste entry into the open sea. A linear relationship is assumed between these two parameters. Most (but not all) of the rivers have a marked discharge seasonality with a dry season during July, August and September (figure 14).

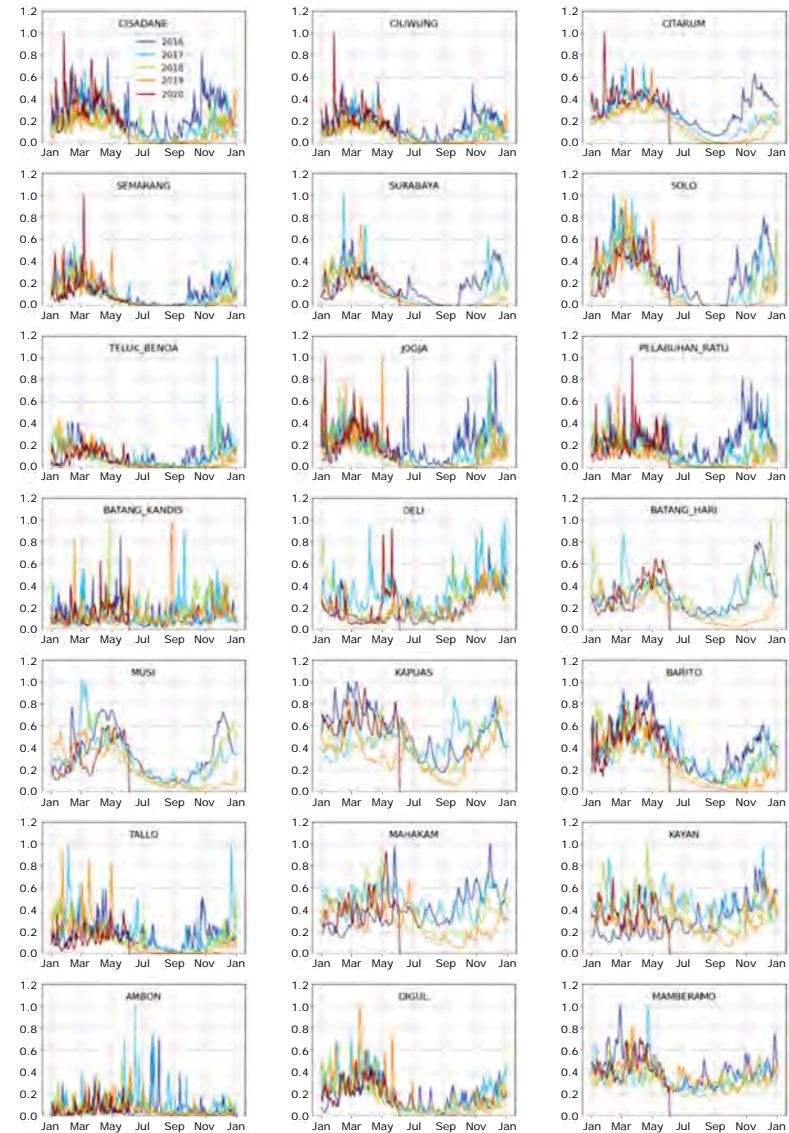


Figure 14: Time evolution of river discharge, using the GloFAS dataset values at the river mouth of the 21 selected rivers. Values have been normalized by the maximum discharge value of each river

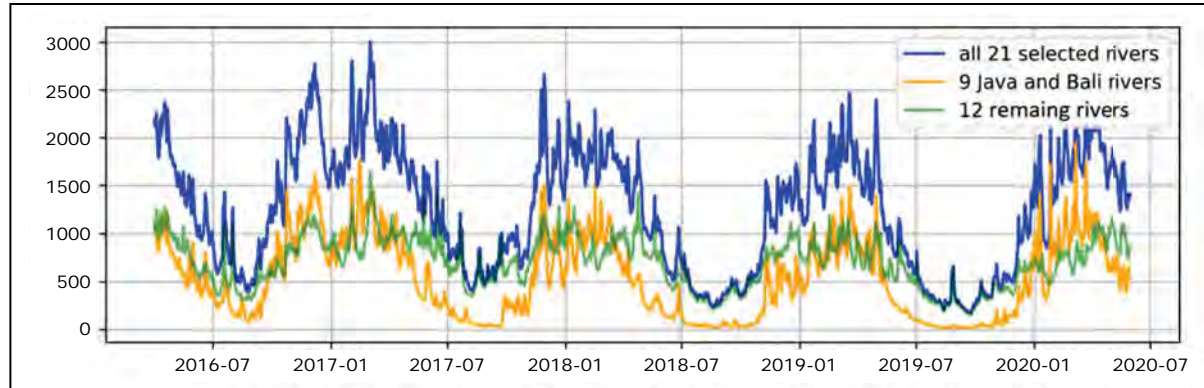


Figure 15: Time evolution of the sum of released particles for all rivers in blue line and for two subgroups of rivers: The 9 rivers of Java and Bali islands in orange line, and the 11 remaining rivers in green line

As no further information on relative pollution was available, the same number of particles was released for each river. This number was set to 90,000 particles by river to reach a total of 1,890,000 particles to be statistically representative. With a particle release scenario following the river discharge time evolution, 500 to 2,500 particles were released each day (figure 15, blue line). It is noteworthy that the 9 rivers from Java and Bali islands have a marked dry season in August and September (figure 15, orange line close to zero in August and September) compared to the remaining 12 rivers from Sumatra, Kalimantan, Maluku and Papua (figure 15, green line close to 500 in August and September).

## Particle strandings

### Definition of a numerical stranding

The modelling assumptions need to be reviewed before defining what a "stranding" is from a numerical point of view.

First, the resolution of the surface currents is limited:

- close to the shore, surface currents are considerably disturbed and the induced fine-scale perturbation can not be resolved by the  $1/12^\circ$  spatial resolution of the OGCM numerical model
- waves are considered through the addition of surface Stokes drift to OGCM surface currents. However, because these two surface currents result from coupled processes (Stoke drift and the Eulerian flow impact each other), simply adding them may induce

an overestimate of the Stokes drift impact (Couvelard *et al.*, 2020; van Sebille *et al.*, 2020)

- similarly, tides are considered through their addition to OGCM surface currents, whereas a coupled model would be more accurate. The tidal ebb and flow is not simulated either

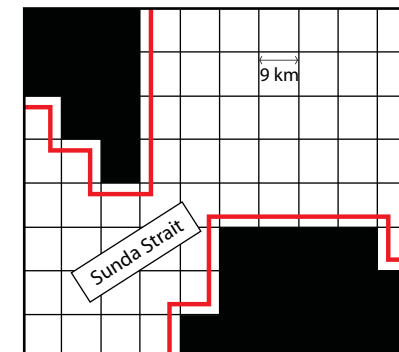


Figure 16: Illustration of the numerical definition of a stranding in the Sunda Strait. The grid of the numerical model is in black. The red lines illustrate the threshold distance to the numerical coast: if a particle enters the zone in between the red line and the coast, it will then be considered as stranded. The distance expressed on this figure is exaggerated in purpose, to be illustrative. The threshold is in fact set to 9 meters or 0.001 grid cell size

Second, processes leading to particle stranding are complex and difficult to parameterize. They depend on several factors such as the beach type (sand, cliffs, rocks, etc), tidal conditions, coastal currents, wind and waves, sand burying, unburying, and subsequent back-release into the sea (Critchell and Lambrechts, 2016; Lebreton *et al.*, 2019; van der Mheen *et al.*, 2020).

Finally, within the Ariane Lagrangian software, particles are allowed to drift along smooth (numerical) coastlines.

Considering the limitations mentioned above, a numerical stranding is hereafter simply defined as follows: "a particle is considered as stranded when it drifts within a given distance to the numerical coastline" (as illustrated in figure 16). The rest of the trajectory computed by the Lagrangian software is not considered anymore. Despite its relative simplicity, this definition is consistent with the numerical grid used to compute surface currents, and thus consistent with surface currents themselves.

Finally, the following features should be considered when setting the threshold distance value:

- the threshold distance should be smaller than the width of the narrower straits of the Indonesian region (i.e. smaller than 1 or 2 grid cell size). Otherwise, particles travelling through these straits would be automatically counted as stranded
- some particles have been released at a distance down to a 0.01 grid cell size to coastline. Consequently, the threshold distance should be smaller than 0.01 grid cell size
- for numerical memory convenience, part of the post-treatment results including particle trajectories has been saved in float 32 bits. Thus, the threshold should not be set below the precision limit of 0.001 grid cell size

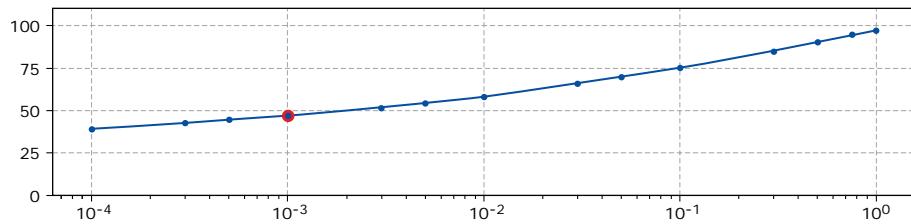


Figure 17: Percentage of stranded particles from Cisadane river plotted against the distance to the coast threshold (in grid cell size unit) below which the particle is considered as stranded. The x-axis follows a logarithm evolution. The red dot corresponds to the threshold finally chosen

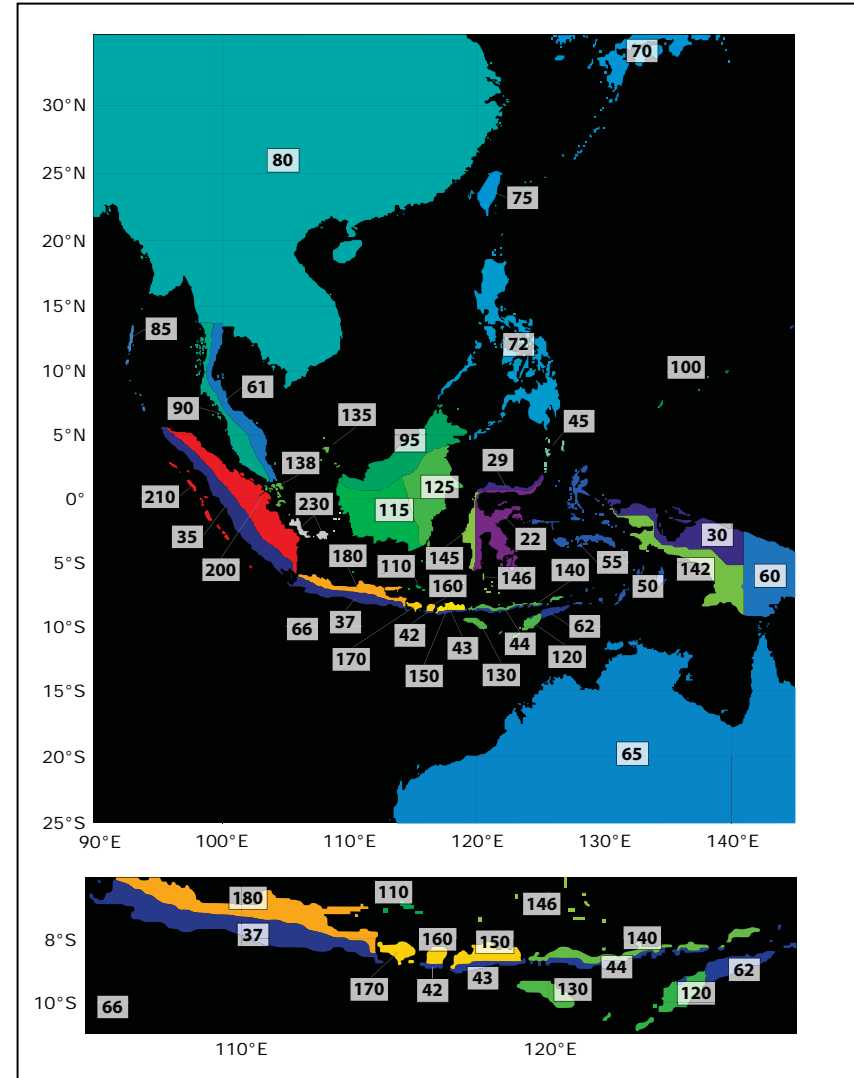


Figure 18: Map of the subzones for the stranding evaluation. Seas are colored in black. Definition of the identification numbers is provided in table 2. Identification numbers were chosen to facilitate visual differentiation between subzones when displaying the map in shades of grey with the GIMP software (during the building process), these numbers are recorded inside an 8-bits parameter and values are accordingly coded inside a [0,255] range

id	stranding subzone description
22	East Sulawesi on Molucca and Banda Sea
29	North Sulawesi on Sulawesi Sea
30	North Papua
35	West Sumatra
37	South Java
42	South Lombok
43	South of West Nusa Tenggara
44	South of East Nusa Tenggara
45	Sulawesi Entry
50	Between Timor, Arafura and Banda
55	Maluku
60	Papua New Guinea
61	East Thailand-Malaysia peninsula
62	East Timor
65	Australia
66	Christmas Isle
70	Japan
72	Philippines
75	Taiwan
80	China, Vietnam, Cambodia, Thailand, Myanmar and Bangladesh
85	Andaman and Nicobar Isles
90	West Thailand-Malaysia peninsula
95	Malaysia and Brunei on Borneo Isle
100	Palau
110	Greater Sunda and Kangean Isles
115	South Borneo
120	Timor
125	East Borneo
130	Rote Savu and Sumba Isles
135	Riau Archipelago in South China Sea
138	Riau Archipelago in Malacca Strait Entry
140	East Nusa Tenggara and Wetar Isles
142	South Papua
145	West Sulawesi-Makassar Strait
146	Selayar Isles
150	North of West Nusa Tenggara
160	North Lombok
170	Bali
180	North Java
200	East Sumatra
210	Mentawai Batu Simeulue Isles
230	Bangka and Belitung Isles

Table 2: List of the different stranding zones used in this atlas

The threshold value could range from 0.0001 grid cell size (90 cm) to 0.01 grid cell size (90 m). The sensitivity of the particle stranding rate to the threshold value has been assessed for the Cisadane river (figure 17). As expected, the percentage of stranded particles increases with the threshold value. The threshold is set to 0.001 grid cell size (9 m), which corresponds to the mean stranding rate for the allowed threshold range (red dot in figure 17).

#### Definition of stranding subzones

To understand the spatial variability of the stranding patterns, 42 subzones were defined within the Indonesian regional domain (figure 18 and table 2). The subzone definition is driven by both political and geographical considerations. For instance, the division of the Sulawesi Island into three subzones is only driven by geographical considerations with the western coast on the Makassar Strait, the northern coast on the Sulawesi Sea and the southern and western coasts on the Flores, Banda and Molucca seas. The division of the New Guinea Island is also driven by political considerations with a north-south separation line corresponding to the country boundary between Indonesia on the western part and Papua New Guinea on the eastern part. Because this study is focused on the Indonesian region, there is a high number of subzones within this region only, and much less for the surrounding countries (for instance, no subzone occurs for Australia or China).

To consistently compare the number of strandings from one subzone to another, results were normalized by the length of the subzone coastline. This length is calculated using the numerical grid. It is noteworthy that the lengths of the numerical coastline are smaller than values provided from real topography as found by any online search because features below the grid resolution of 9 km are smoothed out in the former case. For instance, the Australian Christmas Isle in the Indian Ocean has the smallest coastline length of 37 km while it is closer to 80 km in "reality". The longest numerical coastline length (17,737 km) is found in the Philippines (vs. 36,289 km in "reality"), followed by the multiple country subzone of China, Vietnam, Cambodia, Thailand, Myanmar and Bangladesh with 14,196 km of numerical coastline. The subzone of Australia comes last with 11,702 km. Additional details are synthesized in the table 3 of the results section.





# Results

This section is organized as follows: first, the regional dispersion of particles into the Indonesian region is presented, then the spatio-temporal variability of stranded particle along the Indonesian and surrounding countries' coasts is investigated. Finally, the impacts of the physical processes are discussed.

## Regional dispersion of particles originating from Indonesian rivers

To have a synoptic view of the regional dispersion, the average number of particles per grid cell (i.e., by approximately 80 km<sup>2</sup>) was computed over the simulation last year (i.e., from April 2019 to April 2020) and over its four trimesters (figure 19).

Almost all particles are located within a latitude band extending from 15°S to 12°N. Particles are abundant in the Java, Flores and Banda seas as well as in the Malacca Strait. Some of them drift inside the southern part of the South China Sea. It is noteworthy that there is almost no particle along the northwestern coast of Borneo. During the Northwest Monsoon, offshore Ekman currents seem to prevent particles from flowing into this area (Yan *et al.*, 2015) while during the Southwest Monsoon the Tanjung Datu cape and the main northeastern surface currents prevent them from flowing into it. There is no major dispersion inside the Sulu Sea but some particles enter nonetheless through the Balabac Strait and the Sibutu passage. Many particles can be found in the Sulawesi Sea, originating from both close-by and remote rivers.

The particles leave the Indonesian regional domain mainly through the South Indian Ocean, following a large pathway extending from 15°S to 5°S at 90°E, and drifting along with the Indian South Equatorial Current. This pathway is particularly followed in July, August and September (figure 20).

Three secondary pathways are also observed:

- through the North Indian Ocean in a narrow pathway extending from 6°N to 8°N at 90°E mostly from January to June. Particles exit through the Malacca Strait and follow the Northwest Monsoon Current
- through the North Pacific Ocean in a narrow pathway extending from 6°N to 8°N at 90°E mostly from end of June to December. Particles are often drifting within the Halmahera Eddy before being advected away from the Indonesian region along with the Pacific North Equatorial Counter Current
- through the South Pacific Ocean in a narrow pathway extending from 4°S to 2°S at 145°E mostly from November to May. Particles follow the Papua New Guinea southeast coastal current occurring during the Northwest Monsoon (Cresswell, 2000)

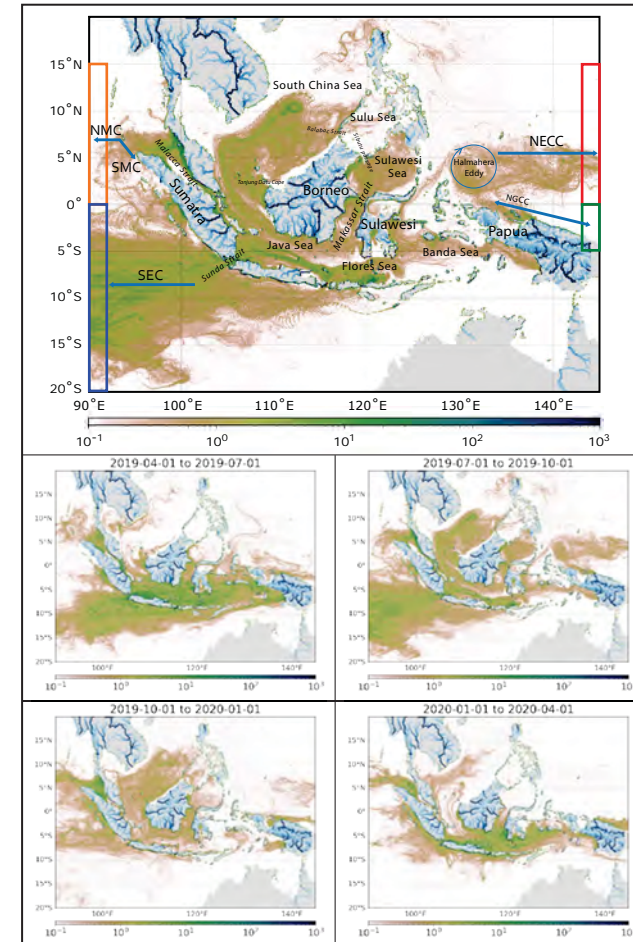


Figure 19: Upper panel: Average number of particles per grid cell over the last year of simulation (1<sup>st</sup> of April 2019 to 1<sup>st</sup> of April 2020) using the SMOC product. The colored boxes in the upper panel represent the areas used to compute the time evolution of the number of particles leaving the Indonesian domain in figure 20. Lower panels show the three-month averages. Straits and cape are given in black italics. Acronyms: NMC, Northwest Monsoon Current (Jan-Feb); SMC, Southeast Monsoon Current (Jul-Aug); SEC, South Equatorial Current; NECC, North Equatorial Counter Current; NGCC, New Guinea Coastal Current (Northwestward during the trade winds period and Southeastward during the Monsoon from November to March)

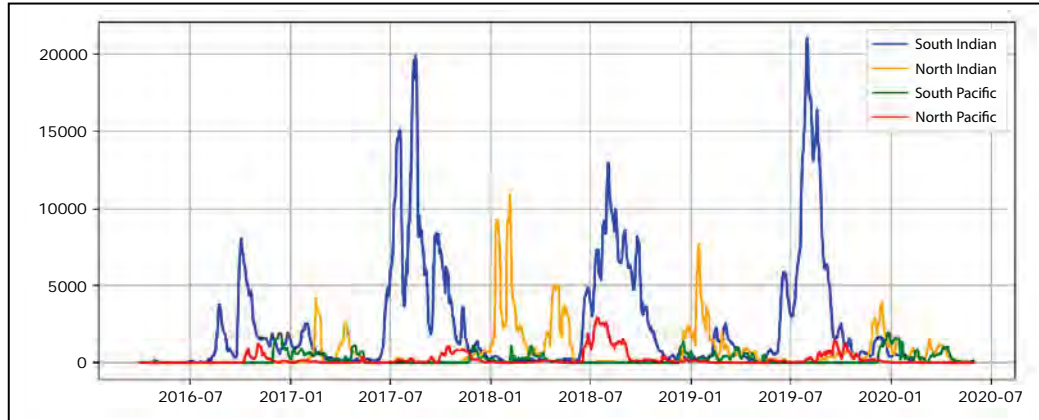


Figure 20: Total number of particles leaving the Indonesian region from the four boxes drawn in the upper figure 19:  $[90,92]^{\circ}\text{E} \times [20,0]^{\circ}\text{S}$  for South Indian Ocean in blue,  $[90,92]^{\circ}\text{E} \times [0,15]^{\circ}\text{N}$  for North Indian Ocean in yellow,  $[143,145]^{\circ}\text{E} \times [5,0]^{\circ}\text{S}$  for South Pacific Ocean in green and  $[143,145]^{\circ}\text{E} \times [0,15]^{\circ}\text{N}$  for North Pacific Ocean in red

## Spatio-temporal patterns of stranded particles

At the end of the 4-year simulation, 60.4% of the particles are stranded in the Indonesian region, 9.7% still drift inside it while 29.9% drifted away (87% through the Indian Ocean -13% through the Pacific Ocean). In this section, the spatio-temporal variability of the stranded particles is investigated.

### Regional patterns

Inside the Indonesian region, the particles mainly strand along the Indonesian coasts (92.6%). The remaining 7.4% strand along the coasts of surrounding countries included in the defined regional domain (Australia, Papua New Guinea, Philippines, Taiwan, Japan, China, Vietnam, Cambodia, Thailand, Myanmar and Bangladesh). The subzones supporting most of stranded particles are North and South Java (figure 21). West Sulawesi and Bali come next in normalized number whereas they are respectively ranked 6 and 12 in total number. Results are detailed in table 3.

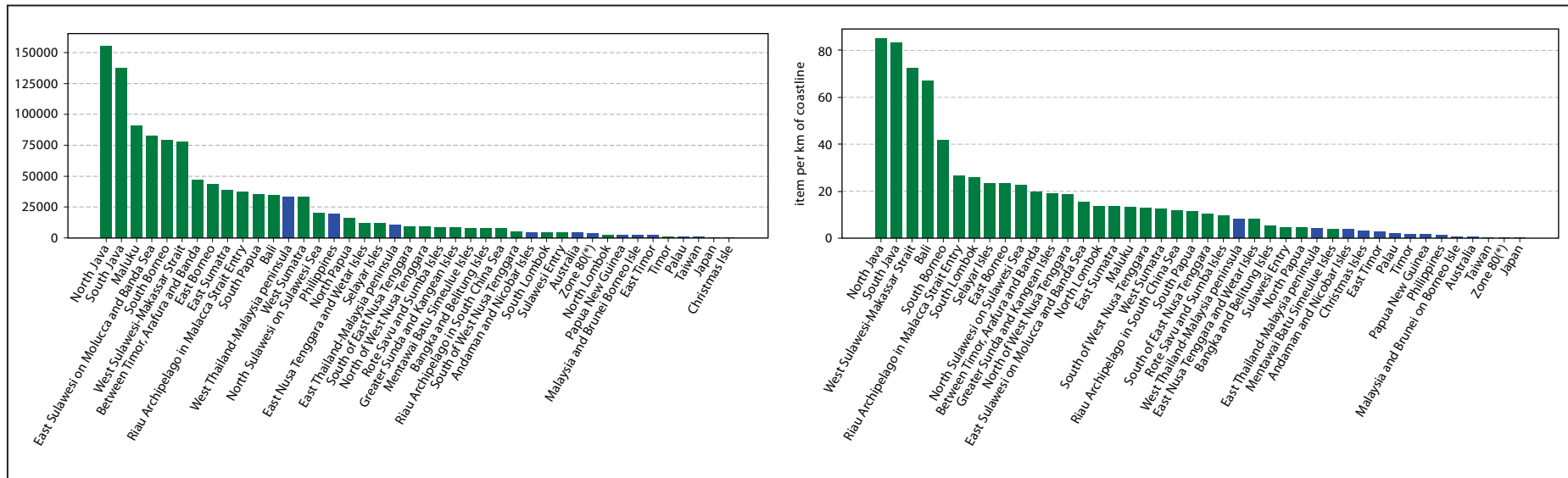


Figure 21: Left panel: Total number of particles according to the stranding areas. Right panel: Number of particles normalized by the coastline length of the stranding subzone. (\*) zone 80 gathers "China, Vietnam, Cambodia, Thailand, Myanmar and Bangladesh". Green bars illustrate particles stranding along the Indonesian coasts. Blue bars illustrate particles stranding along the surrounding countries' coasts

id	stranding subzone description	length of coastline [km]	total stranding [item]	normalized stranding [item/km]
22	East Sulawesi on Molucca and Banda Sea	5,413	82,546	15.2
29	North Sulawesi on Sulawesi Sea	909	20,434	22.5
30	North Papua	3,570	15,670	4.4
35	West Sumatra	2,659	32,959	12.4
37	South Java	1,667	138,881	82.3
42	South Lombok	165	4,242	25.6
43	South of West Nusa Tenggara	404	5,099	12.6
44	South of East Nusa Tenggara	911	9,358	10.3
45	Sulawesi Entry	926	4,219	4.6
50	Between Timor, Arafura and Banda	2,421	47,126	19.5
55	Maluku	6,935	90,471	13.0
60	Papua New Guinea	1,559	2,394	1.5
61	East Thailand-Malaysia peninsula	2,506	10,249	4.1
62	East Timor	754	1,950	2.6
65	Australia	11,702	3,945	0.3
66	Christmas Isle	36	107	2.9
70	Japan	7,490	336	0.0
72	Philippines	17,737	19,239	1.1
75	Taiwan	1,507	466	0.3
80	China, Vietnam, Cambodia, Thailand, Myanmar and Bangladesh	14,196	3,563	0.3
85	Andaman and Nicobar Isles	1,217	4,385	3.6
90	West Thailand-Malaysia peninsula	4,004	33,032	8.2
95	Malaysia and Brunei on Borneo Isle	3,046	2,128	0.7
100	Palau	406	754	1.9
110	Greater Sunda and Kangean Isles	425	8,012	18.9
115	South Borneo	1,909	79,408	41.6
120	Timor	570	927	1.6
125	East Borneo	1,882	43,521	23.1
130	Rote Savu and Sumba Isles	918	8,624	9.4
135	Riau Archipelago in South China Sea	648	7,465	11.5
138	Riau Archipelago in Malacca Strait Entry	1,428	37,433	26.2
140	East Nusa Tenggara and Wetar Isles	1501	11,832	7.9
142	South Papua	3,155	35,013	11.1
145	West Sulawesi-Makassar Coast	1,075	77,906	72.4
146	Selayar Isles	499	11,592	32.2
150	North of West Nusa Tenggara	498	9,193	18.5
160	North Lombok	203	2,736	13.5
170	Bali	516	34,578	67.0
180	North Java	1,855	157,433	84.9
200	East Sumatra	2,864	38,551	13.5
210	Mentawai Batu Simeulue Isles	2,058	7,858	3.8
230	Bangka and Belitung Isles	1,465	7,510	5.1

Table 3: Number of particles according to stranding subzones: Correspondence between the identification number (id), the stranding subzone description, the length of the numerical coastline in km at a 1/12° spatial resolution, the total number of stranded particles (number of numerical particles drifting within 9 m to the coast), and the number of stranded particles normalized by the length of the coastline

Another noteworthy feature is the timing of the stranding process. Although the longest drift before stranding is 1,470 days (4 years), most of the particles quickly strand: 63% before 3 months, 84% before 6 months and 96% before 1 year (figure 22). Only 0.1% of the particles strand immediately. Three rivers clearly stand out of the general pattern: Particles released from the Deli river drift the longest before stranding and particles from the Jogja and Pelabuhan Ratu rivers, which are both located in the south of Java, strand the fastest.

The stranded particles mainly come from local riverine sources. Indeed, while the longest distance between the particle initial release position and the stranding location is 5,442 km, 99% are shorter than 3,000 km, 76% are shorter than 1,000 km (which corresponds to the length of Java Island for instance), and 33% are shorter than 100 km (figure 23). Consistently with the particle stranding age, particles from the Jogja and Pelabuhan Ratu rivers show the shortest distance between the particle initial release position and the stranding location. On the other hand, particle drifts from the Citarum river are the longest one in terms of distance.

#### Spatio-temporal variability

Floating marine debris strand at any time of the year and originate from all the rivers with a close relative contribution: from 1.9 % of the total number of stranded particles for the Deli River to 6.7 % for the Ambon River (figure 24). Some of the rivers that contribute the most to the total number of strandings are located in enclosed bays (such as Surabaya or Ambon). There is a marked seasonality with two main peaks, one centered on June and July and one centered on January and February. This result may seem obvious because of the seasonality of the particle release and of the surface currents. However, the time evolution of the number of strandings is not a linear function of surface currents and particle release scenario. Consistently with this experiment performed with the SMOC currents, this seasonal variability also appears through the same experiment performed with the OGCM surface currents only (i.e. : excluding Stokes drift and tides), or with surface currents from a reanalysis instead of near-real time products (figures not shown). Lastly, the beginning of an inter-annual variability can be observed in figure 24. It is probably linked to the ENSO, but the 4 years of simulation are too short to fully assert this assumption.

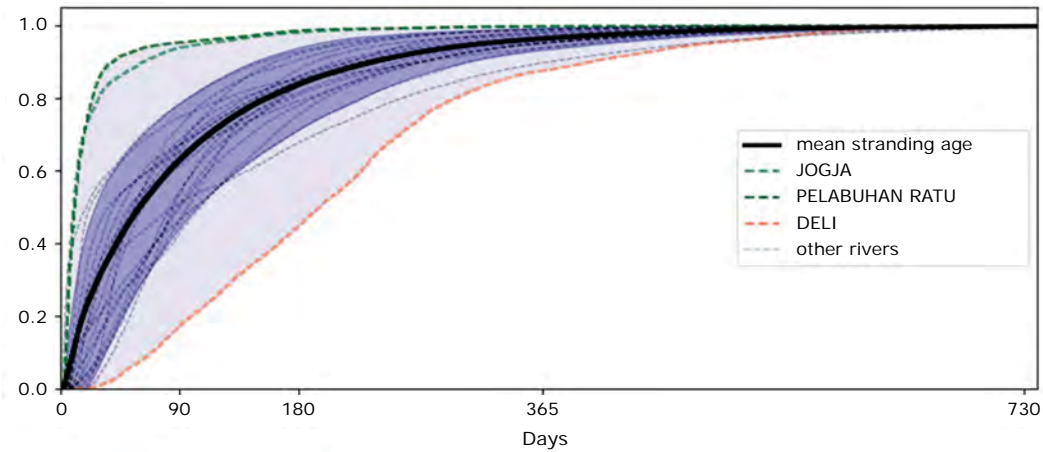


Figure 22: Normalized cumulative histogram of stranding age for particles released from the 21 Indonesian rivers. The thick black line represents the normalized cumulative histogram for all stranded particles, regardless of the riverine origin. The dashed lines correspond to histograms for subsets of stranded particles grouped by their riverine origin. The dark purple shaded area corresponds to the standard deviation with respect to the riverine origin. The light purple shaded area highlights curves with the minimum and maximum values. Three rivers with extreme patterns are highlighted in the legend and their associated dashed lines are colored in green for the Jogja River, in seagreen for the Pelabuhan Ratu River and in orange for the Deli River

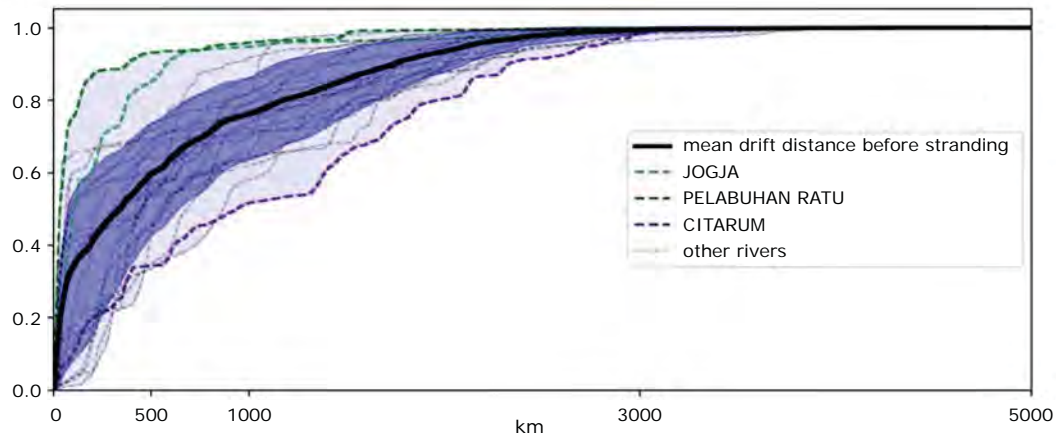


Figure 23: Normalized cumulative histogram of the distance between the particle initial release position and the stranding location. The thick black line represents the normalized cumulative histogram for all stranded particles, regardless of the riverine origin. The dashed lines correspond to histograms for subsets of stranded particles grouped by their riverine origin. The dark purple shaded area corresponds to the histograms standard deviation with respect to the riverine origin. The light purple shaded area highlights the minimum and maximum values. Three rivers with extreme patterns are highlighted in the legend and their associated dashed lines are colored in green for the Jogja River, in seagreen for the Pelabuhan Ratu River and in purple for the Citarum River

# All subzones

1,113,145 stranded particles

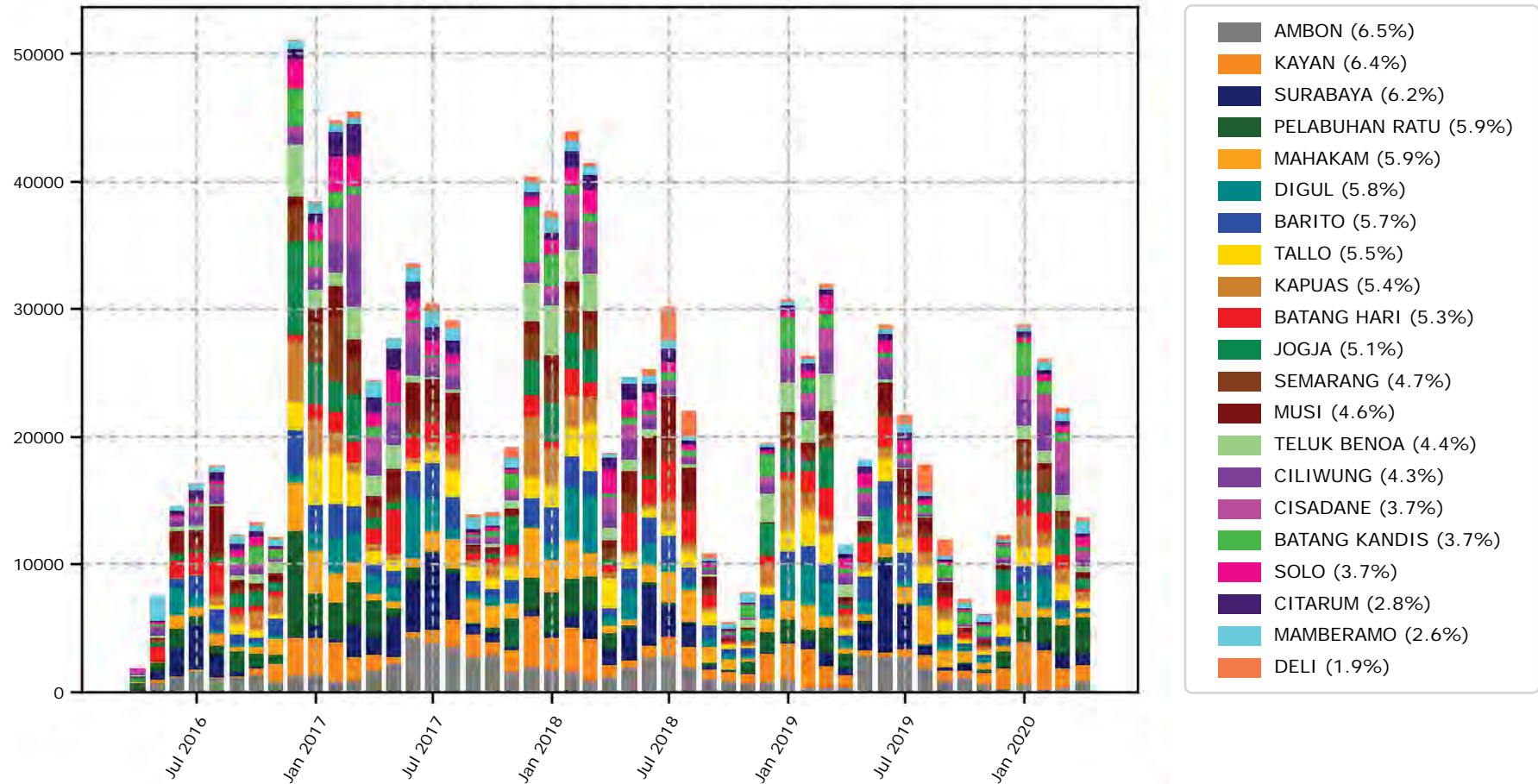


Figure 24: Time evolution of the particle strandings for the whole regional domain. The total number of stranded particles is indicated at the top. The contribution of each river to the total number of stranded particles is provided in the legend on the right side

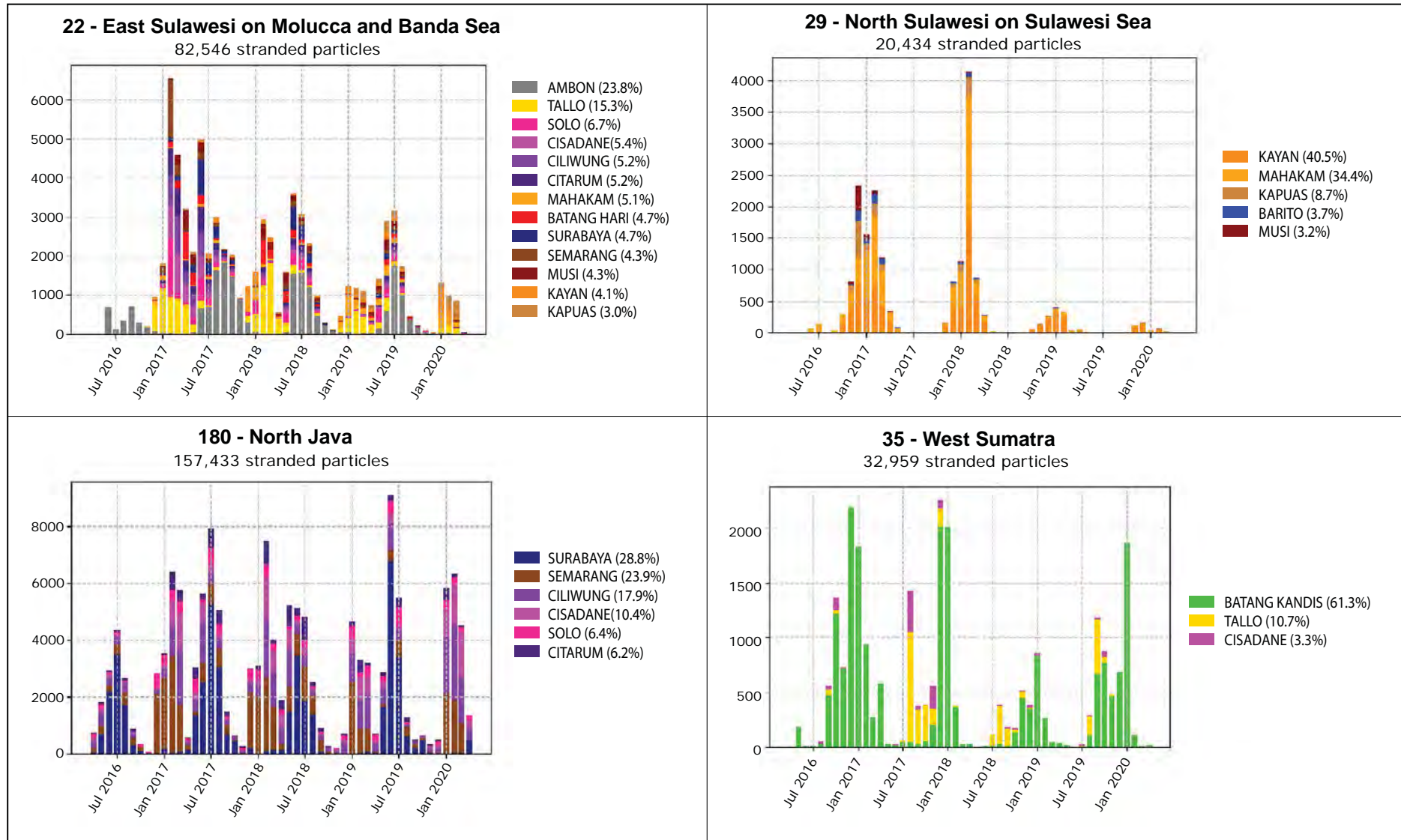


Figure 25: Time evolution of the number of stranded particles along the coasts of East Sulawesi (upper left), North Sulawesi (upper right), North Java (lower left) and West Sumatra (lower right). The subzone identification numbers are provided on the left side of the subzone name

This regional seasonality is spatially modulated. For instance:

- the eastern coast of Sulawesi has two peaks phased with the regional ones but they are shorter and the June-July peak is more intense than the December-March one in 2018 and 2019 (figure 25)
- the northern coast of Sulawesi only has one peak phased with the regional one in December-March
- the northern coast of Java also has two peaks phased with the regional ones
- the western coast of Sumatra only has one peak but between August and February, out of phase with the regional seasonality

A seasonal signal is observed for 24 out of the 42 subzones (see the Atlas in Appendix A for more details): 4 of them seasonally peak twice (East Sulawesi on Molucca and Banda seas, South Borneo, East Borneo and North Java), and 20 of them only peak once. Some peaks are easy to identify (for instance, for North Java) while others are not (for instance, for North Papua). The peaks are mainly centered on January, February and March (for 16 subzones) and on July and August (for 7 subzones) which is consistent with the observed peak seasons in figure 24. There are a few peaks centered on April, May, June, September and December (for 5 subzones) and no peak centered on October and November. The remaining 18 subzones do not show a clear seasonal cycle.

#### Connectivity between river mouths and particle stranding subzones

As presented above, all rivers contribute to the number of stranded particles in the regional domain. The riverine sources of the stranded particles are mainly local in time and space, except in some subzones. For instance, particles stranding along the northern coast of the Java Island almost exclusively originate from local rivers, while particles stranding along the western coast of the Sumatra Island also originate from the remote Tallo River and particles stranding along the northern coast of the Sulawesi Island also originate from the remote Kapuas, Barito and Musi rivers (figure 25).

Rivers, as sources of particles, contribute differently to the total number of stranded particles. Subzones located around the Flores, Banda and Maluku seas show a common pattern of being polluted by more than 9 riverine sources that each contribute more than 3% to the local number of stranded particles (figure 26). On the other hand, Papua, Papua New Guinea and Australia are mostly polluted by 2 riverine sources (Mamberamo and Digul rivers).

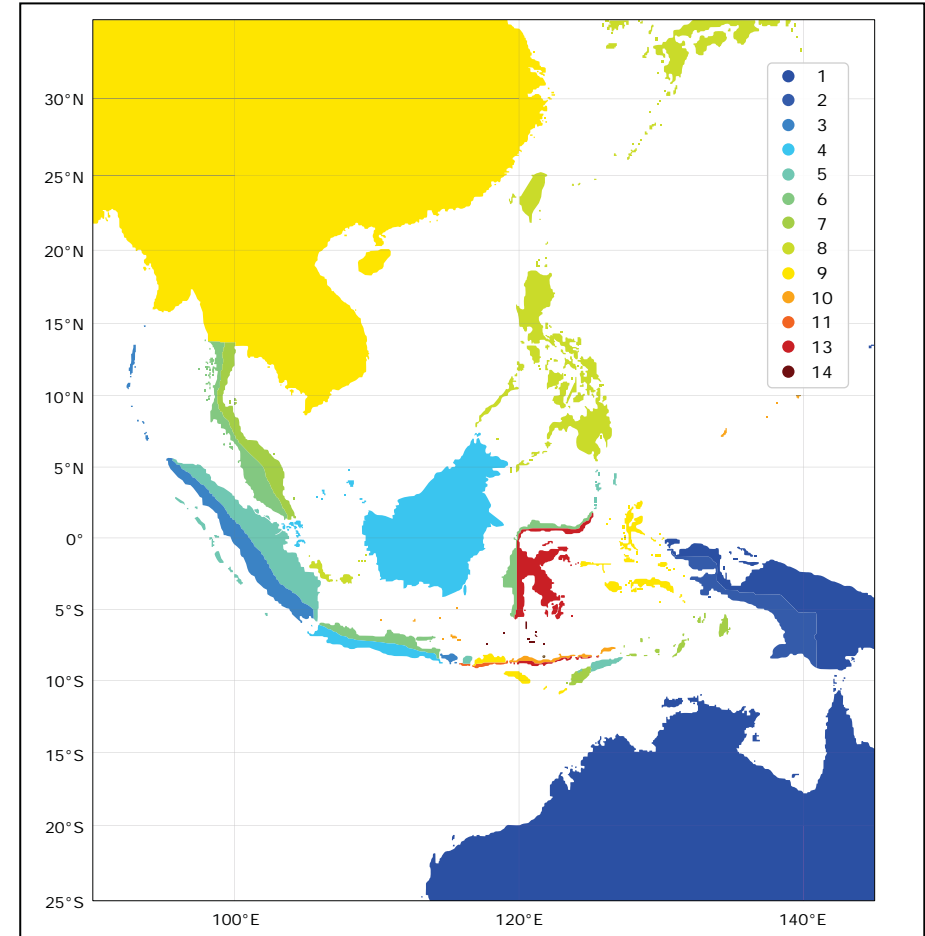


Figure 26: Number of riverine sources contributing more than 3% to the number of stranded particles in the subzone

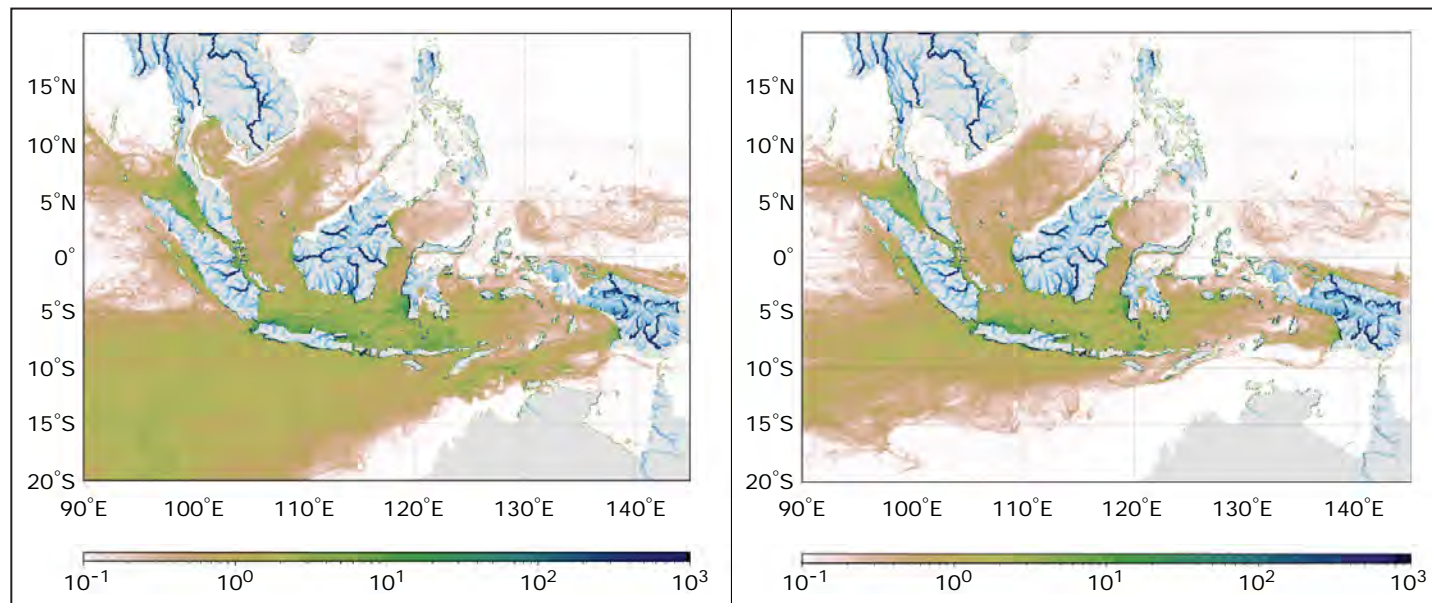


Figure 27: Average number of particles per grid cell for the last year of simulation (1<sup>st</sup> of April 2019 to 1<sup>st</sup> of April 2020) using the OGCM surface currents only (left panel) and using SMOC product that adds tidal currents and surface Stokes drift to the OGCM surface currents (right panel)

### Impact of physical processes on particle trajectories and strandings

This section presents and discusses the impact of the surface Stokes drift and tides addition on the computation of the particle dispersion and strandings. First, considering the regional dispersion of particles, the meridional extension of the exit route towards the South Indian Ocean is much broader when only OGCM surface currents are used than when surface Stokes drift and tidal surface currents are added. This difference is mainly due to the surface Stokes drift addition. The surface Stokes drift is convergent (positive values) southward and eastward of this domain (figure 8). Consequently, adding surface Stokes drift increases the convergence within the Indian South Equatorial Current and limits the meridional extension of the South Indian Ocean exit route. More generally, the addition of the surface Stokes drift seems to limit the poleward dispersion. All these preliminary results warrant further research.

The addition of surface Stokes drift has also a significant impact on the number of stranded particles. Indeed, this number increases by at least 13% and up to

31% depending on the release scenario (this includes the release scenario presented in the Methodology section and other scenarii not presented here). On the other hand, the number of stranded particles decreases by at most 3% when only tidal surface currents are added. Thus, though tides are an important component of the regional dynamics, their addition to the OGCM surface currents has a weak impact on strandings.

To understand why tides have such a small impact on particle dispersion and strandings and why Stokes drift has such a large one, the currents features were investigated (figures 28 and 29). The diverging impact may be due to the fact that the tidal currents are negligible in average (see figure 28 upper left panel) even if their velocity can be greater than 0.5 m/s locally in straits, close to some shores and in shallow waters (see figure 28 upper right and lower panels). On the other hand, the surface Stokes drift maximum is smaller (0.14 m/s) but the direction remains quite constant over time following wind patterns and a variability mostly driven by the seasons (see figure 29).

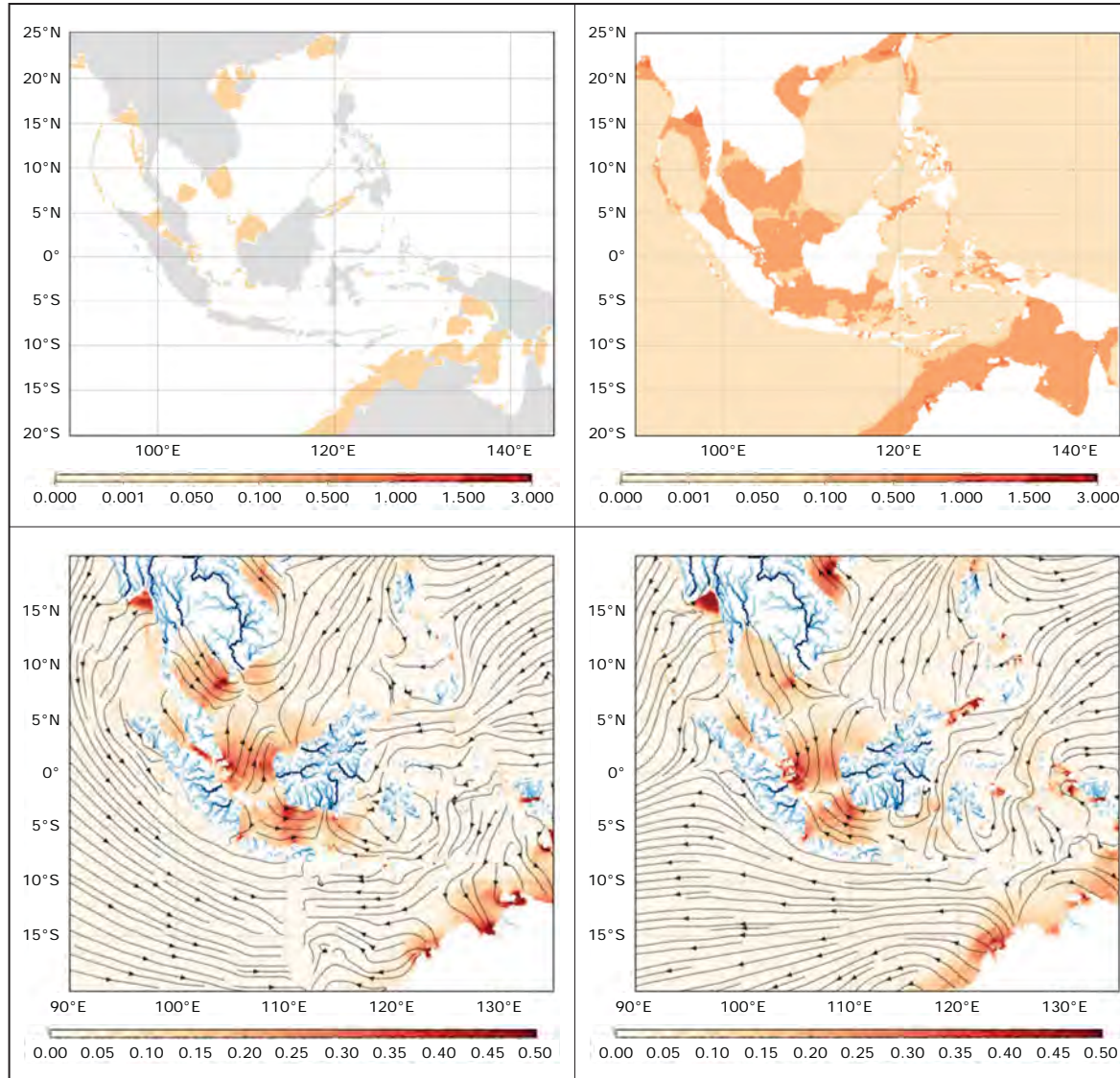


Figure 28: Upper panels: 2017 average of the tidal surface currents (upper left panel) and of the norm of the tidal surface currents (upper right panel). Lower panels: Norm of the tidal surface currents (in shades of orange) and streamlines (in black) with direction indicated by arrows for the 1<sup>st</sup> of April 2016 at 00:00 (lower left panel) and 12 hours later (lower right panel)

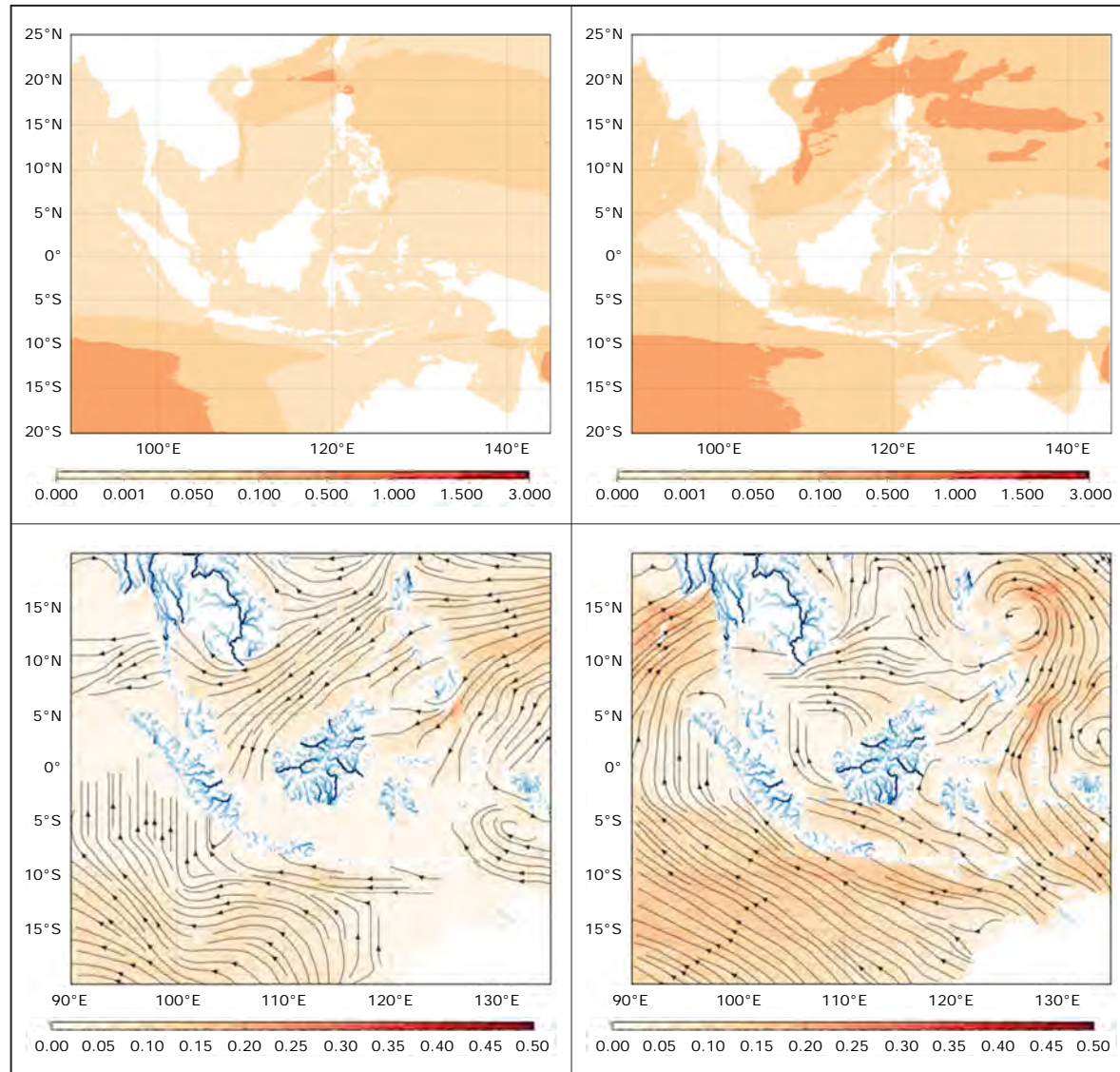


Figure 29: Upper panels: 2017 average of the surface Stokes drift (upper left panel) and of the norm of the surface Stokes drift (upper right panel). Lower panels: Norm of the surface Stokes drift (in shades of orange) and streamlines (in black) with direction indicated by arrows for the 1<sup>st</sup> of April 2016 at 00:00 (lower left panel) and four months later (lower right panel)





© Christophe Maes, IRD

# Detailed strandings for each subzone

This atlas is given for the regional domain and for each subzone of stranding as defined in the methodology section.

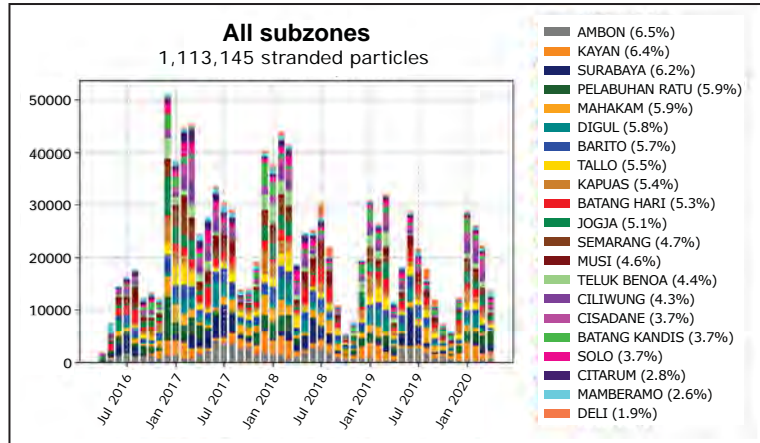


Figure 30: Number of stranded particles by month of stranding and by riverine source for the whole regional domain

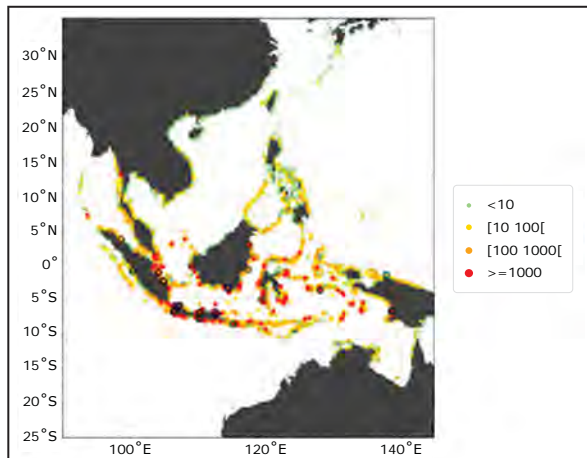


Figure 31: Localization of stranded particles for the whole regional domain, riverine sources are represented by circles

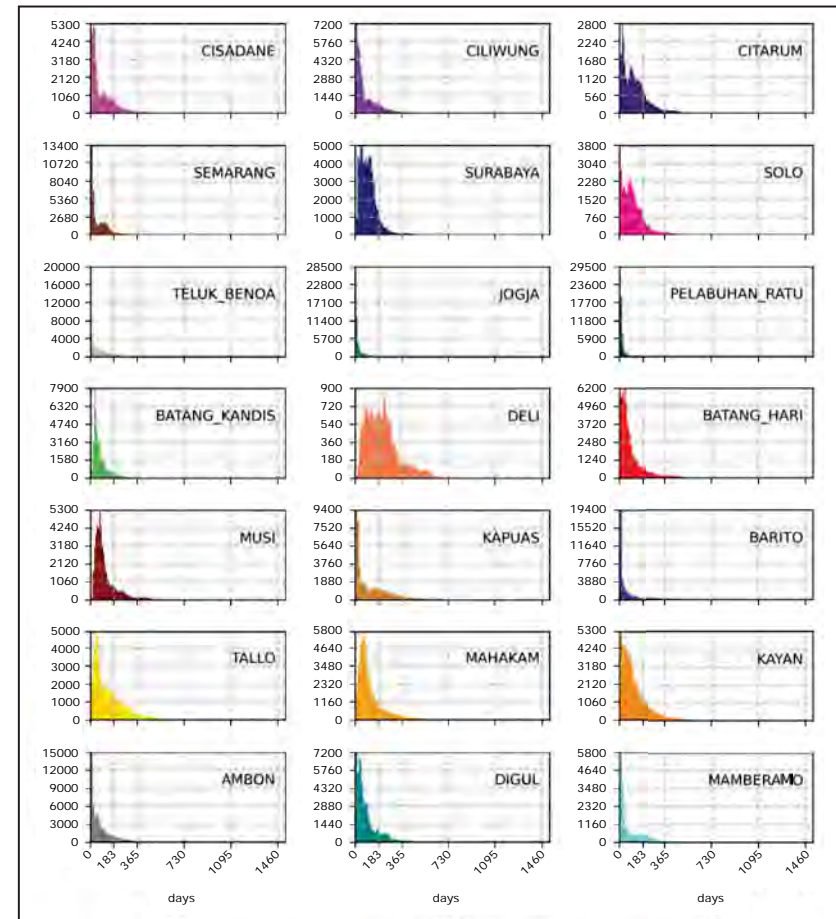


Figure 32: Histograms of stranding age (in days) by riverine source and for the whole regional domain

In figures 33 to 73, the upper left panel presents the number of stranded particles by month of stranding and by riverine source for the subzone; the lower left panel presents the localization of stranded particles for the subzone (the subzone is colored in dark grey); the right panel presents histograms of stranding age (in days) by riverine source and for the subzone.

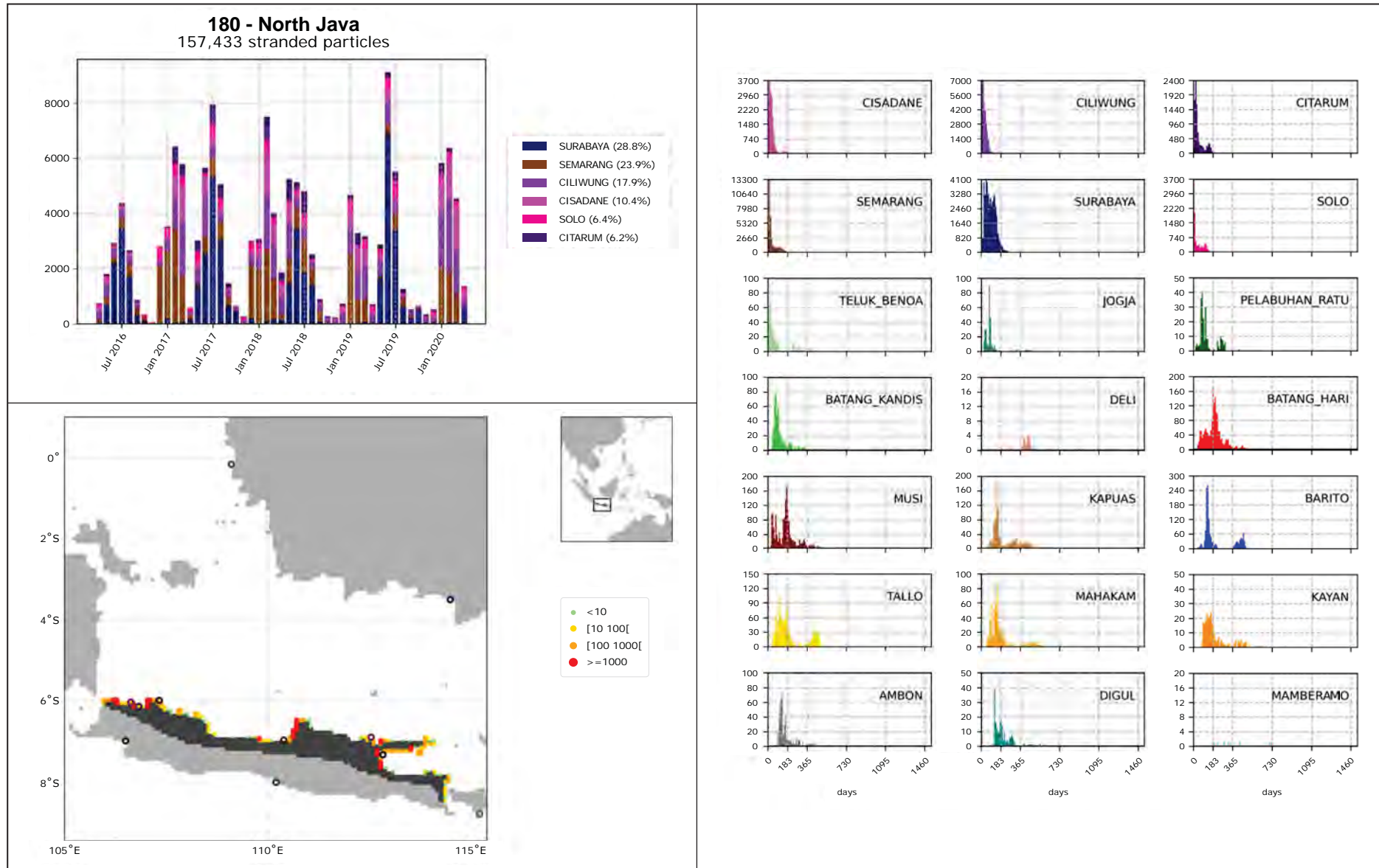


Figure 33: Atlas 180 - North Java

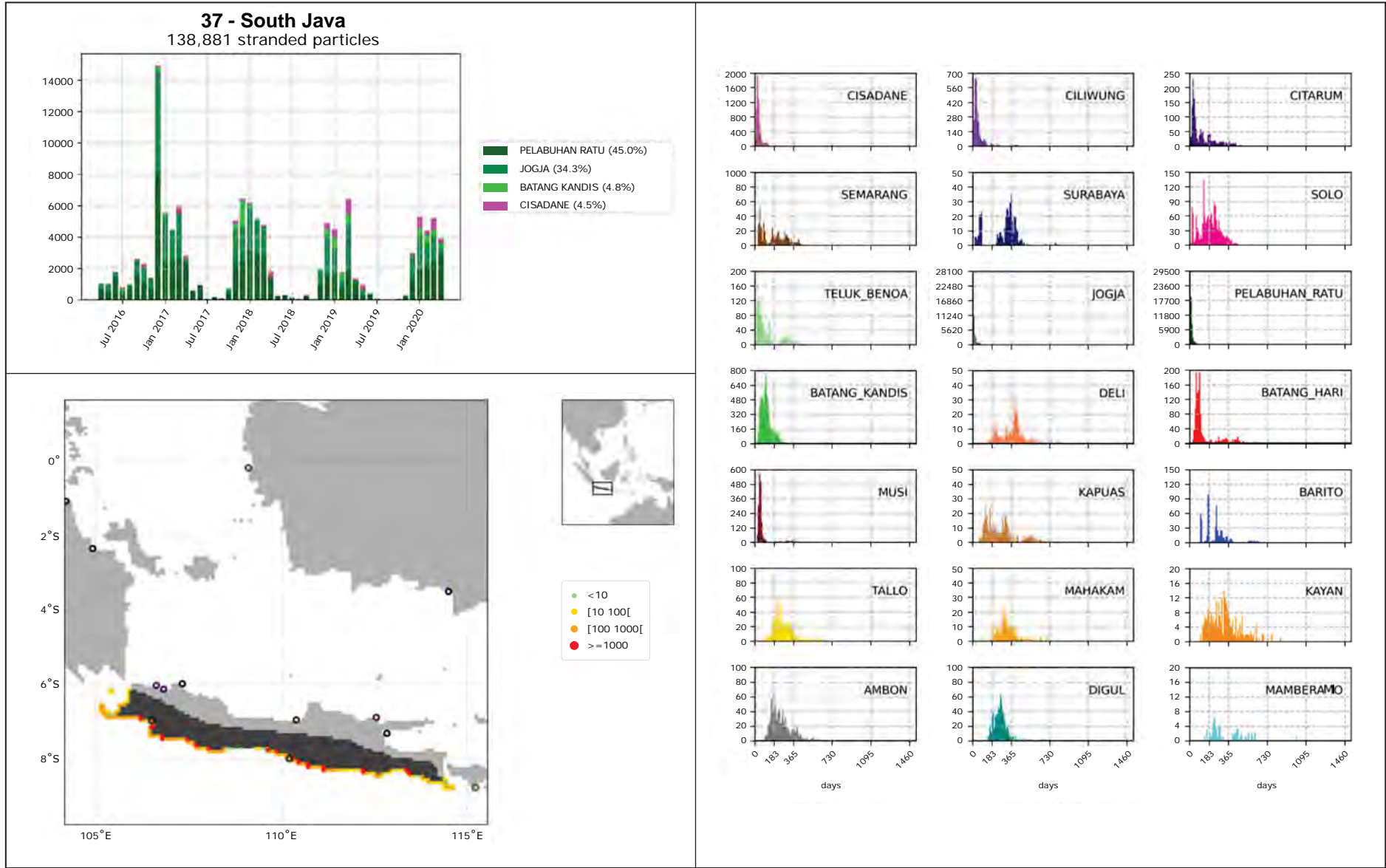


Figure 34: Atlas 37 - South Java

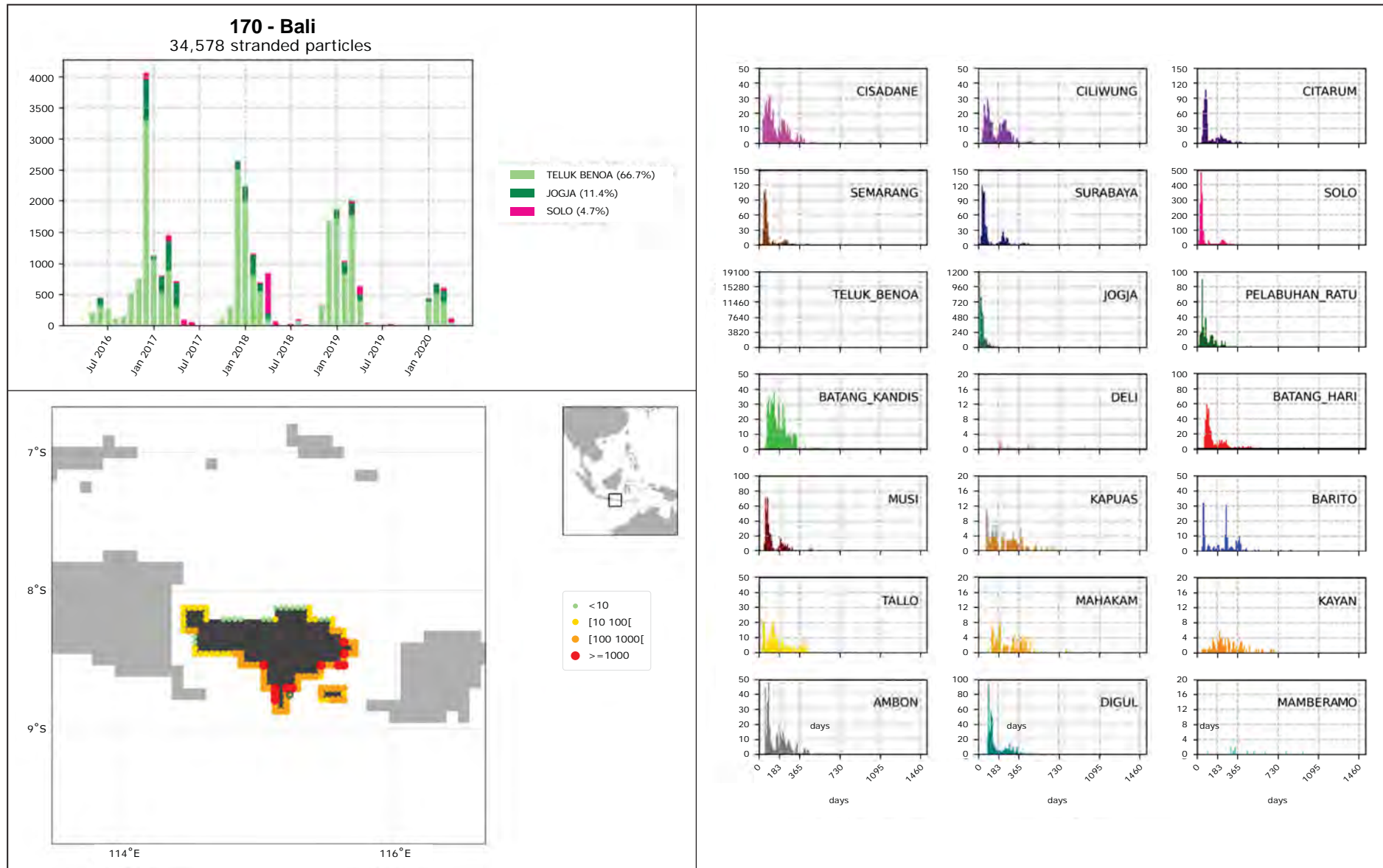


Figure 35: Atlas 170 - Bali

**22 - East Sulawesi on Molucca and Banda Sea**  
82,546 stranded particles

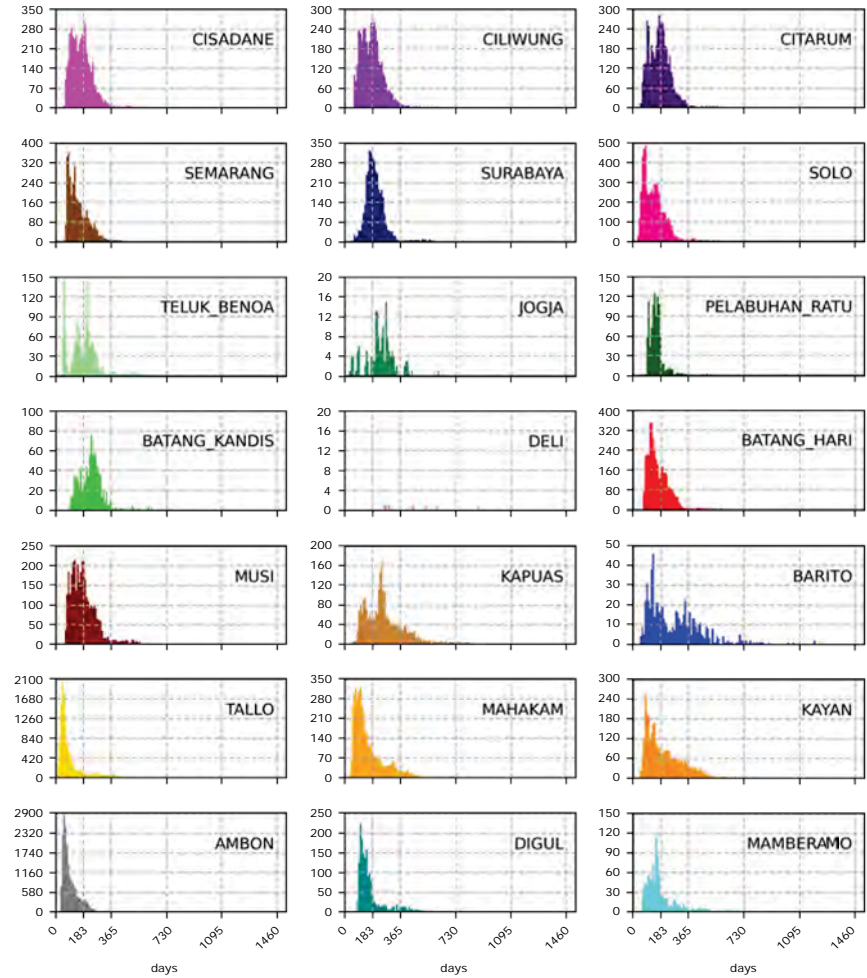
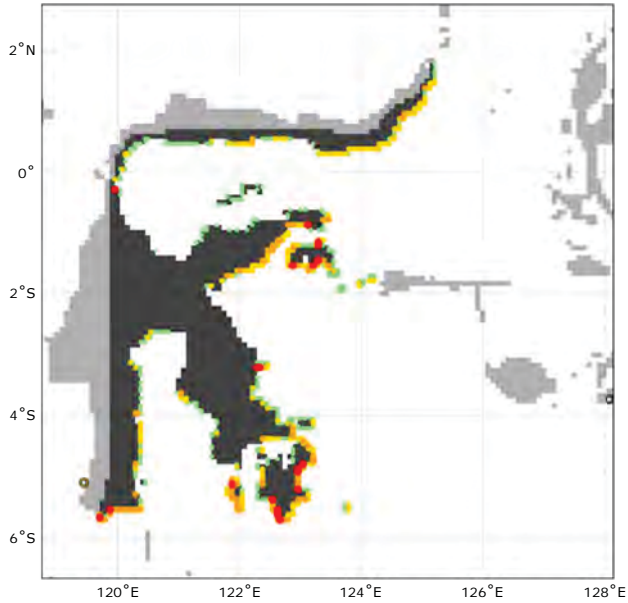
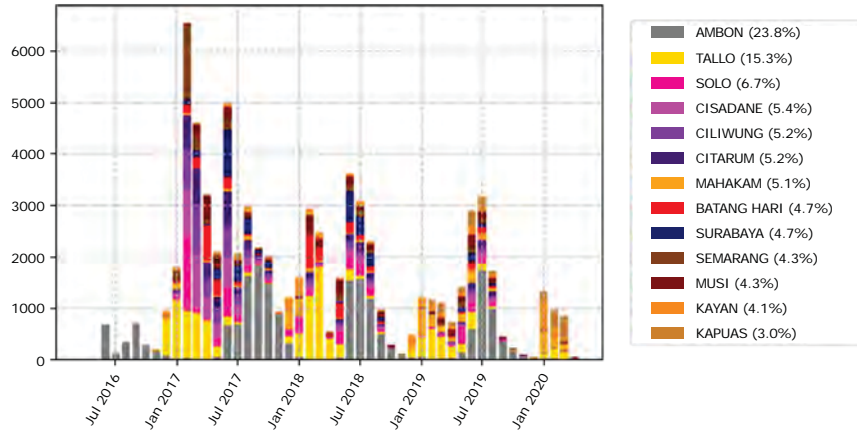


Figure 36: Atlas 22 - East Sulawesi on Molucca and Banda Sea

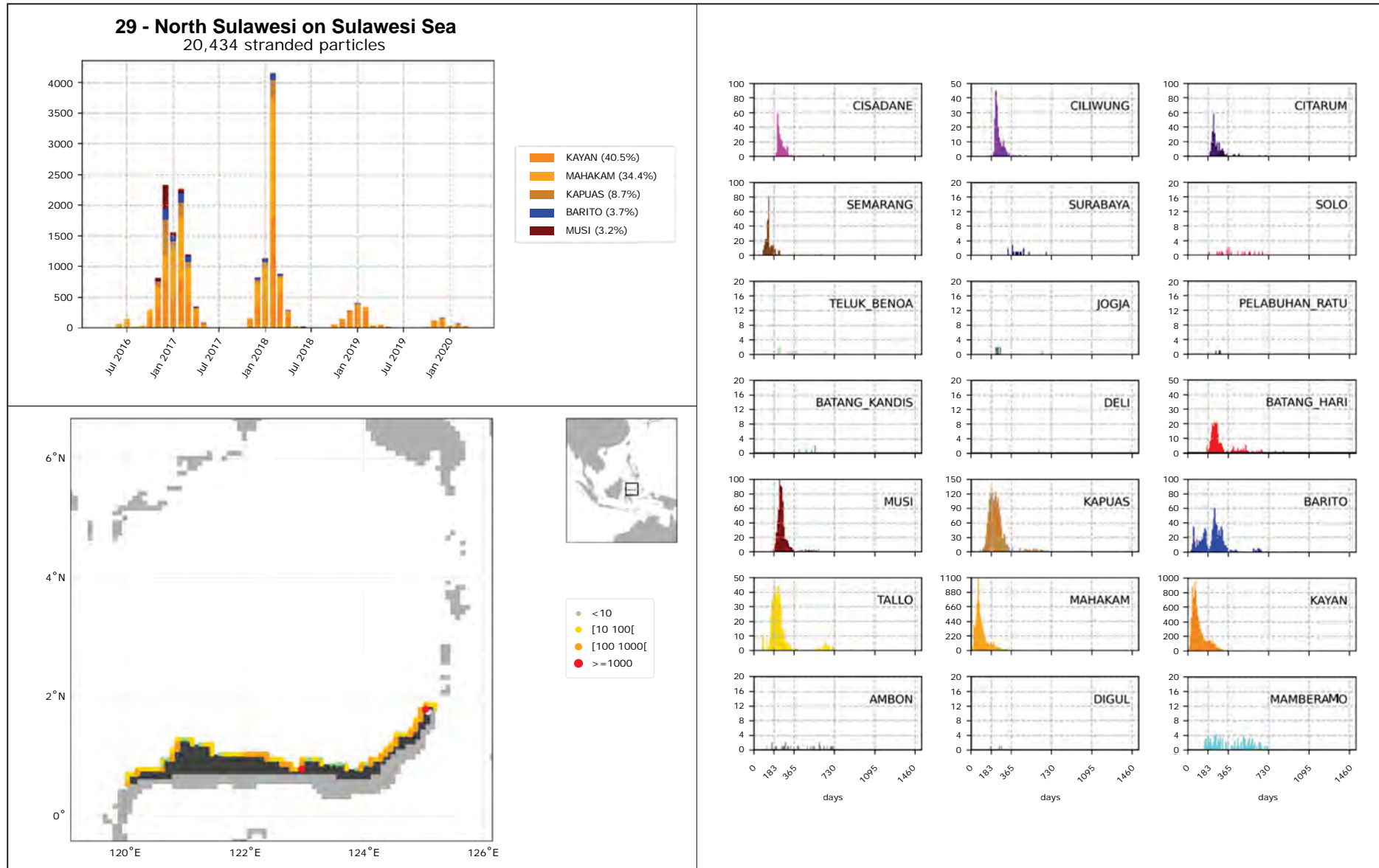


Figure 37: Atlas 29 - North Sulawesi on Sulawesi Sea

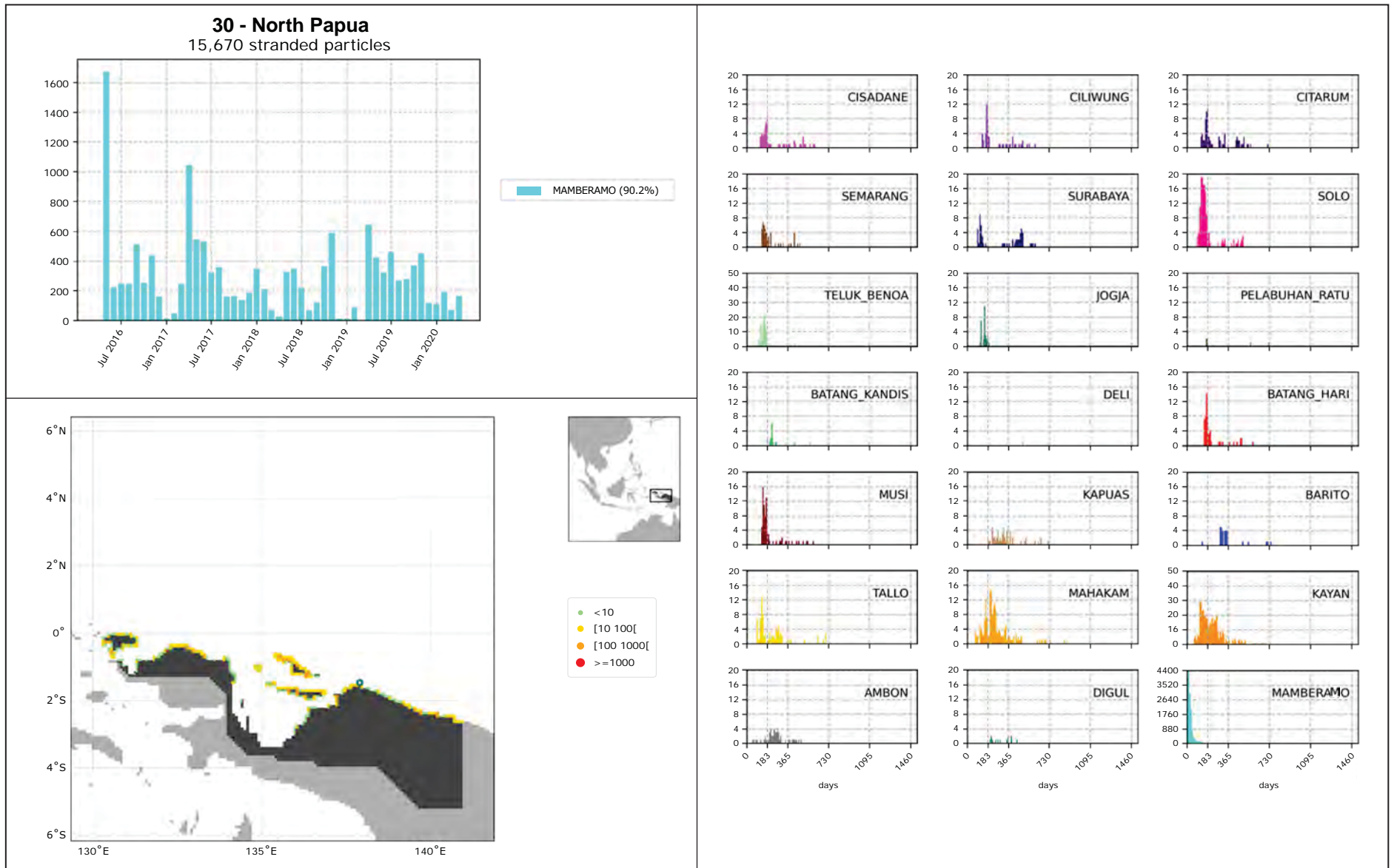


Figure 38: Atlas 30 - North Papua

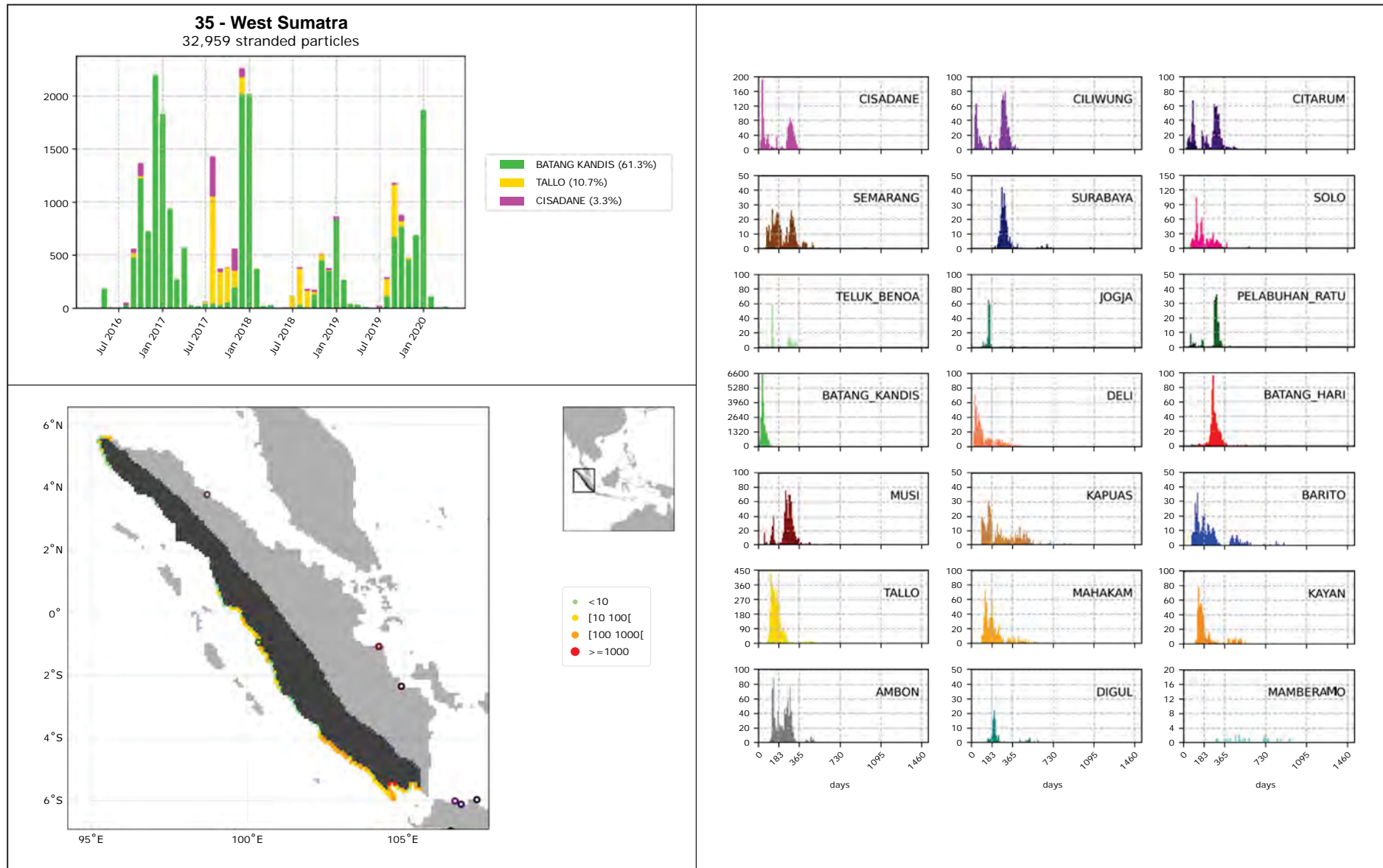


Figure 39: Atlas 35 - West Sumatra

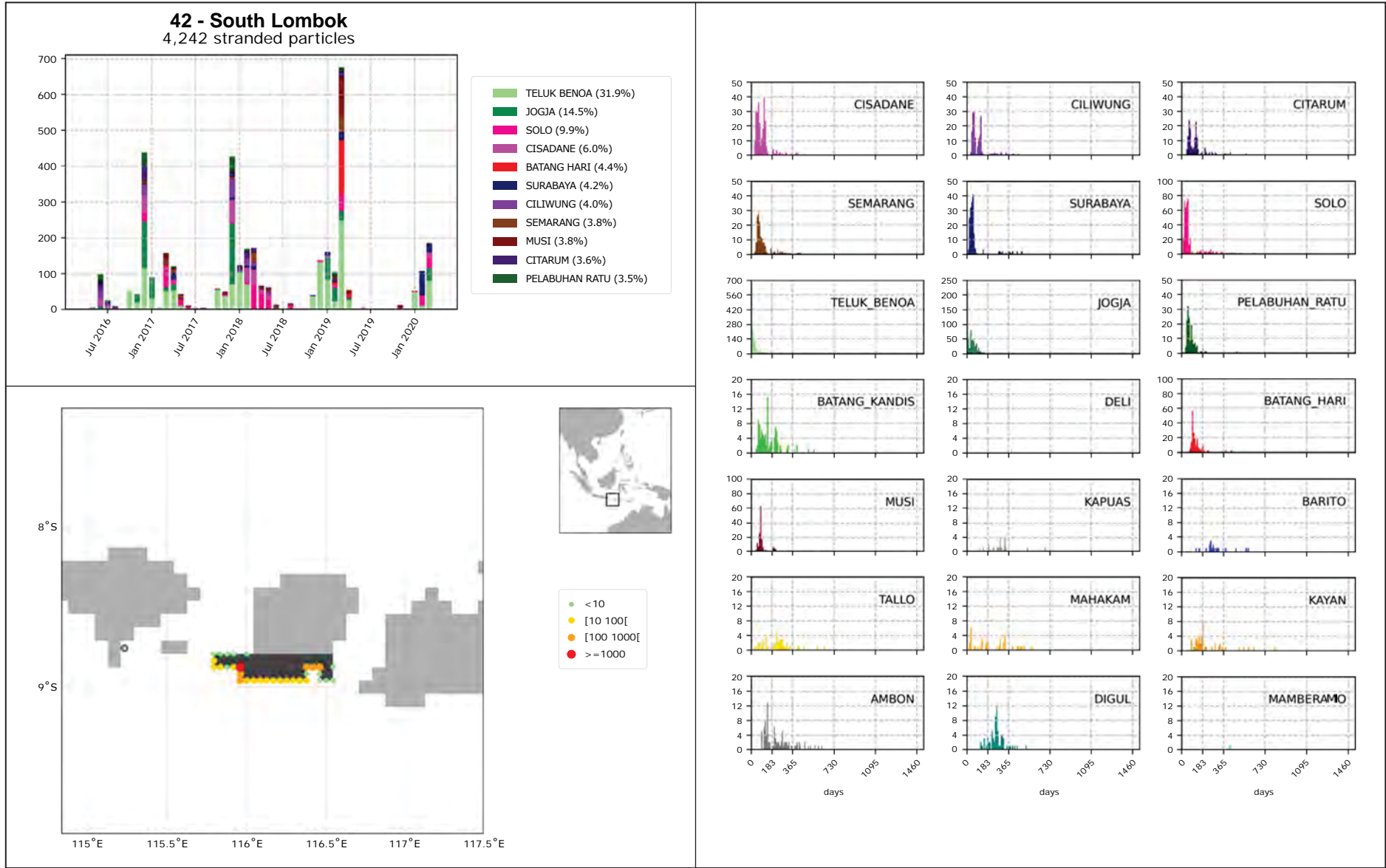


Figure 40: Atlas 42 - South Lombok

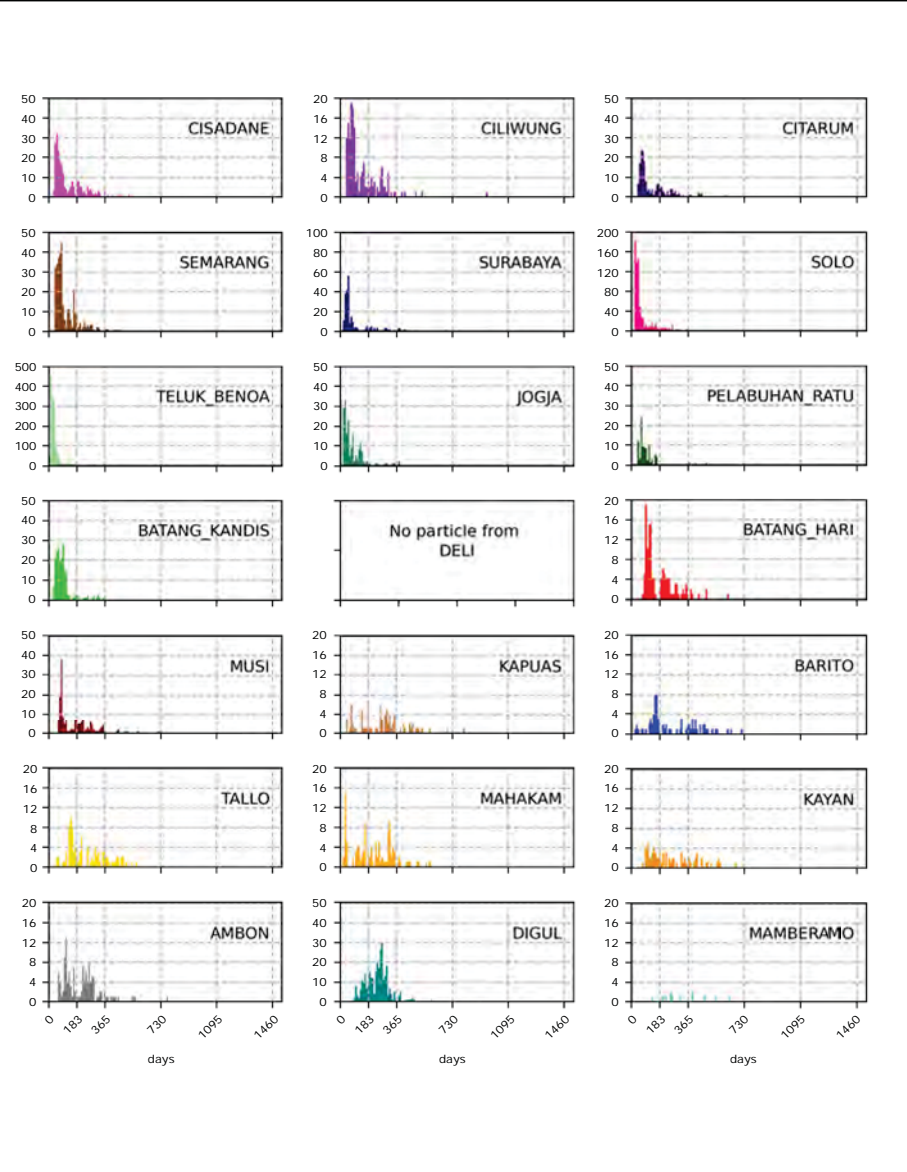
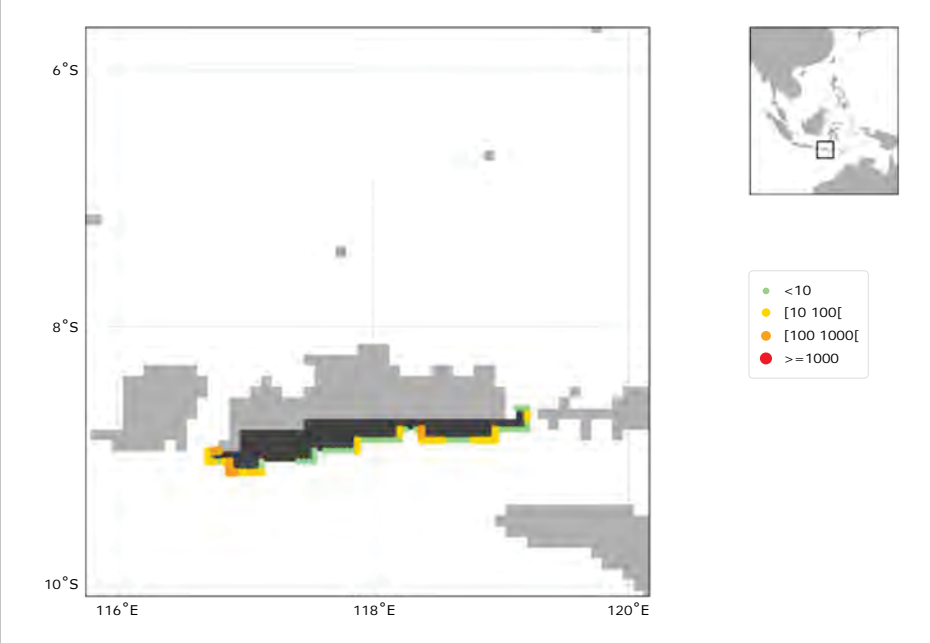
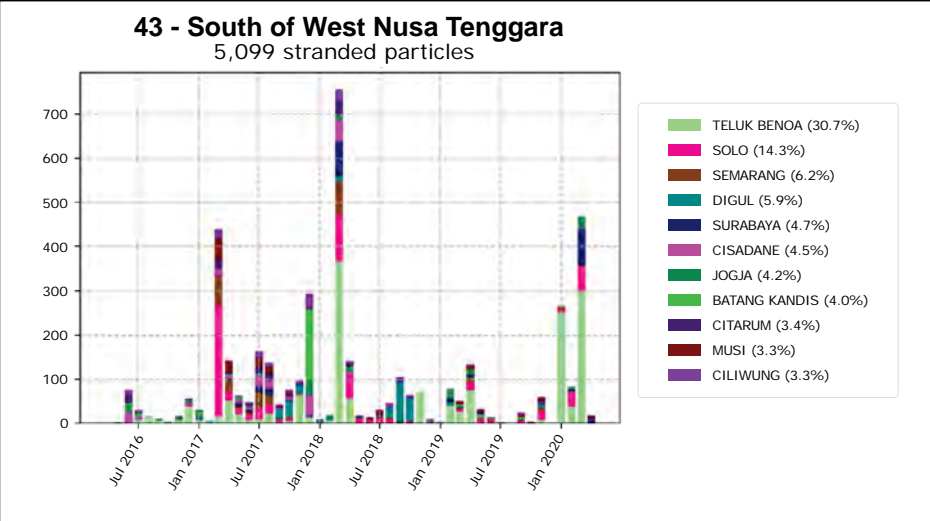


Figure 41: Atlas 43 - South of West Nusa Tenggara

**44 - South of East Nusa Tenggara**  
9,358 stranded particles

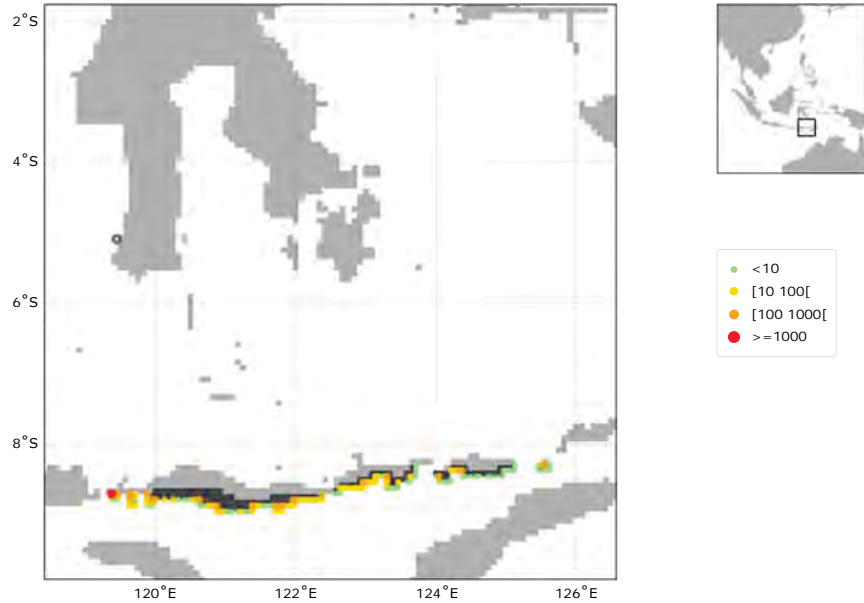
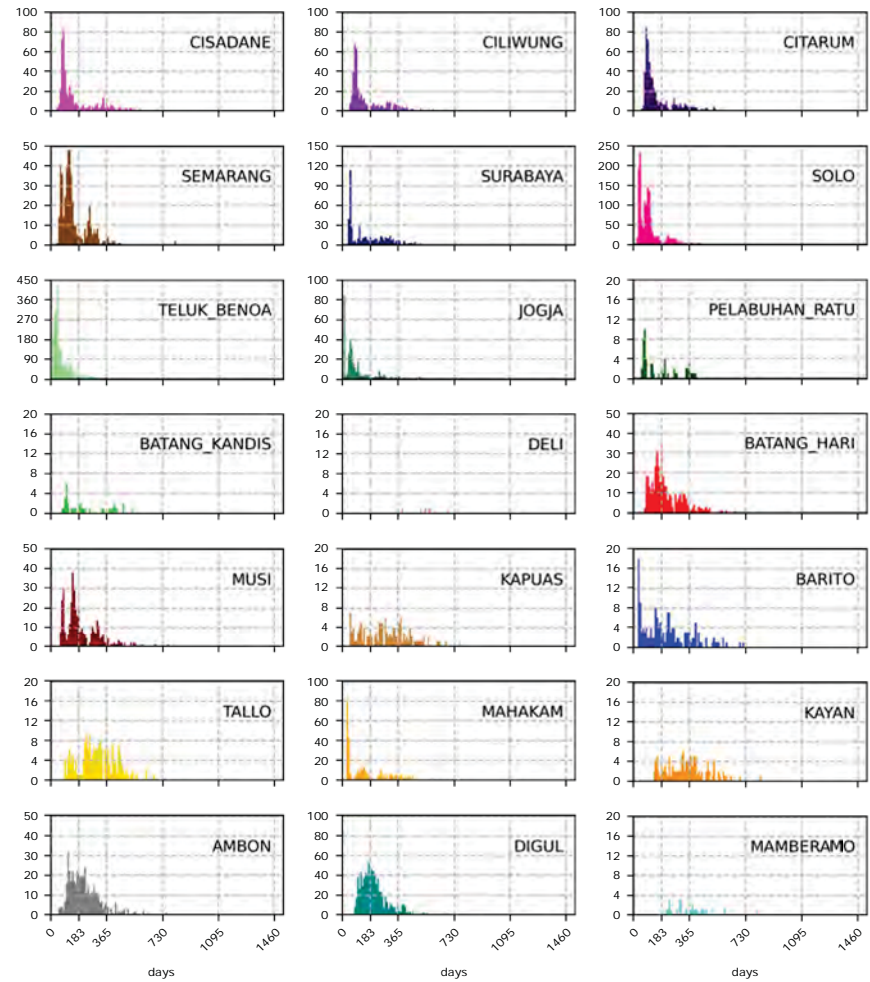
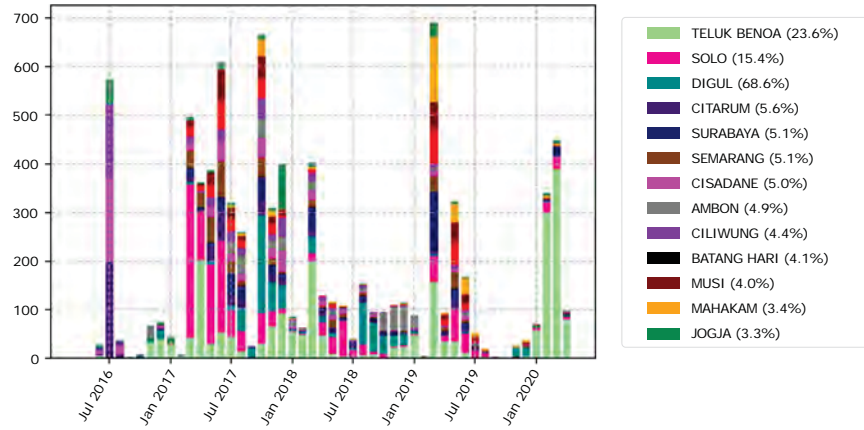


Figure 42: Atlas 44 - South of East Nusa Tenggara

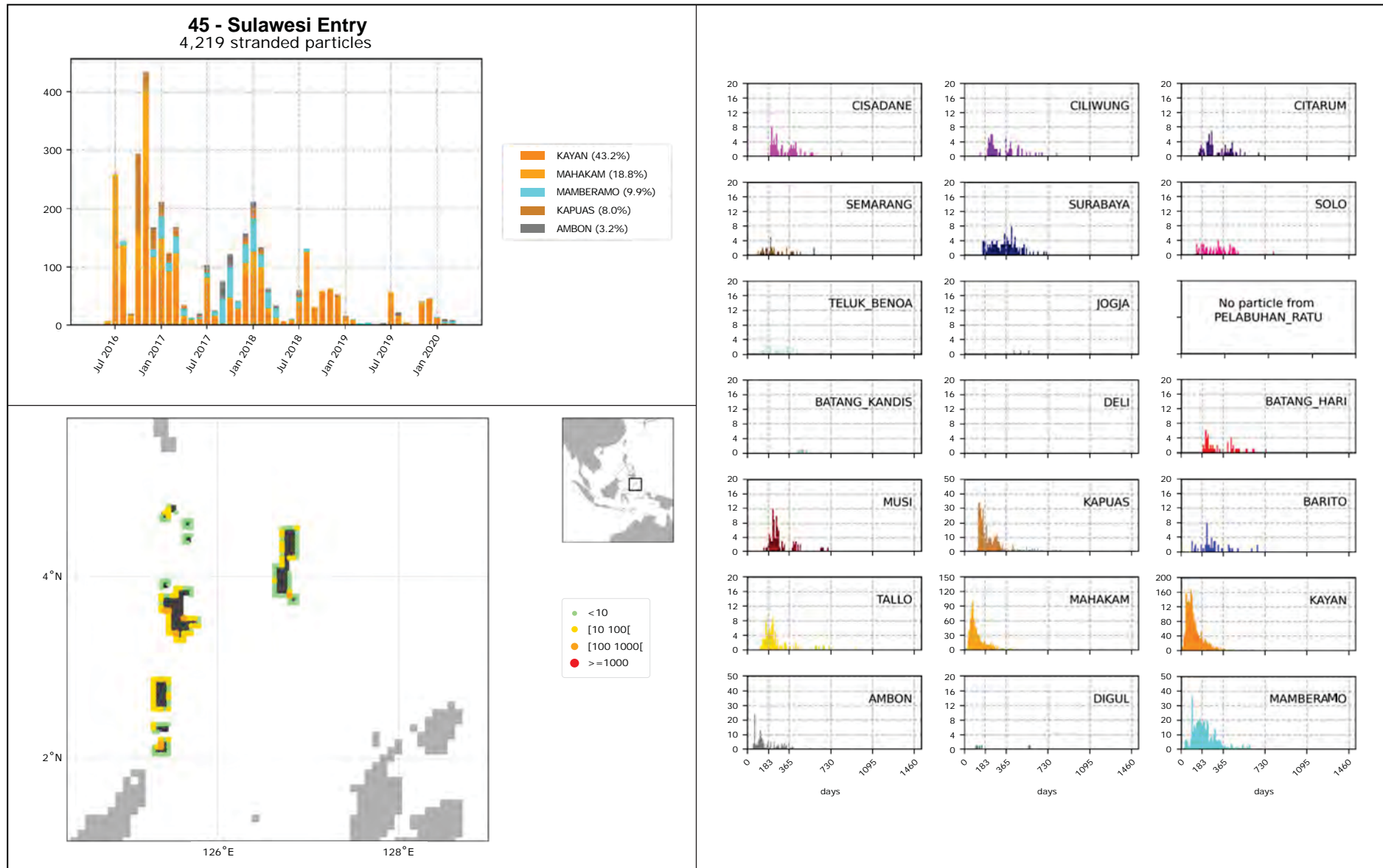


Figure 43: Atlas 45 - Sulawesi Entry

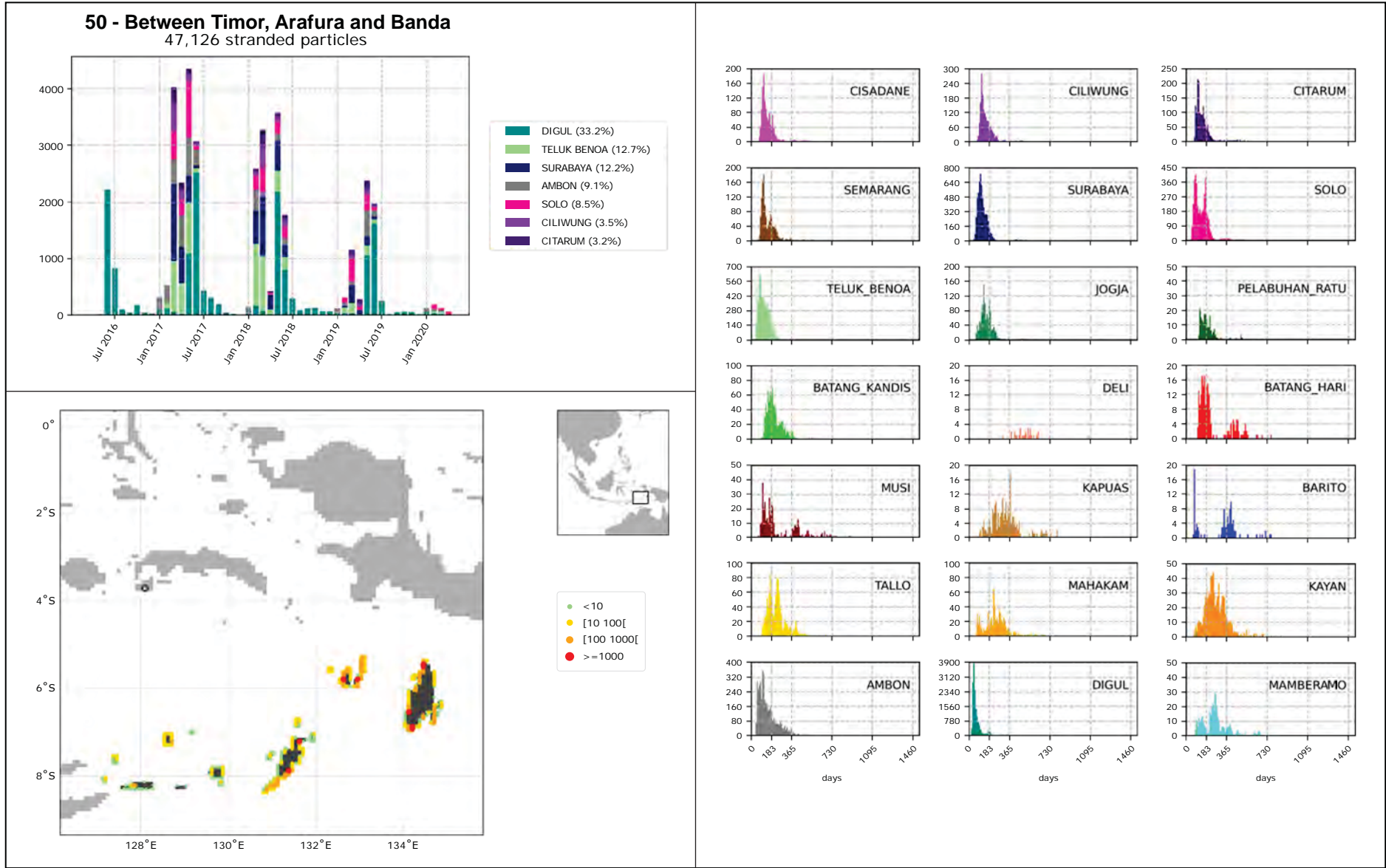


Figure 44: Atlas 50 - Between Timor, Arafura and Banda

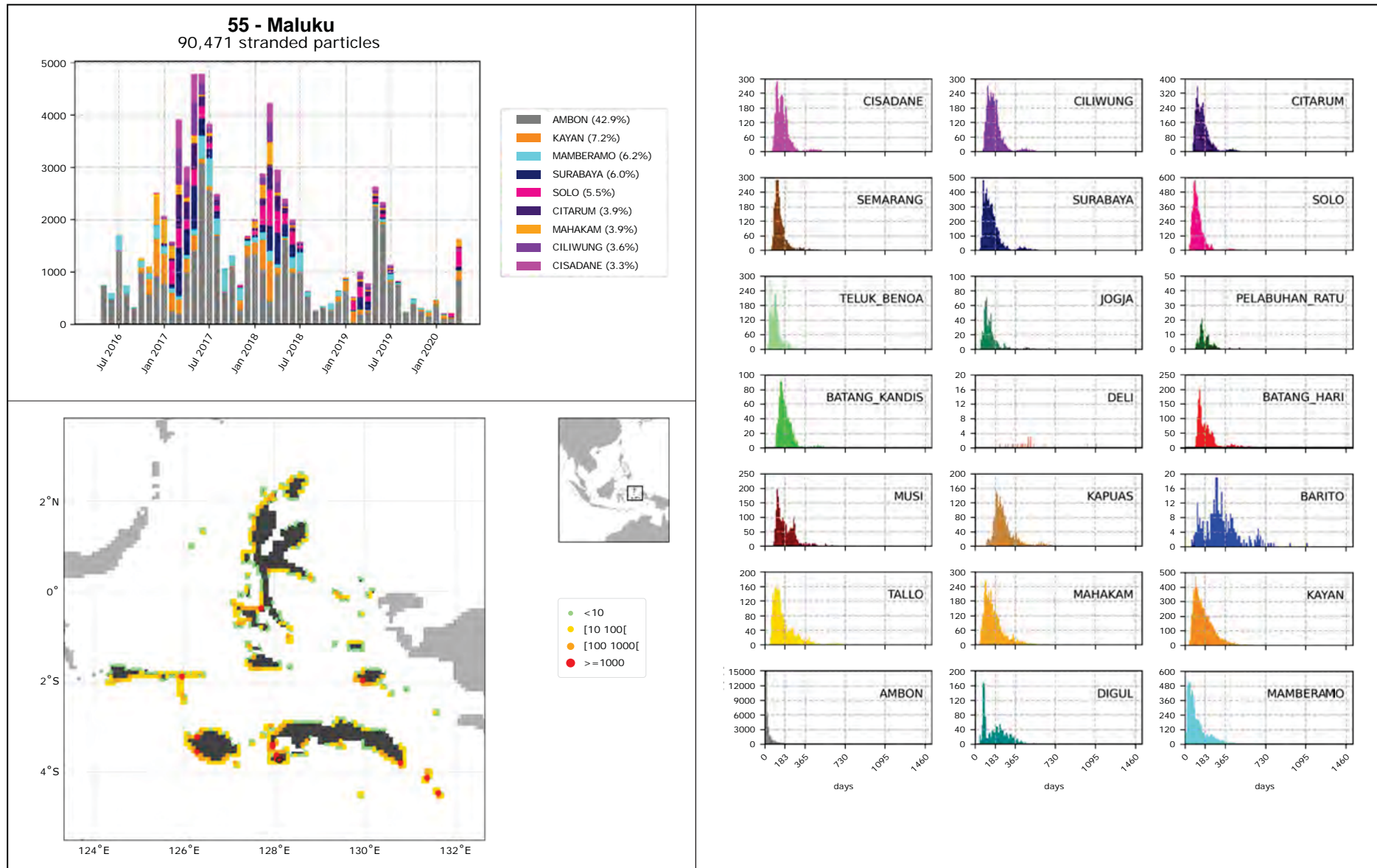


Figure 45: Atlas 55 - Maluku

**110 - Greater Sunda and Kangean Isles**  
8,012 stranded particles

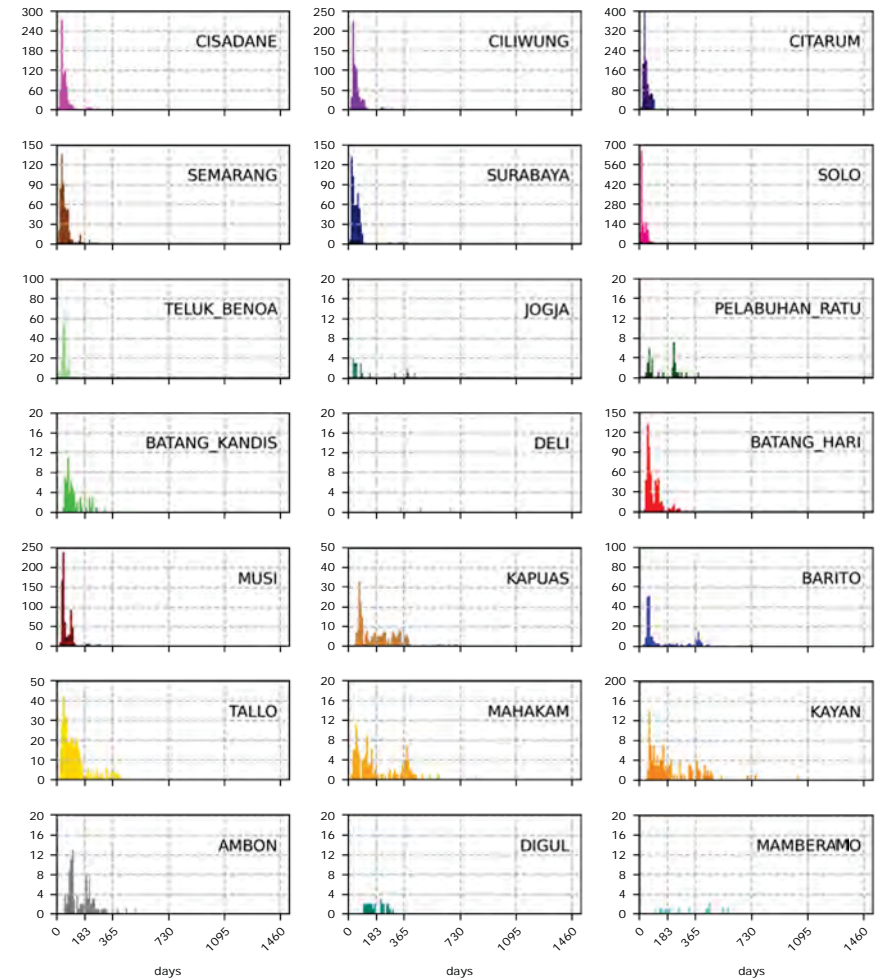
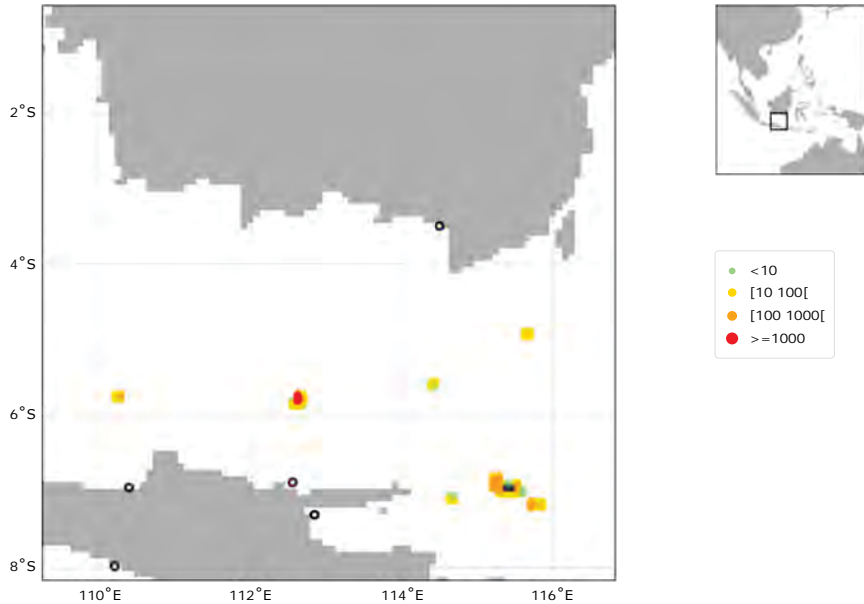
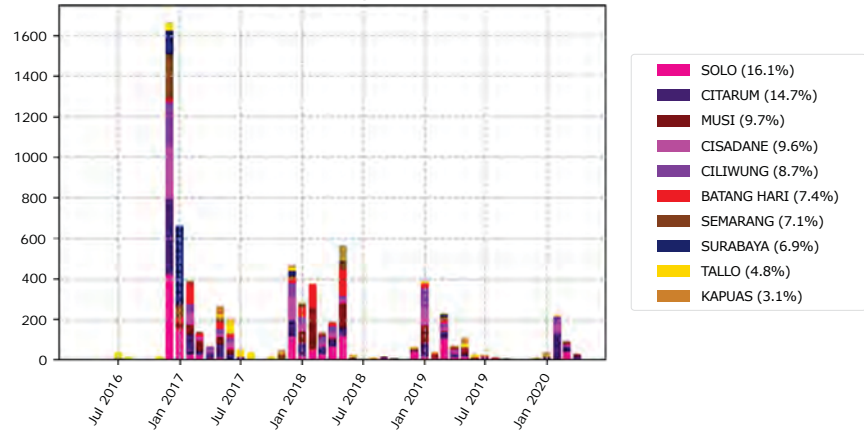


Figure 46: Atlas I10 - Greater Sunda and Kangean Isles

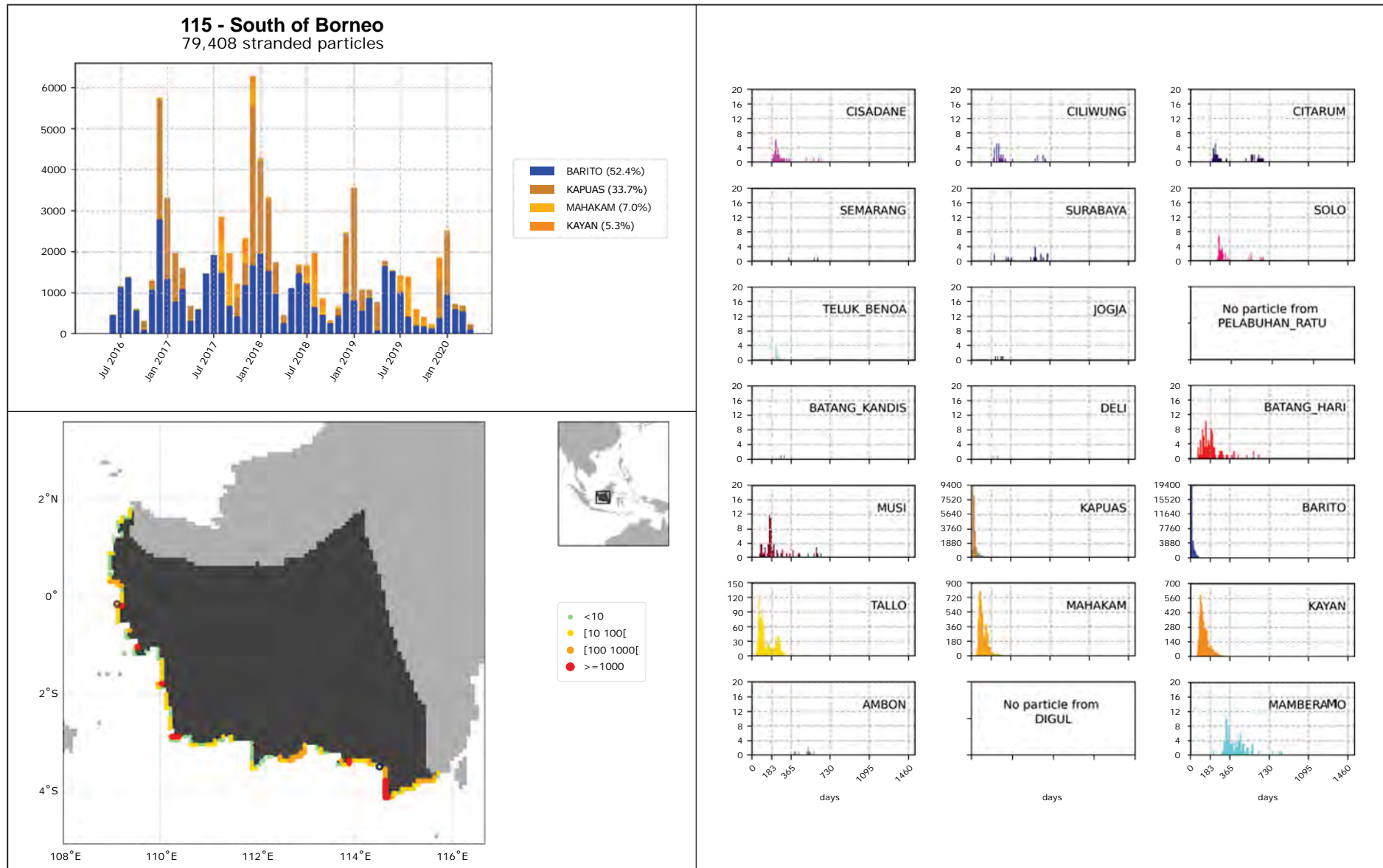


Figure 47: Atlas 115 - South Borneo

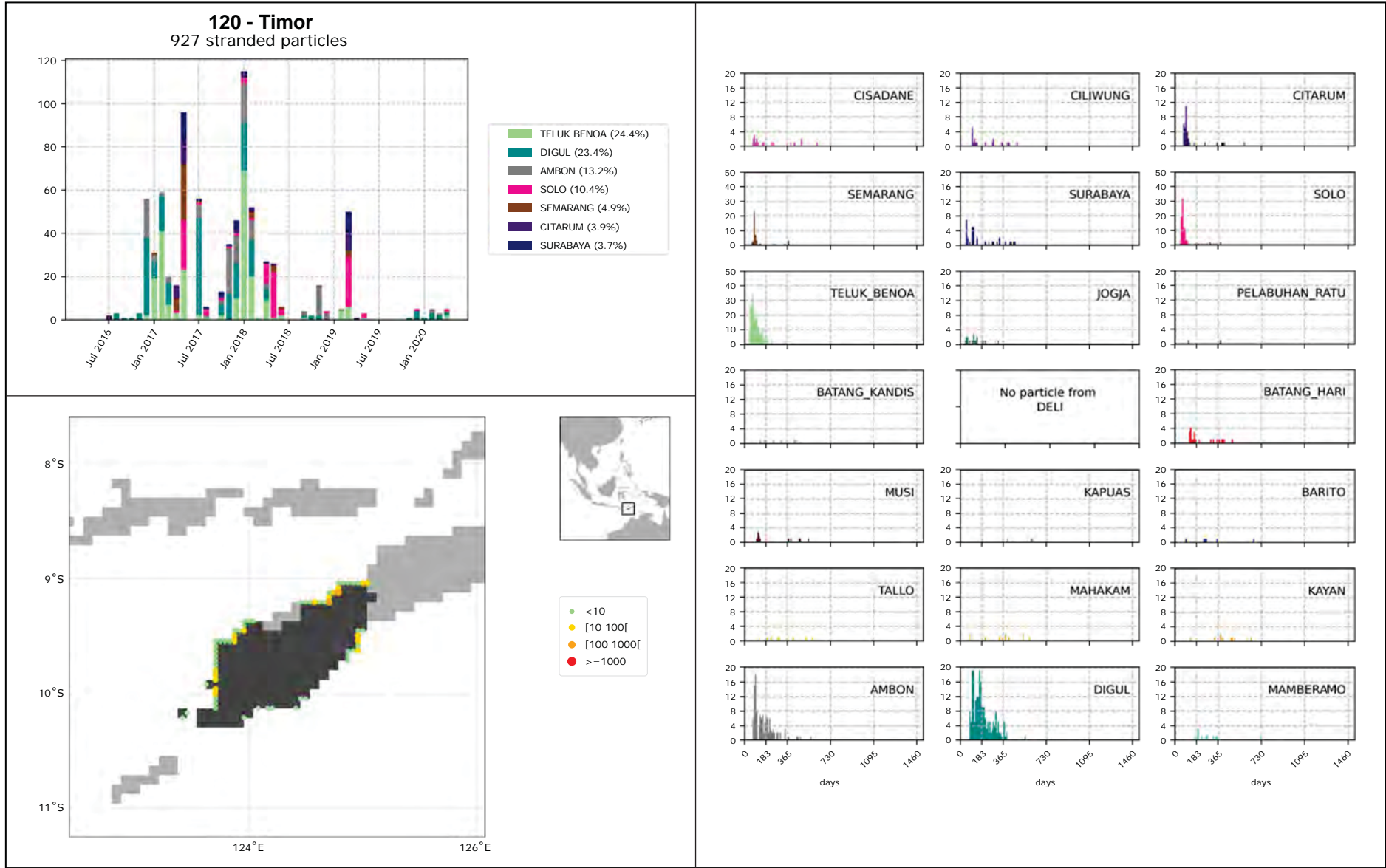


Figure 48: Atlas I20 - Timor

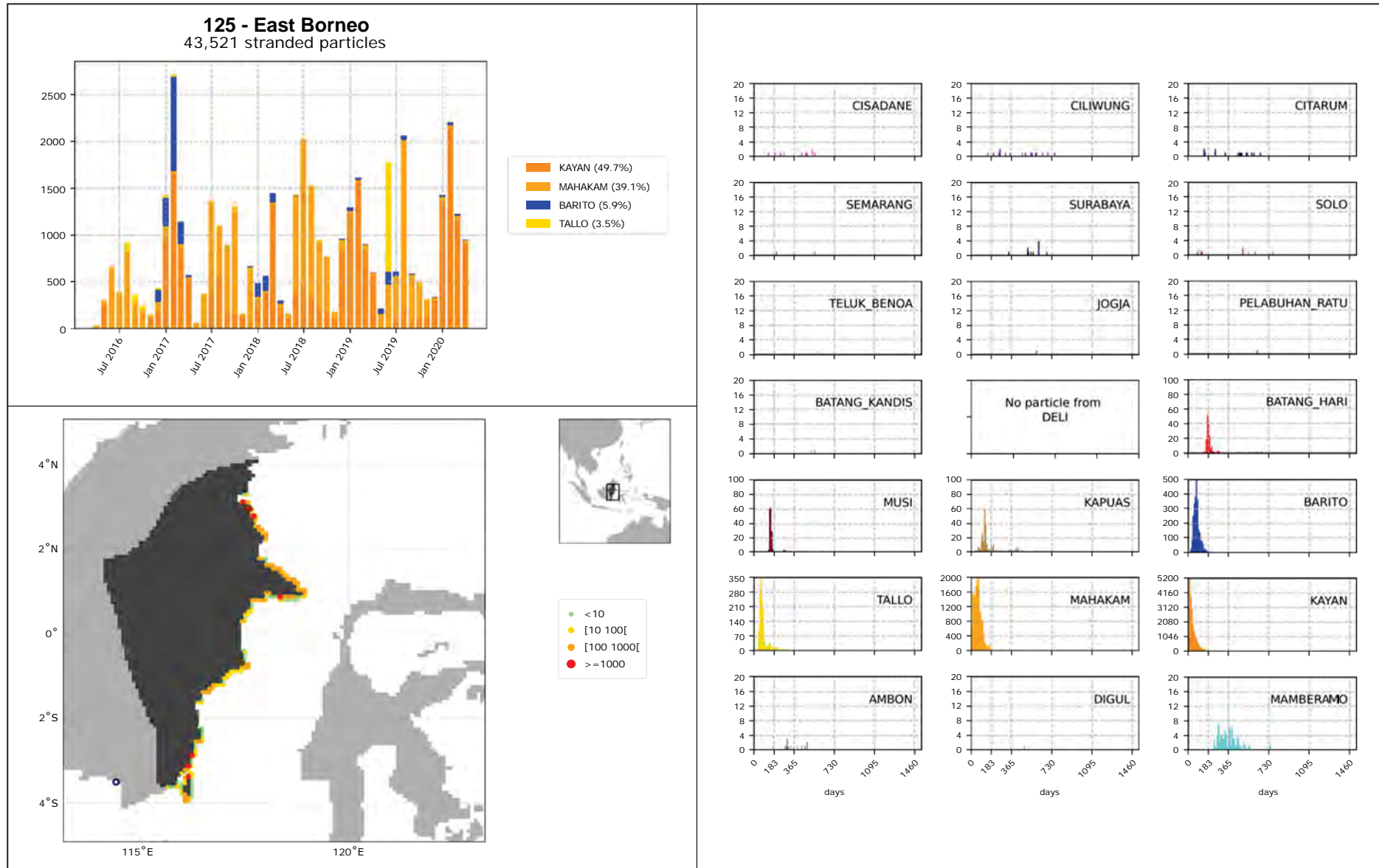


Figure 49: Atlas I25 - East Borneo

**130 - Rote Savu and Sumba Isles**  
8,624 stranded particles

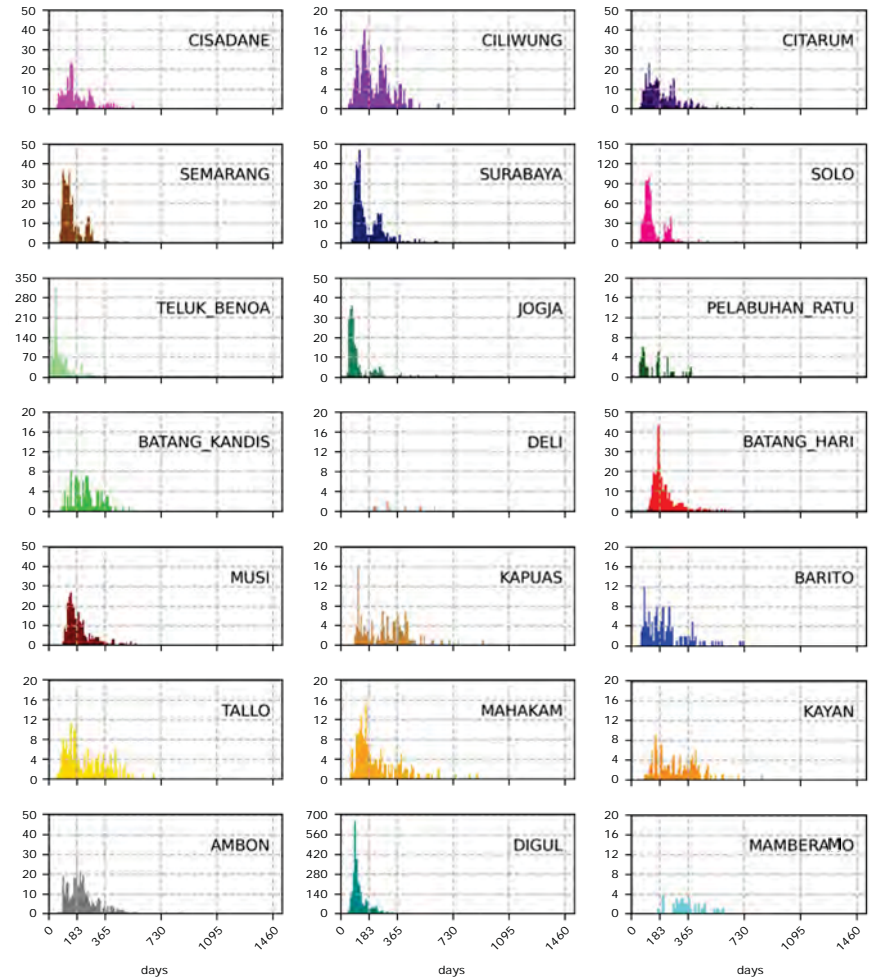
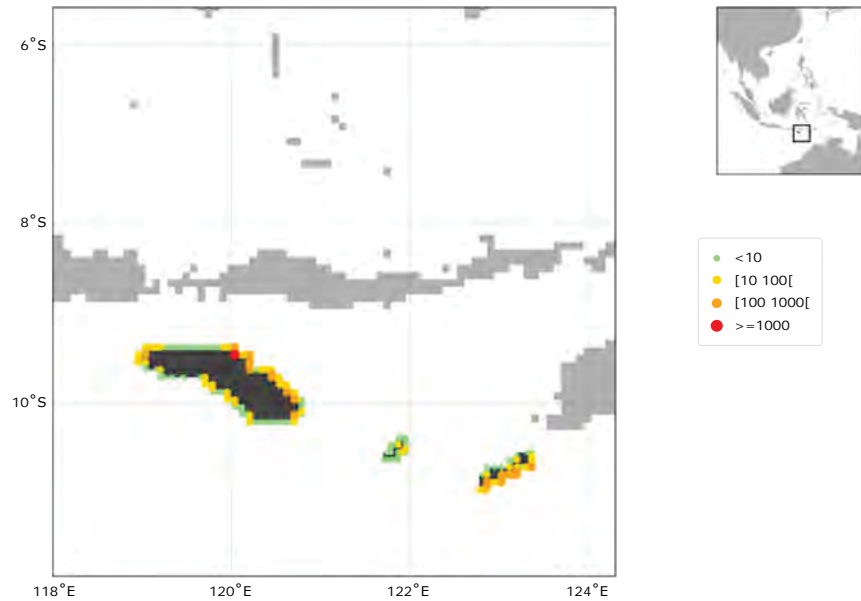
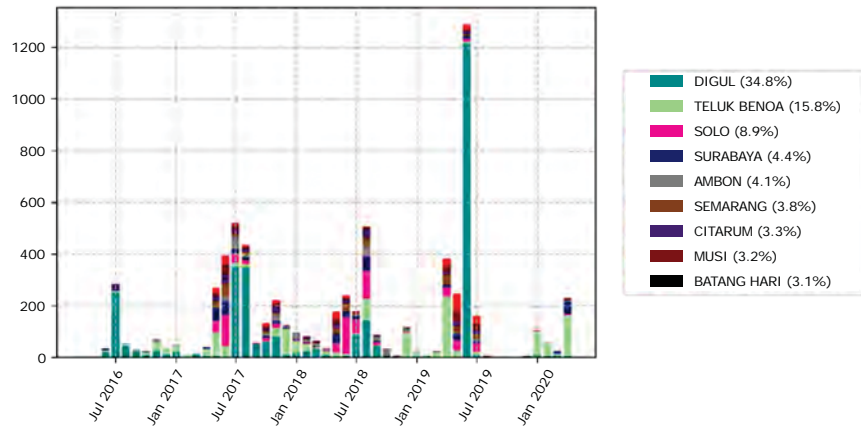


Figure 50: Atlas 130 - Rote Savu and Sumba Isles

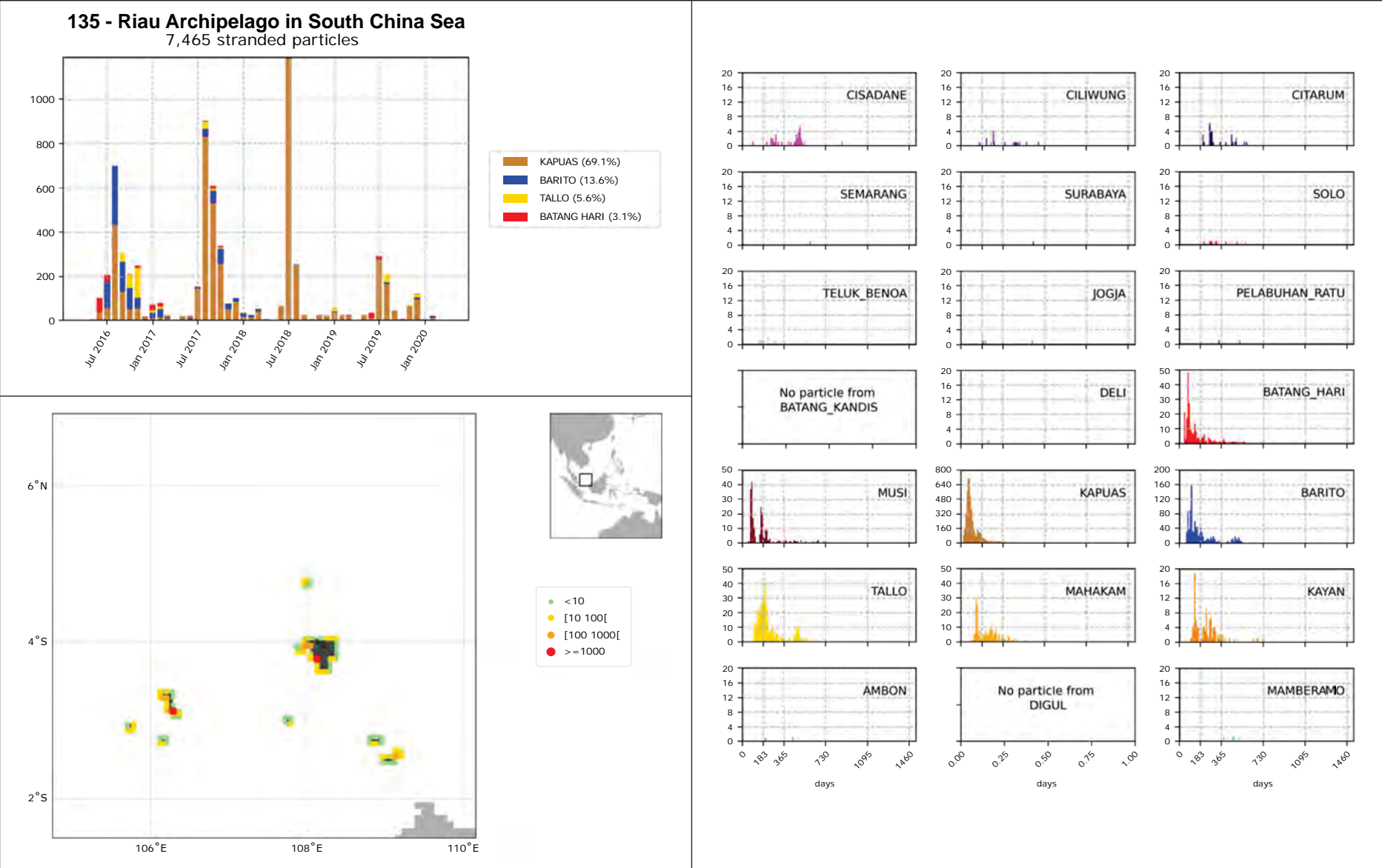


Figure 51: Atlas 135 - Riau Archipelago in South China Sea

**138 - Riau Archipelago in Malacca Strait Entry**  
37,433 stranded particles

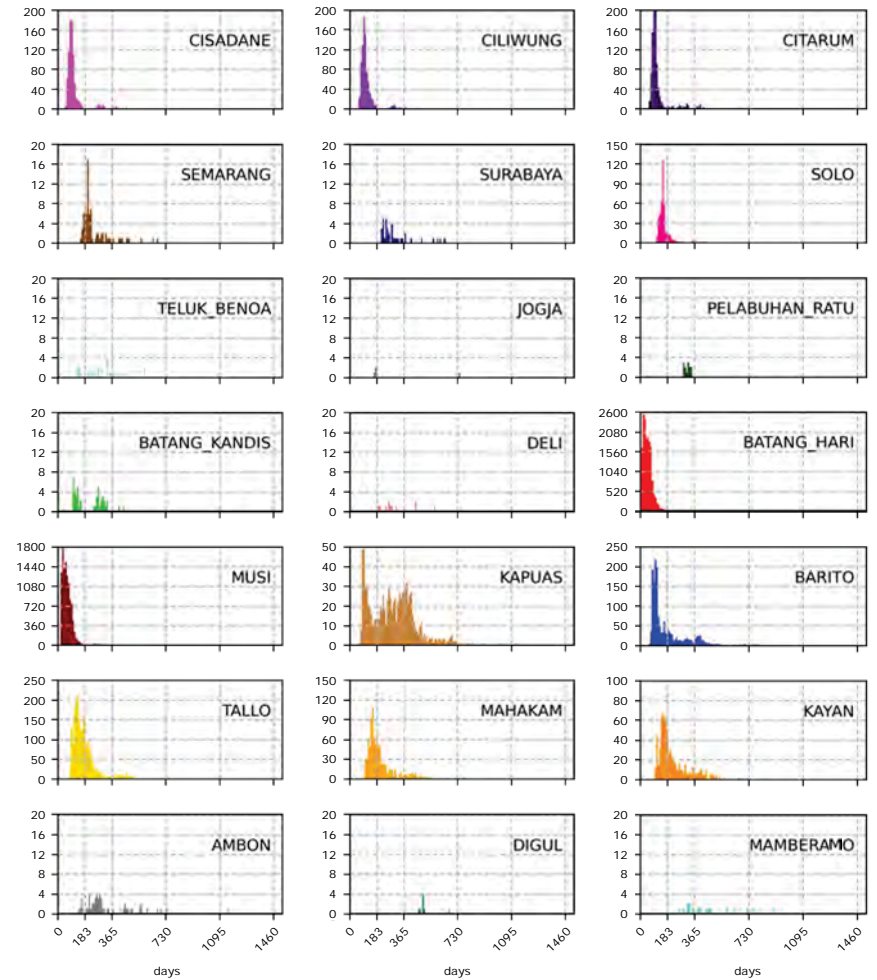
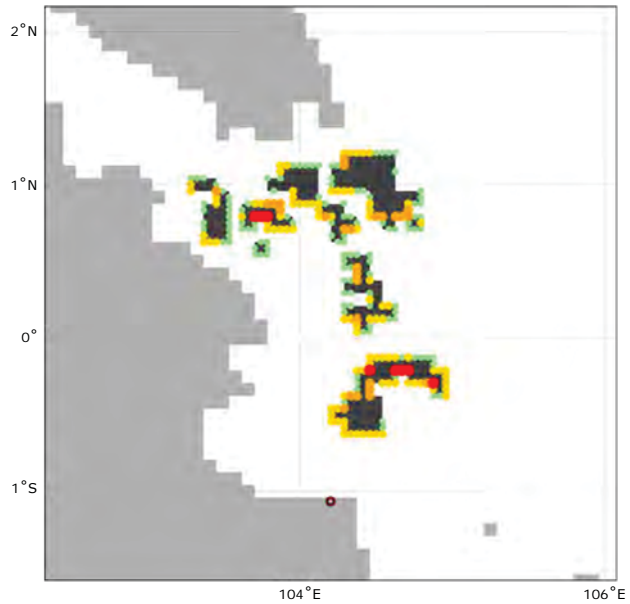
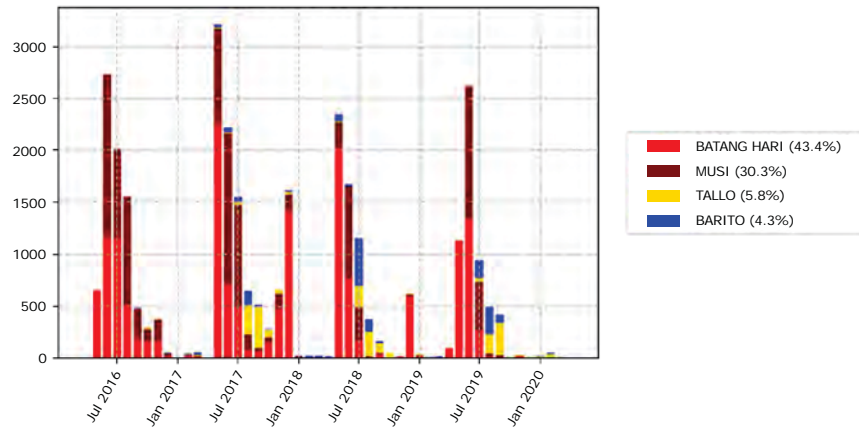


Figure 52: Atlas 138 - Riau Archipelago in Malacca Strait Entry

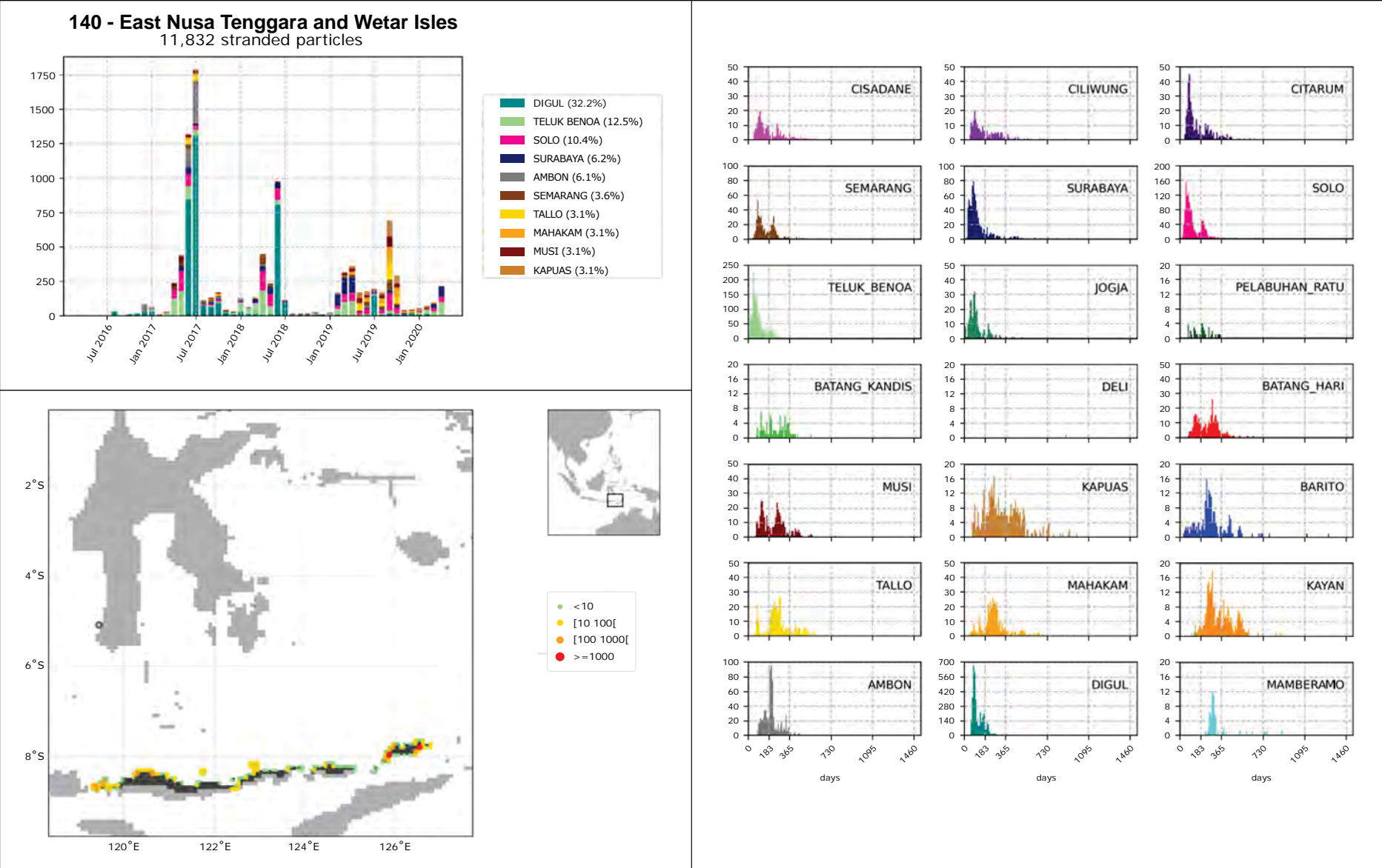


Figure 53: Atlas 140 - East Nusa Tenggara and Wetar Isles

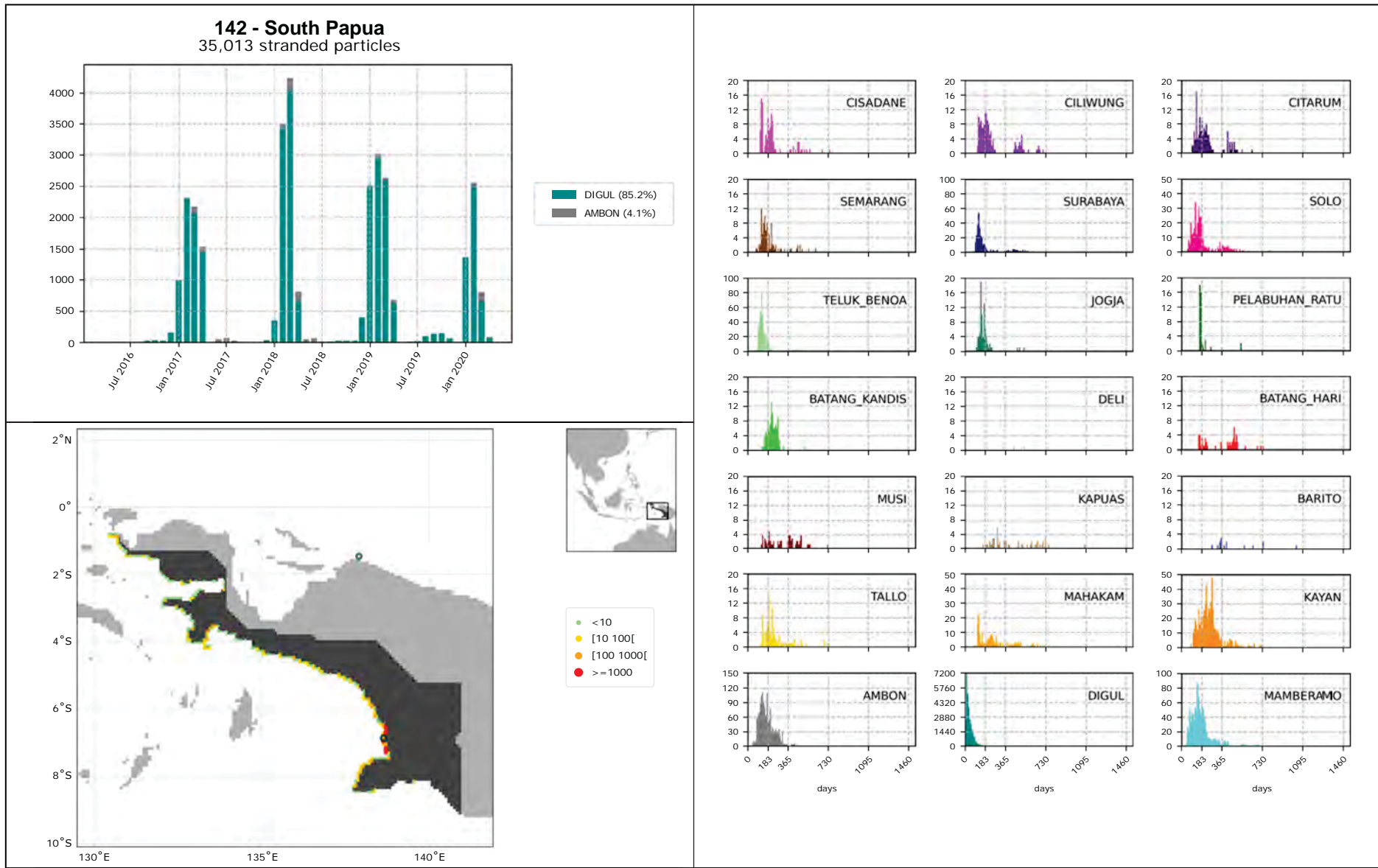


Figure 54: Atlas 142 - South Papua

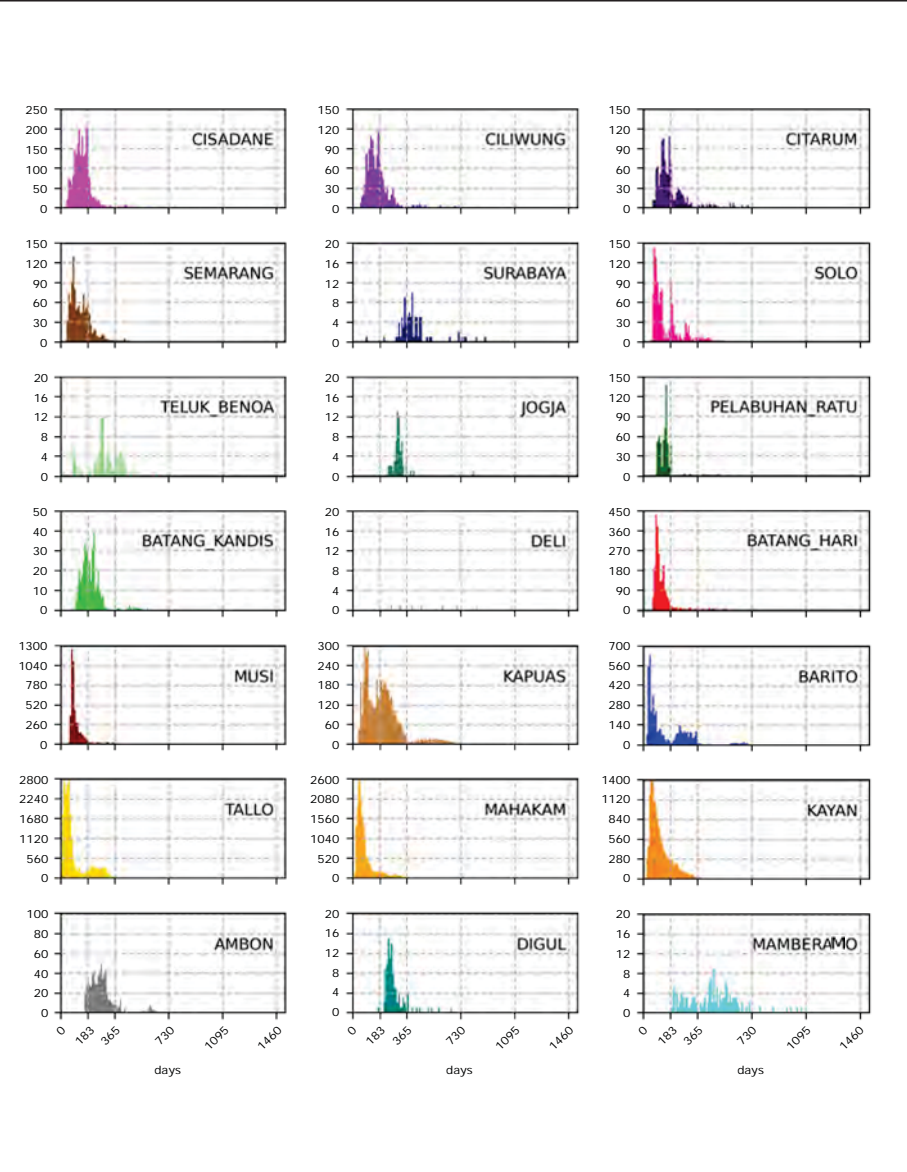
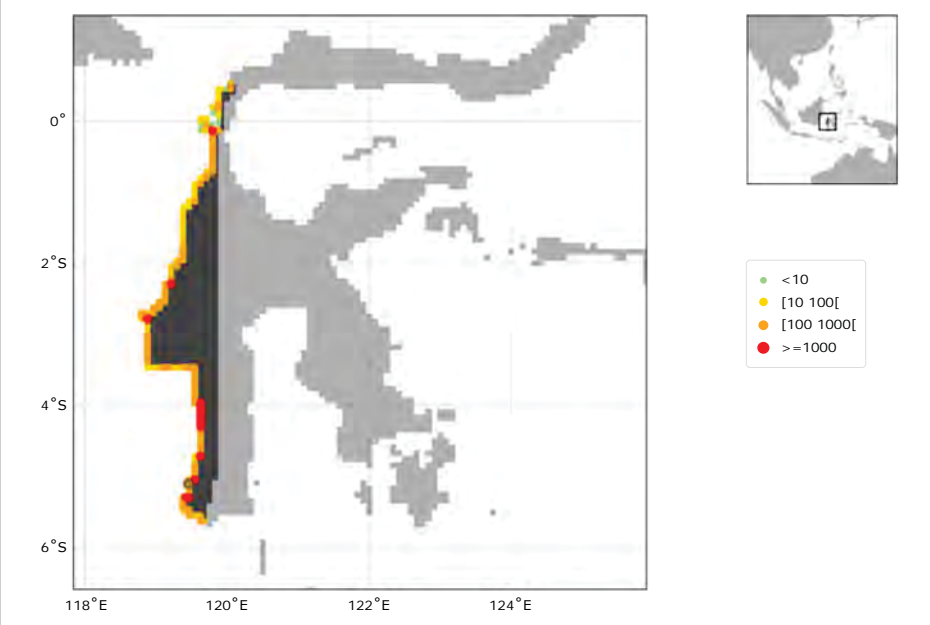
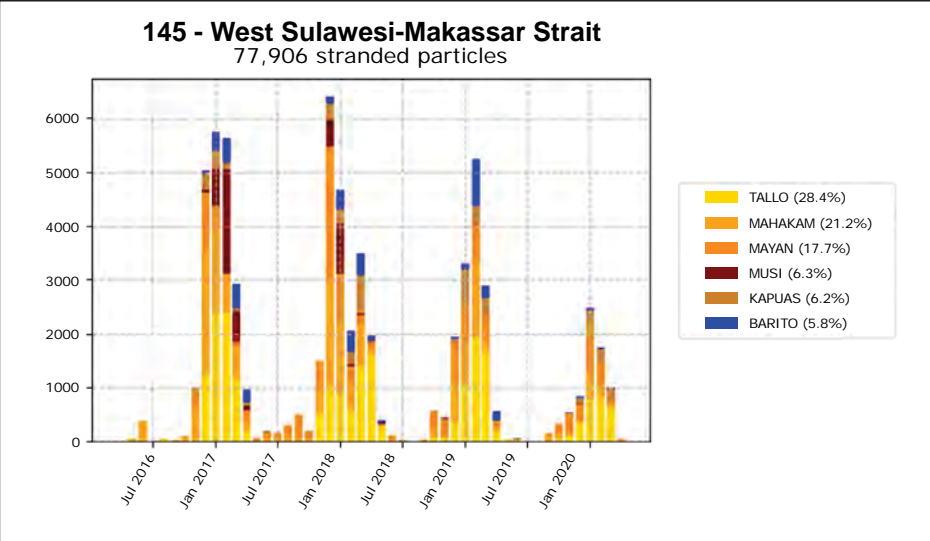


Figure 55: Atlas 145 - West Sulawesi-Makassar Strait

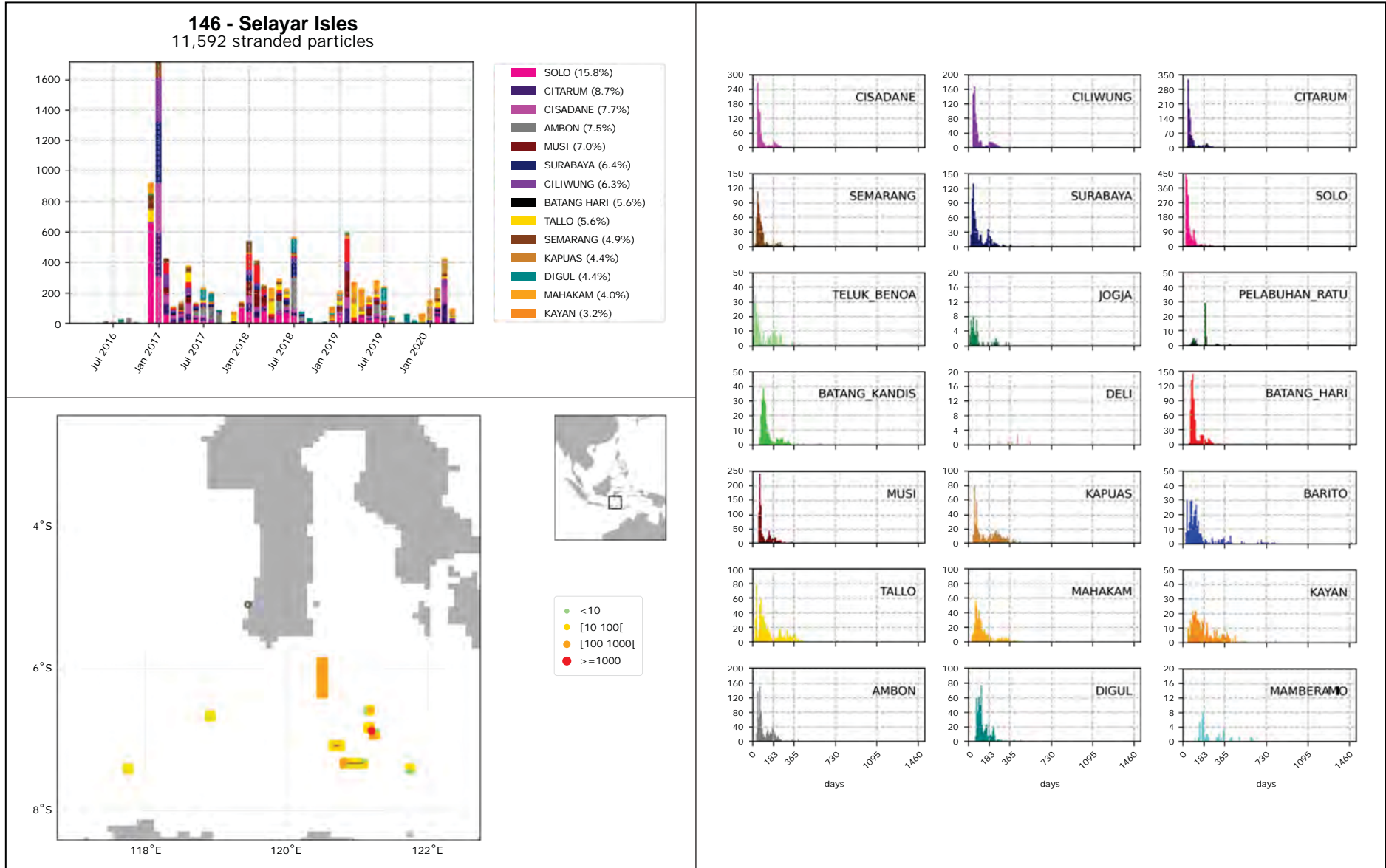


Figure 56: Atlas I46 - Selayar Isles

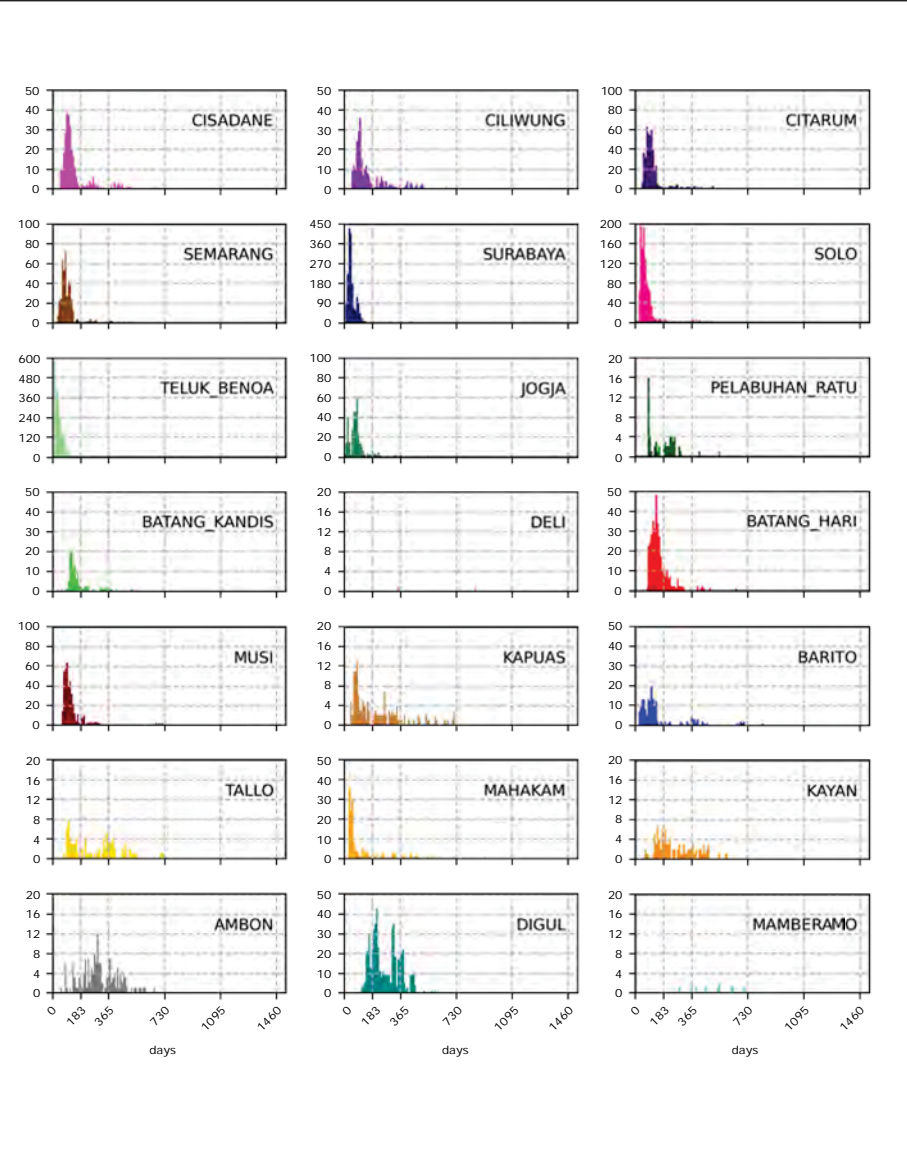
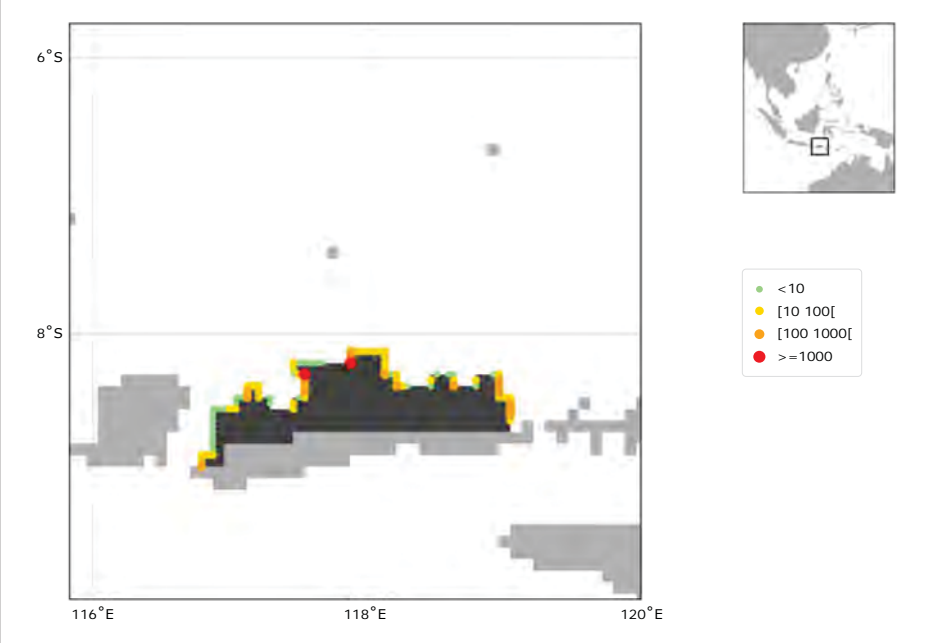
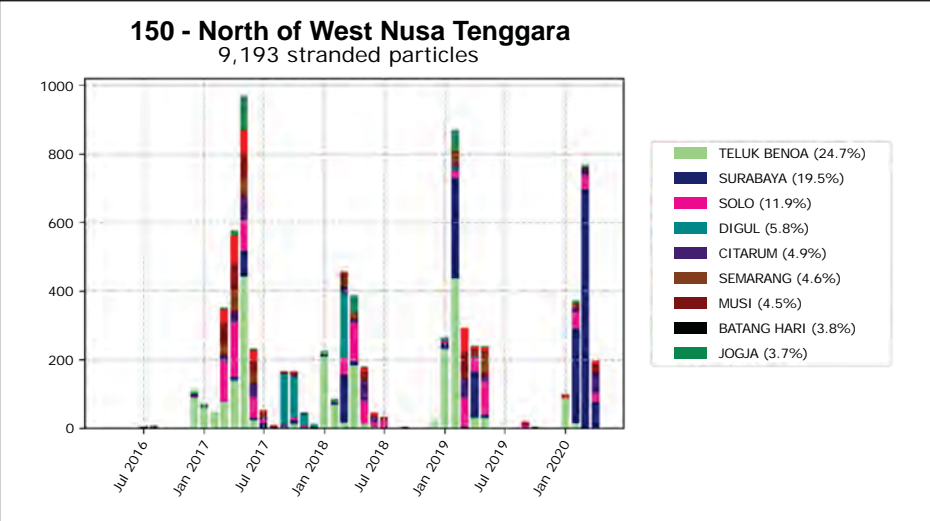


Figure 57: Atlas I50 - North of West Nusa Tenggara

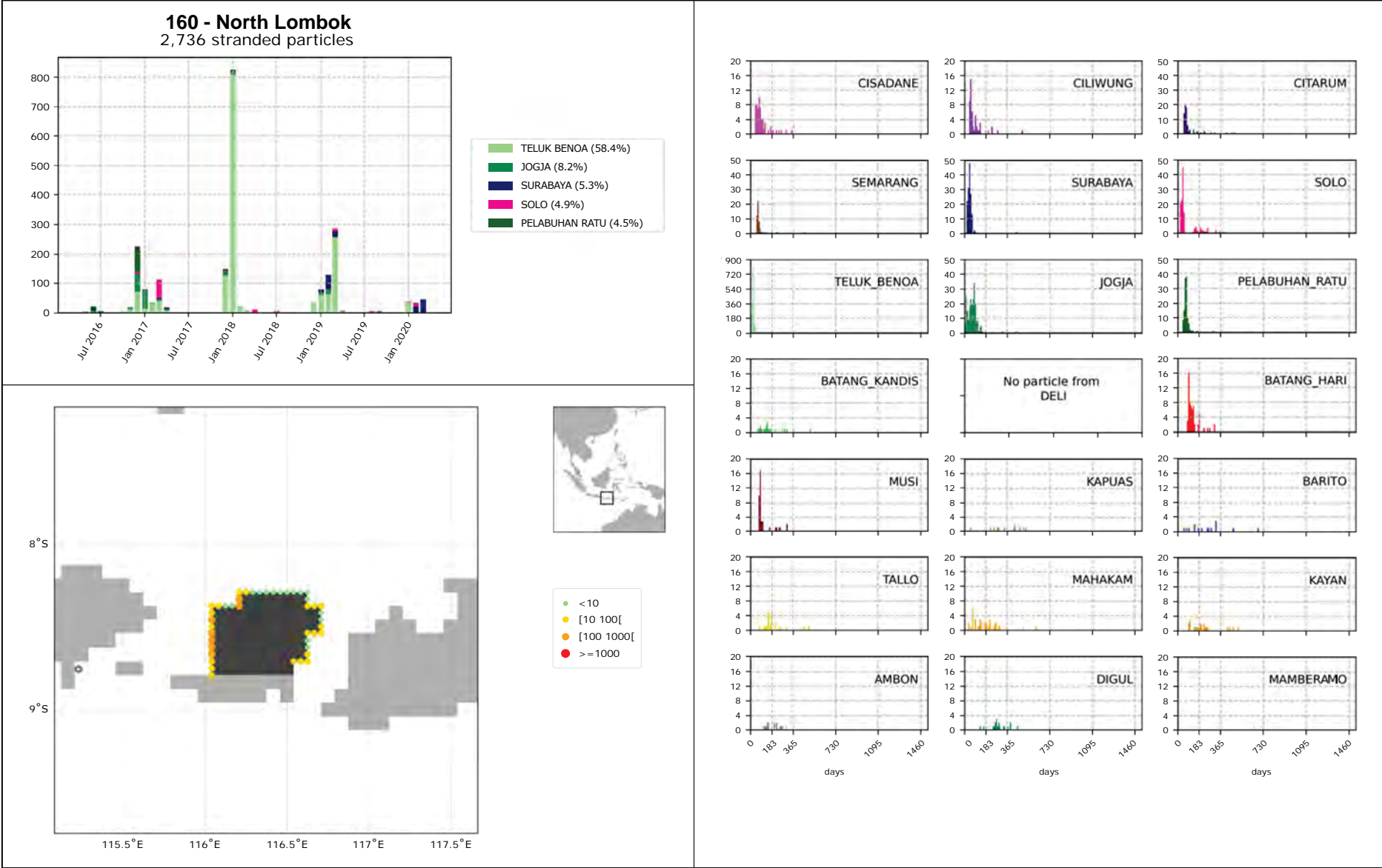


Figure 58: Atlas 160 - North Lombok

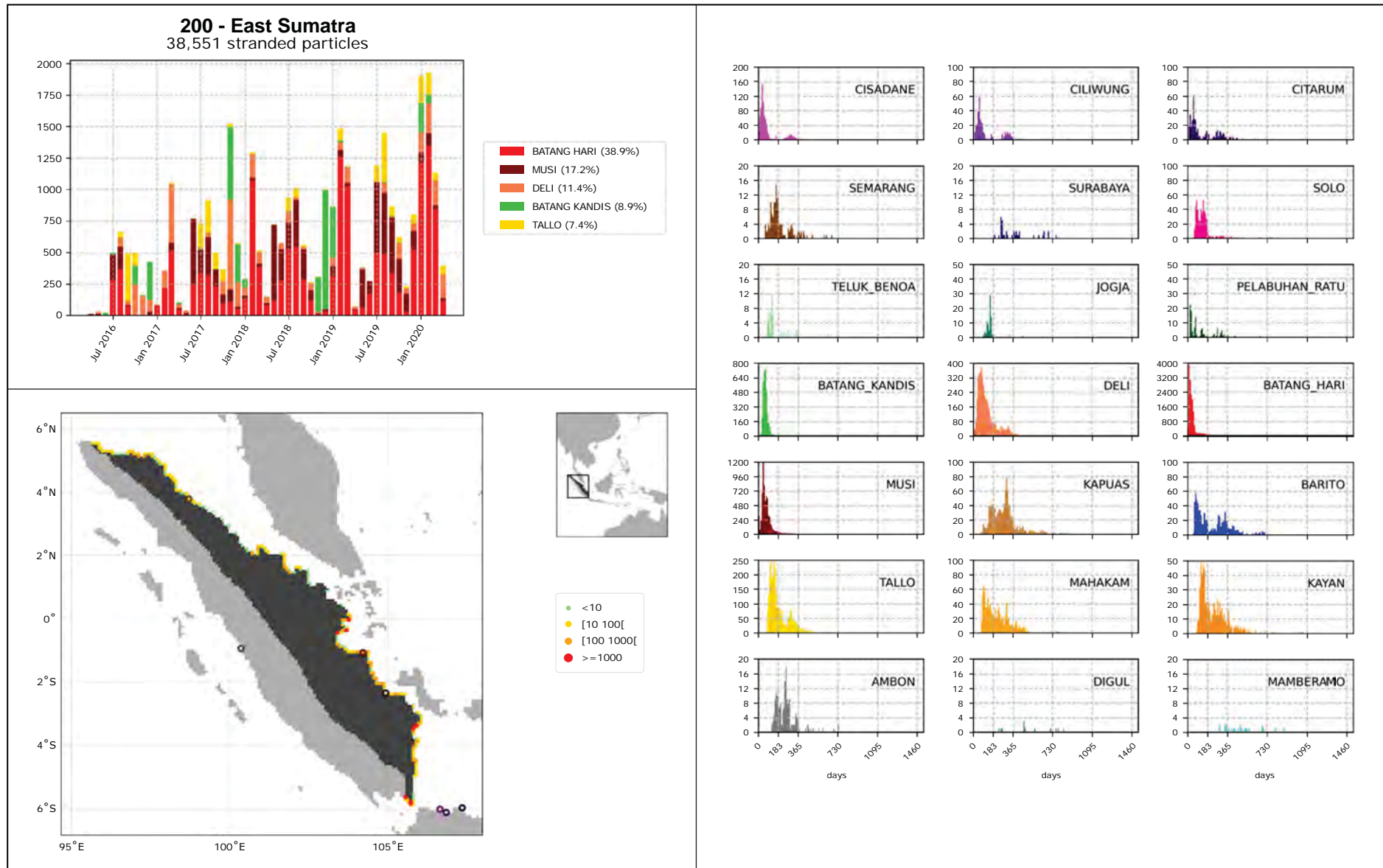


Figure 59: Atlas 200 - East Sumatra

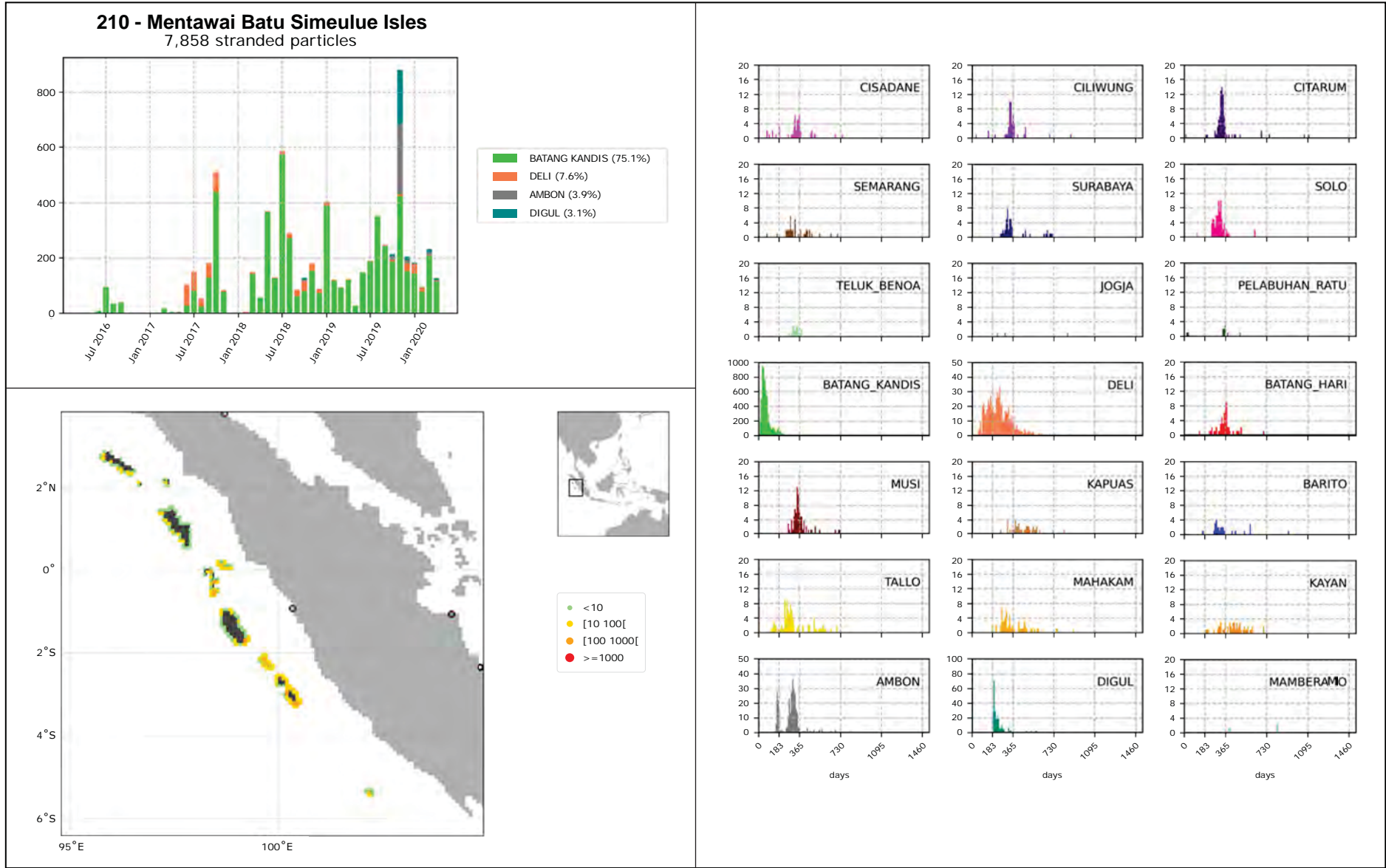


Figure 60: Atlas 210 - Mentawai Batu Simeulue Isles

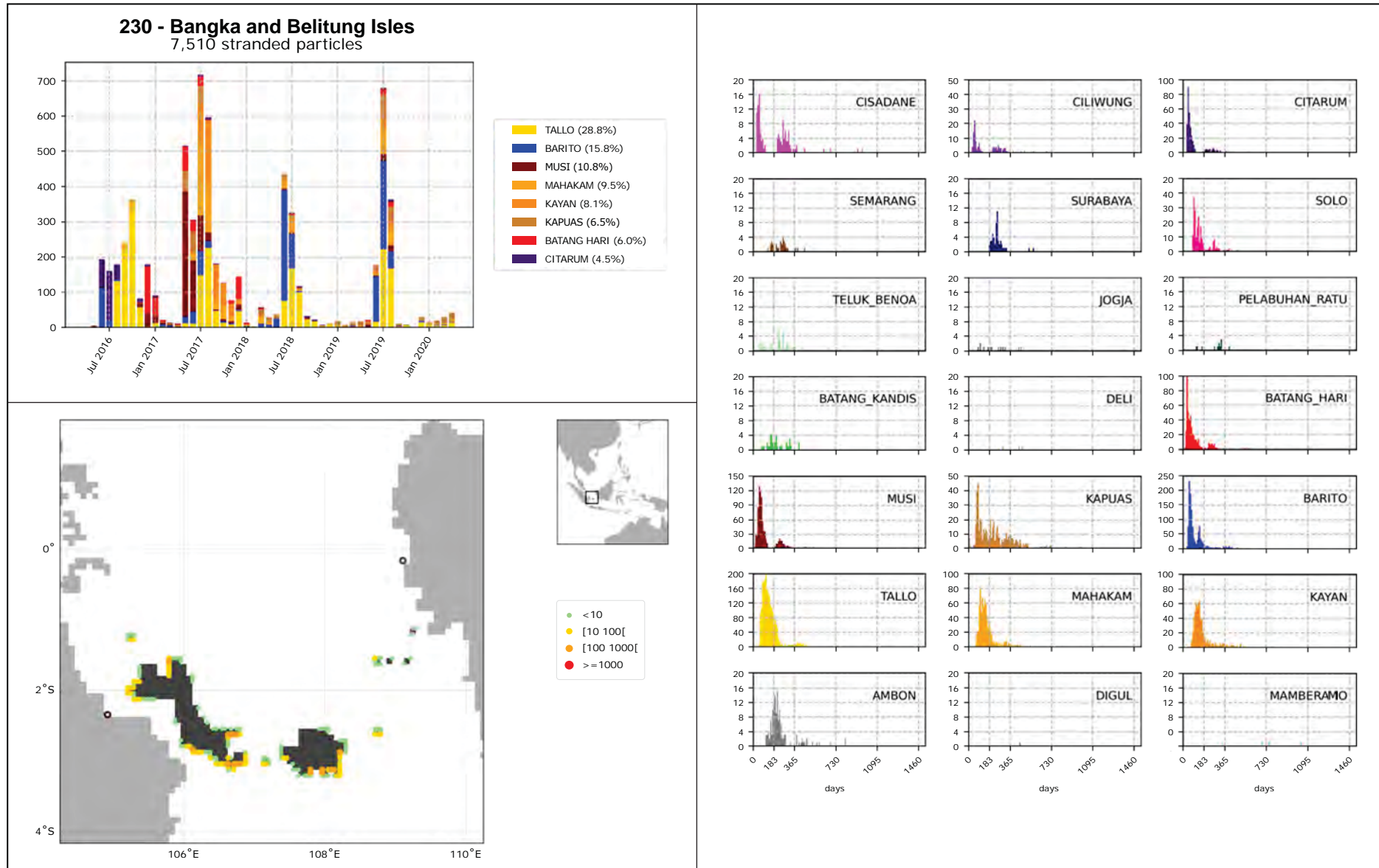


Figure 61: Atlas 230 - Bangka and Belitung Isles

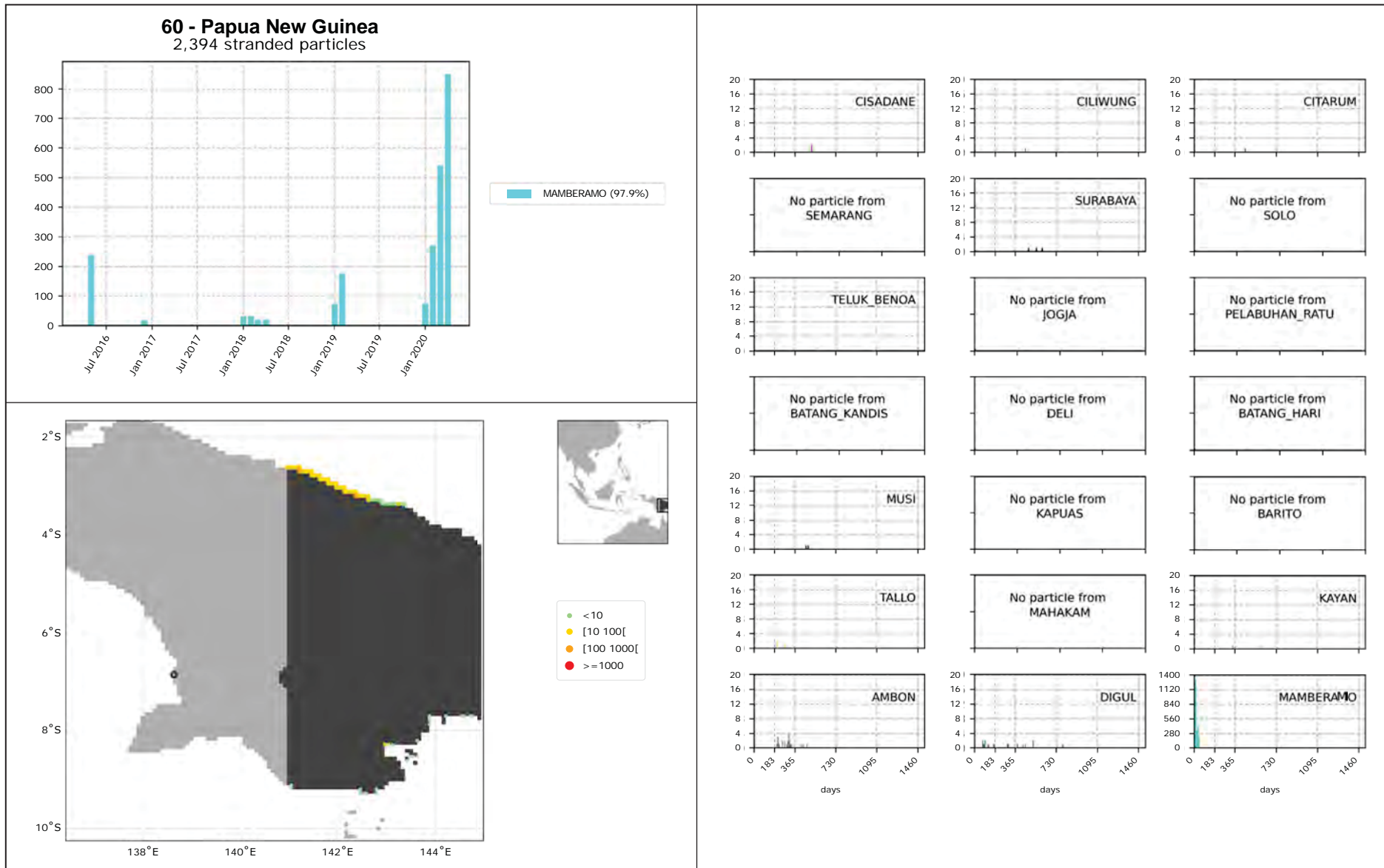


Figure 62: Atlas 60 - Papua New Guinea

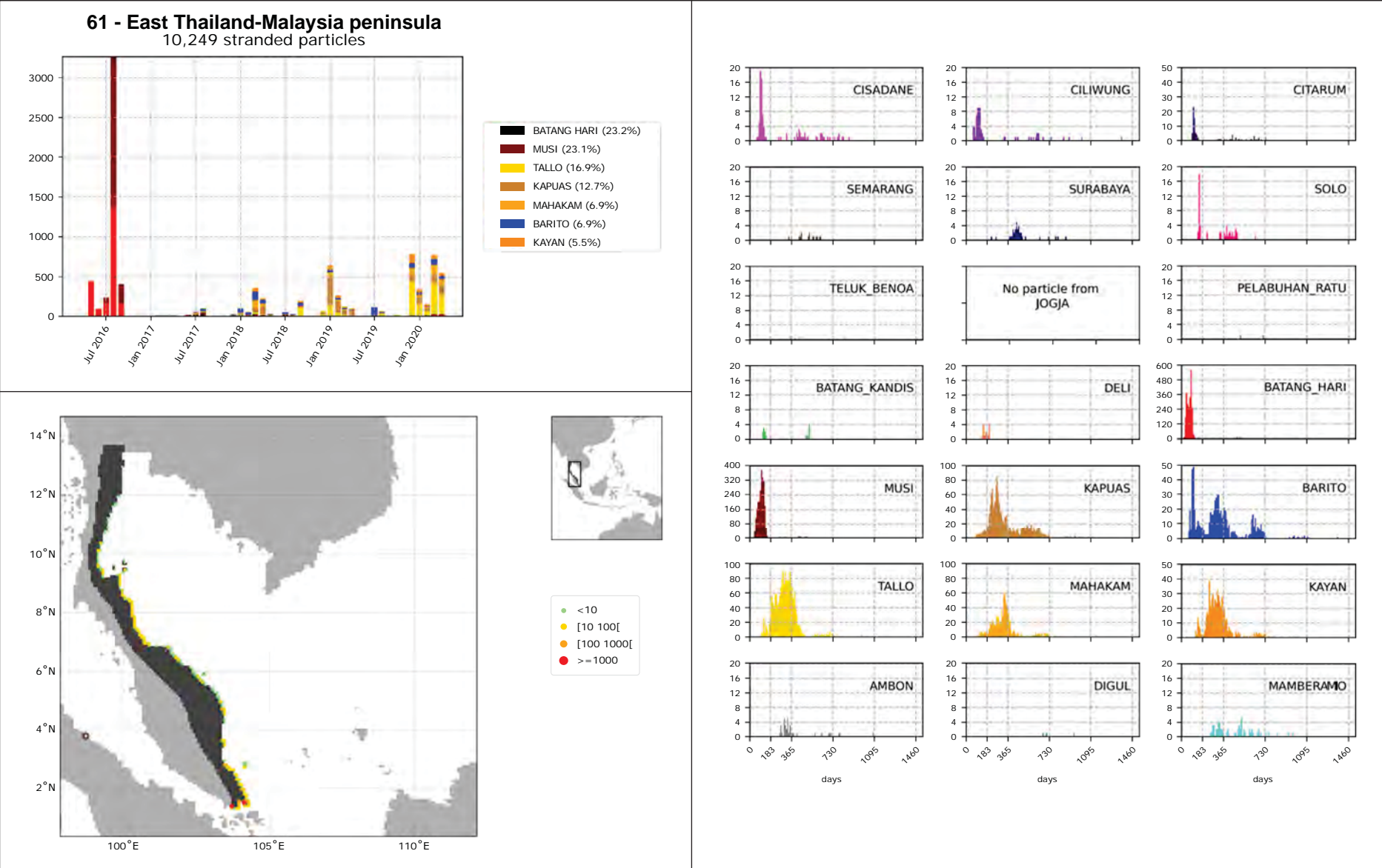


Figure 63: Atlas 61 - East Thailand - Malaysia peninsula

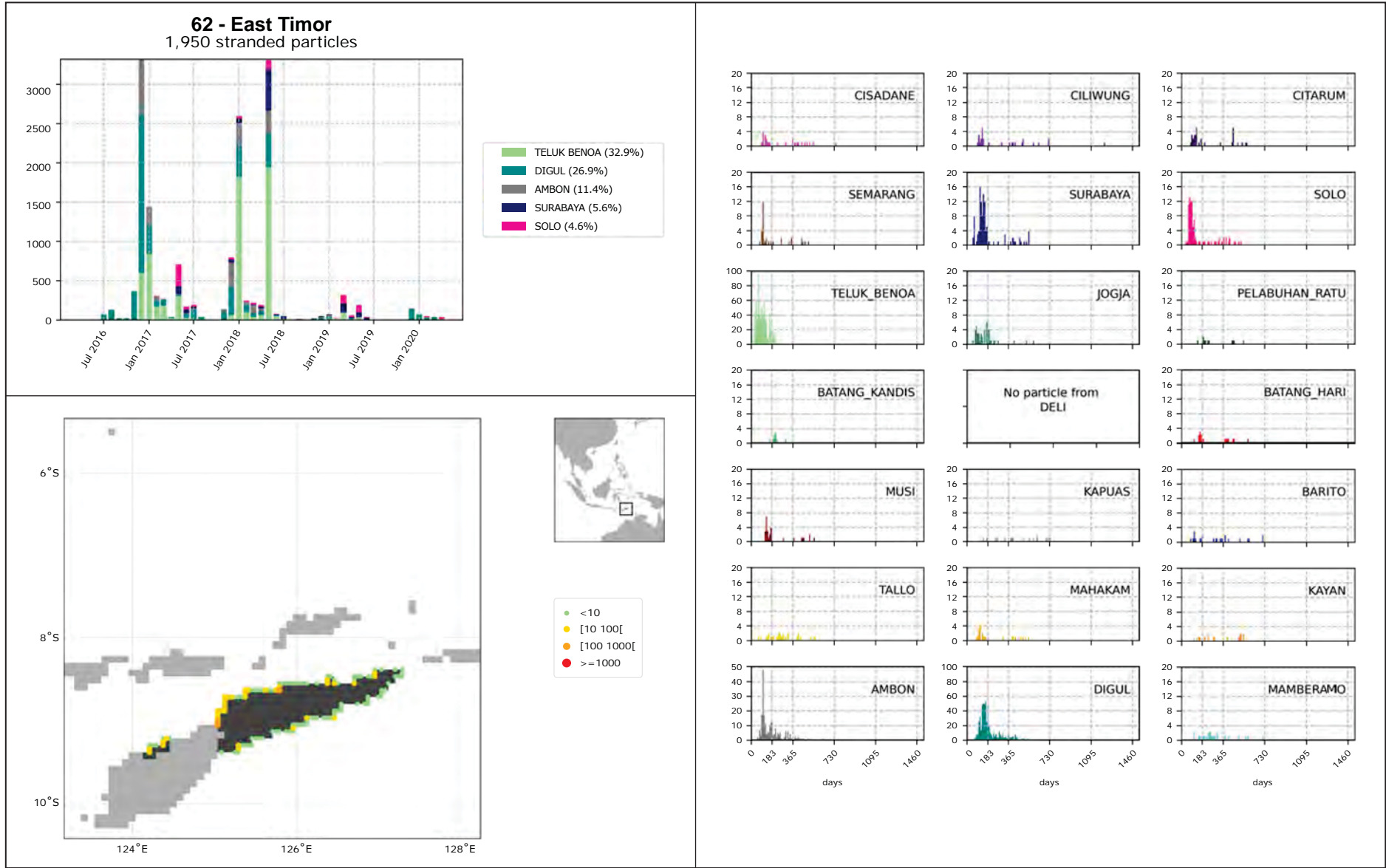


Figure 64: Atlas 62 - East Timor

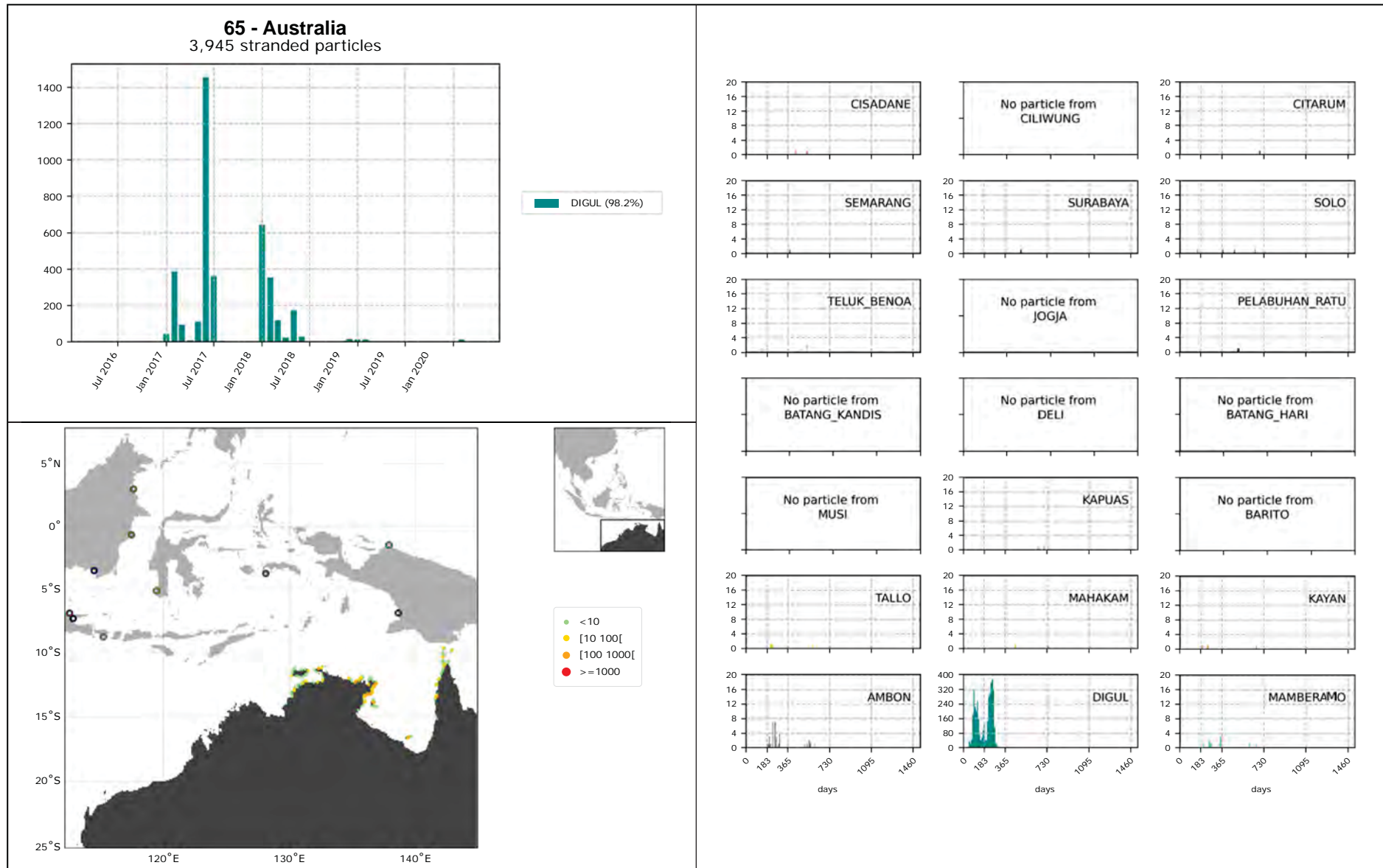


Figure 65: Atlas 65 - Australia

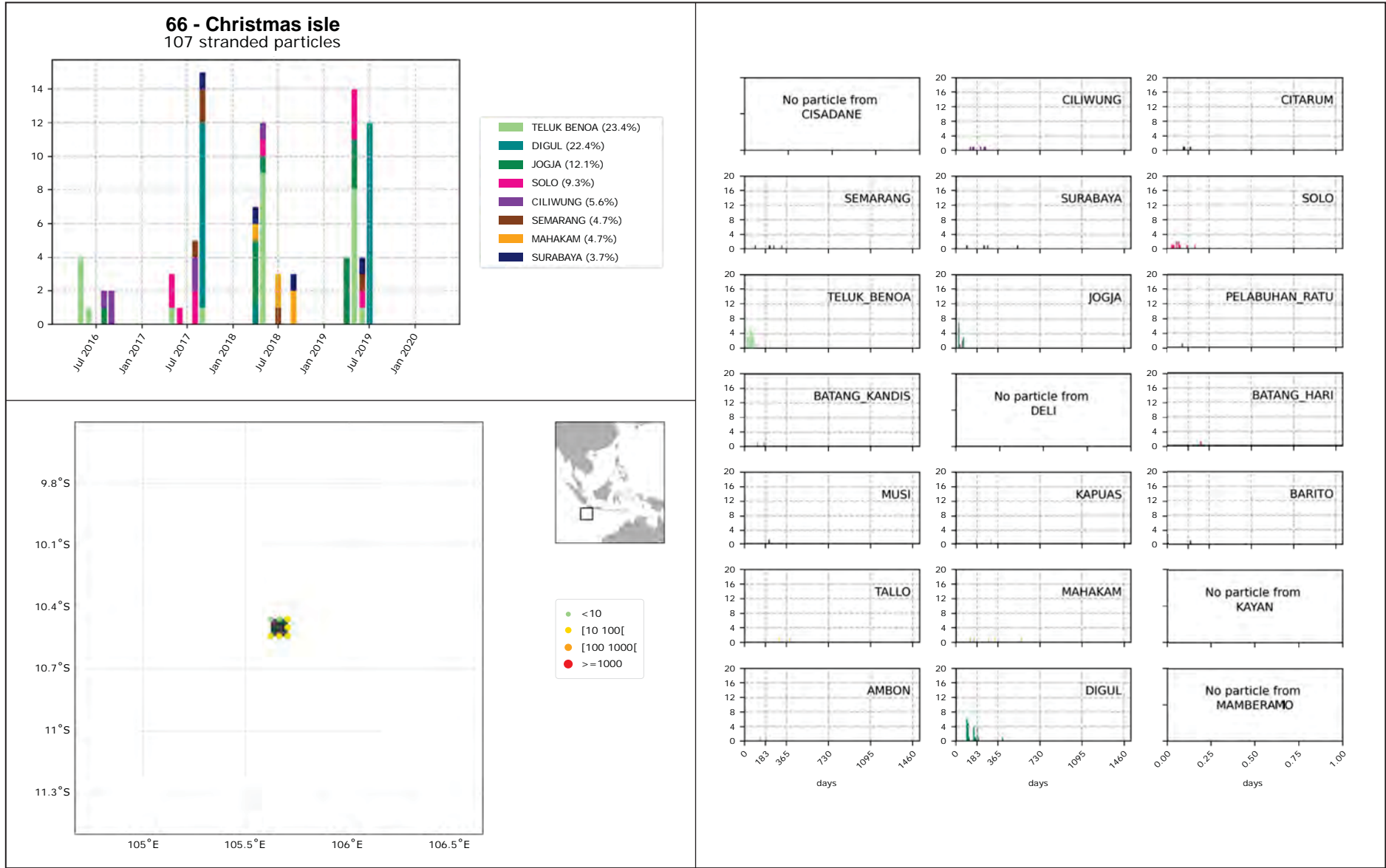


Figure 66: Atlas 66 - Christmas isles

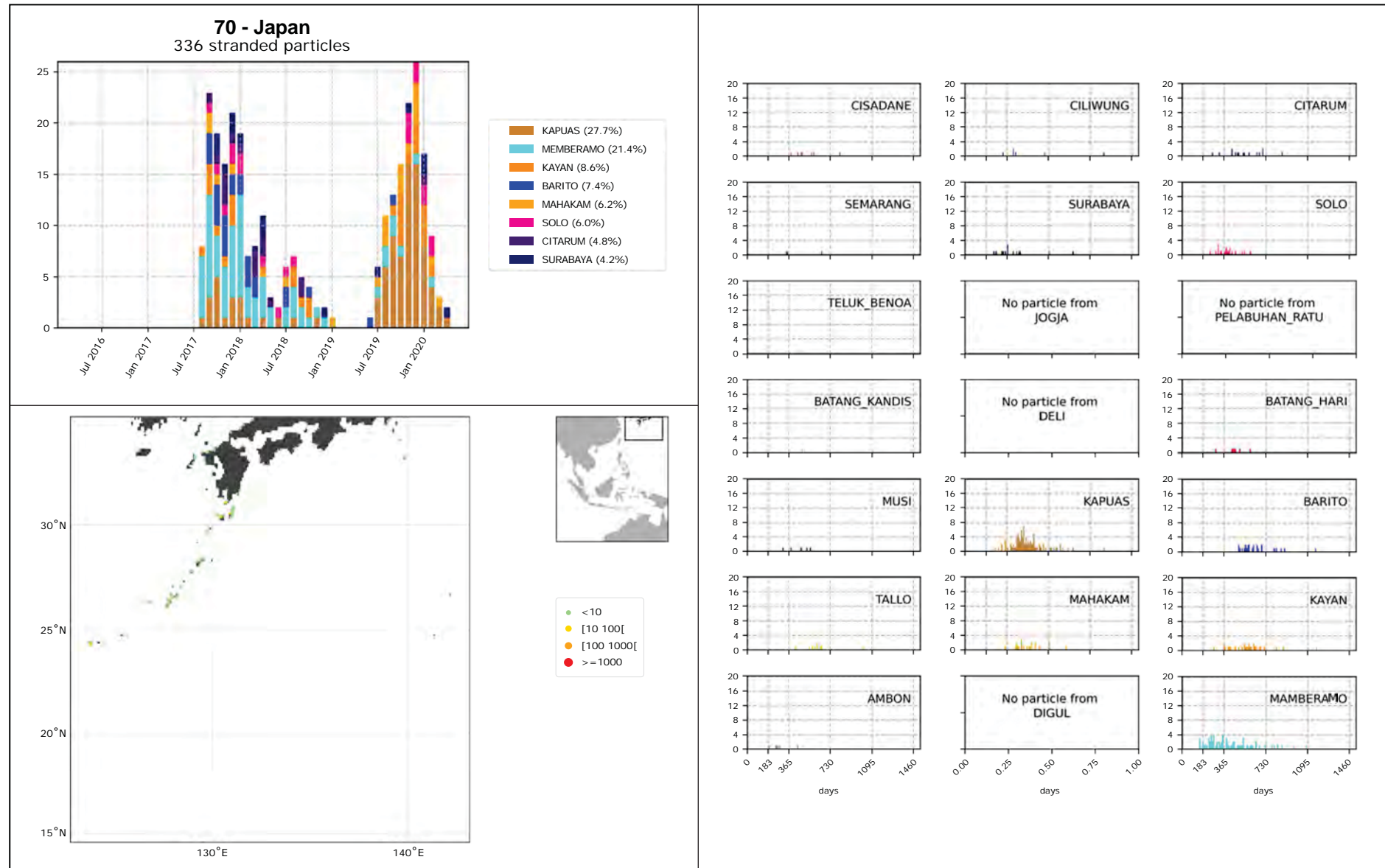


Figure 67: Atlas 70 - Japan

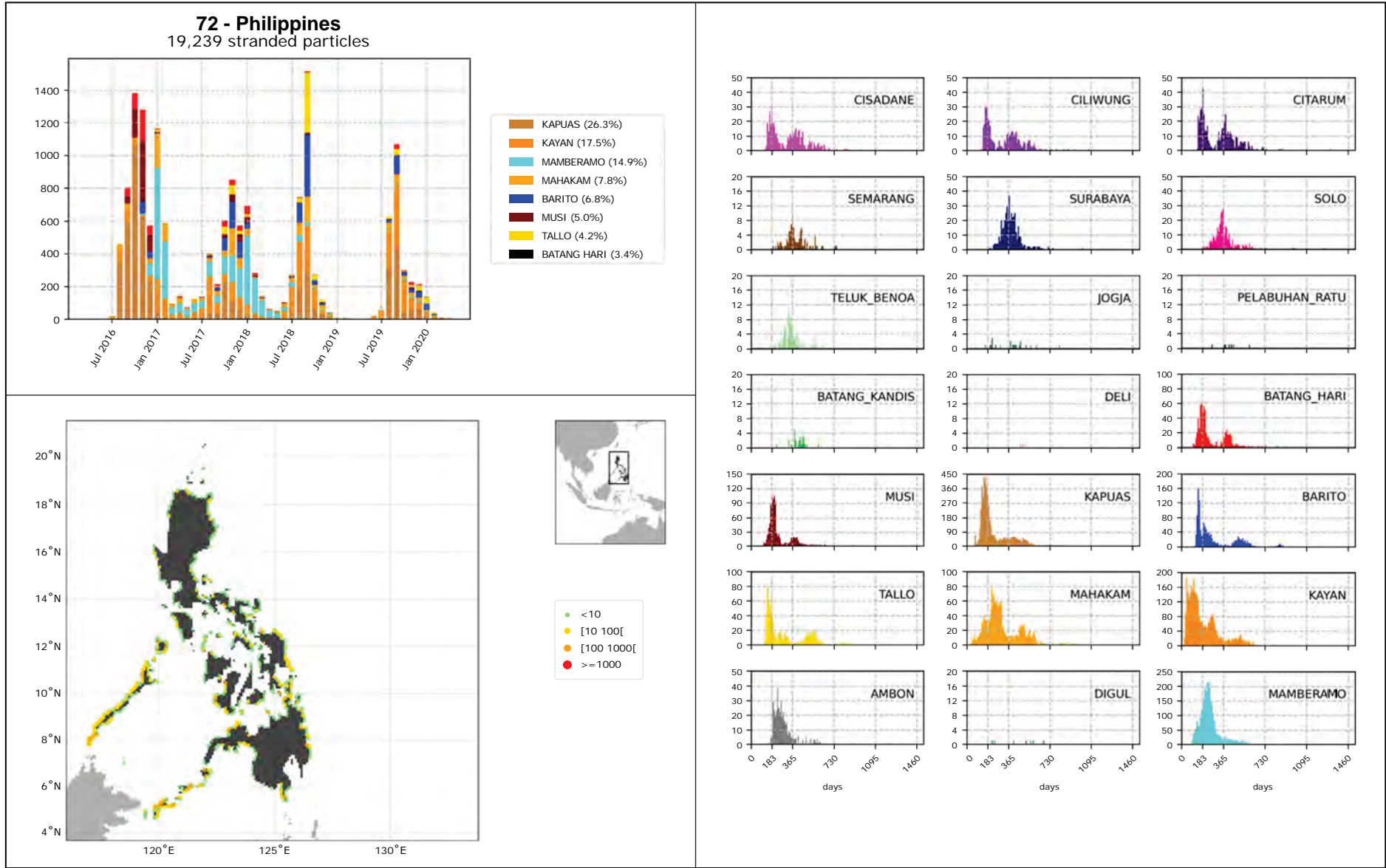


Figure 68: Atlas 72 - Philippines

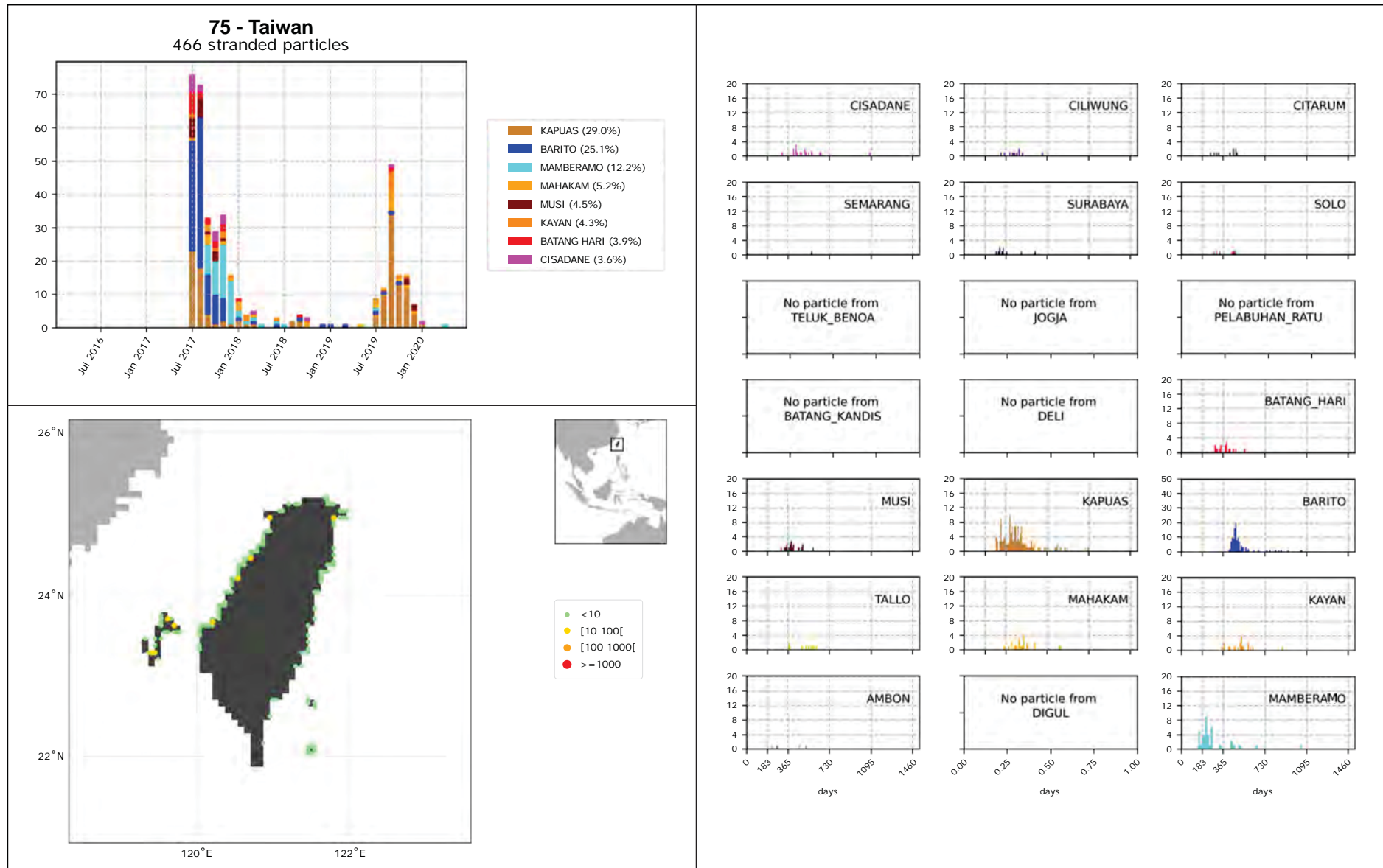


Figure 69: Atlas 75 - Taiwan

**80 - China, Vietnam, Cambodia, Myanmar and Bangladesh**  
3,563 stranded particles

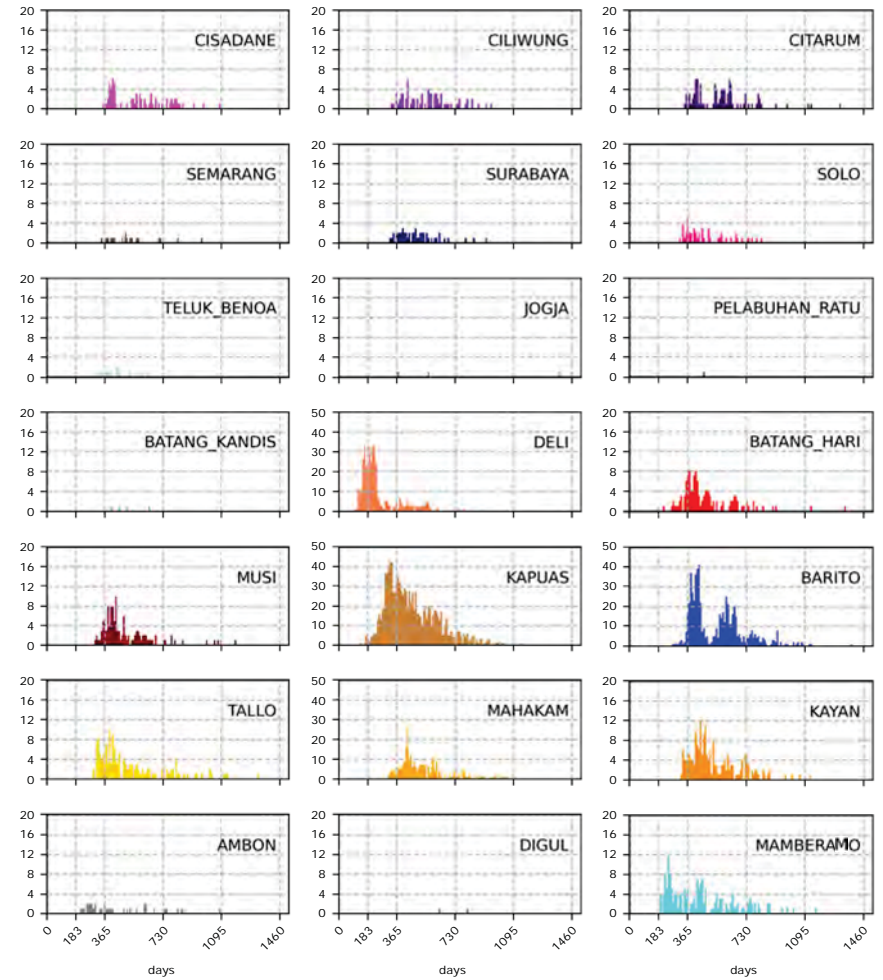
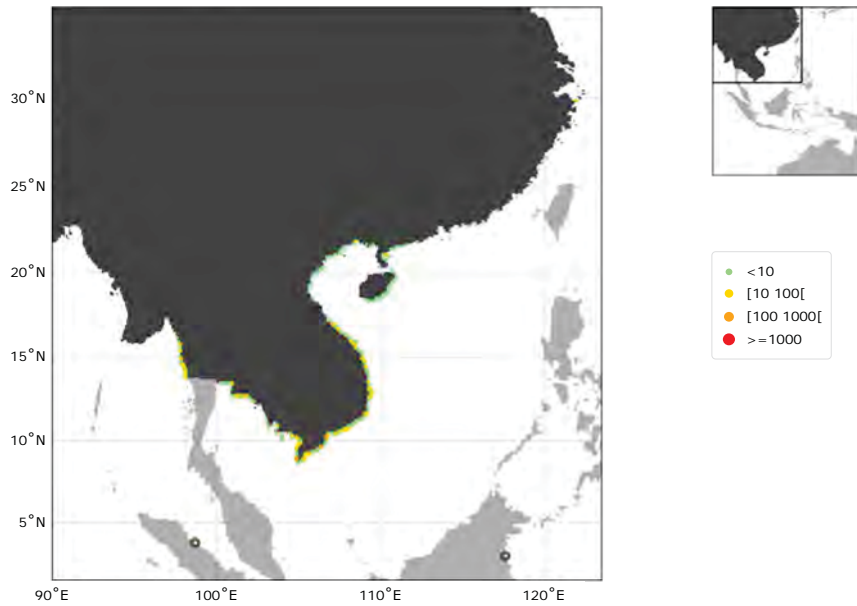
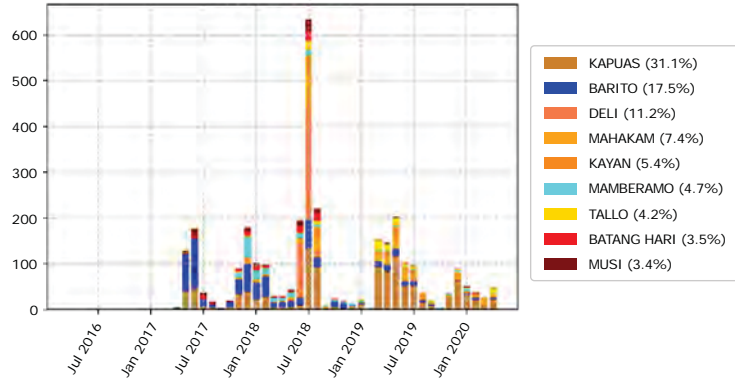


Figure 70: Atlas 80 - China, Vietnam, Cambodia, Thailand, Myanmar and Bangladesh

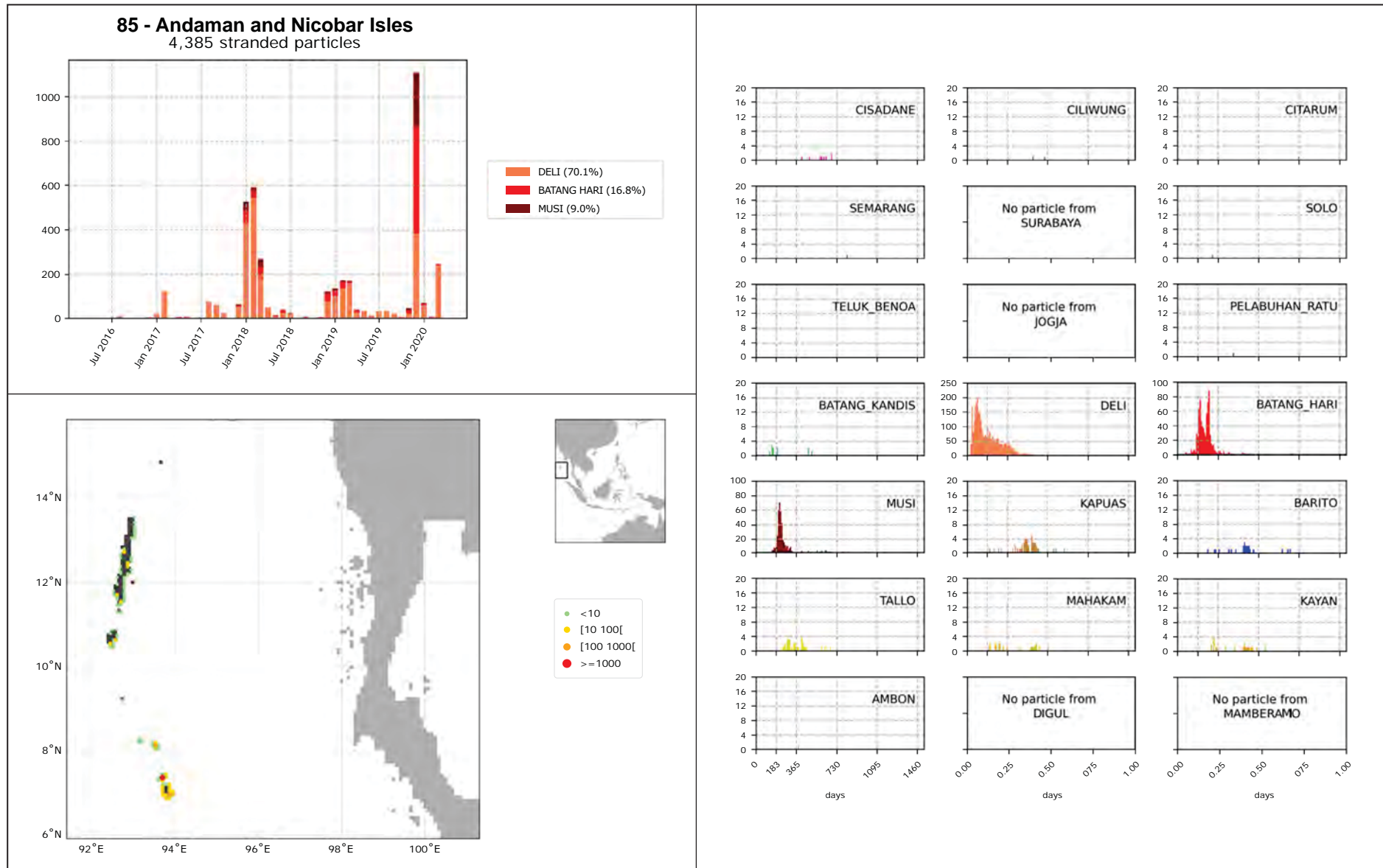


Figure 71: Atlas 85 - Andaman and Nicobar Isles

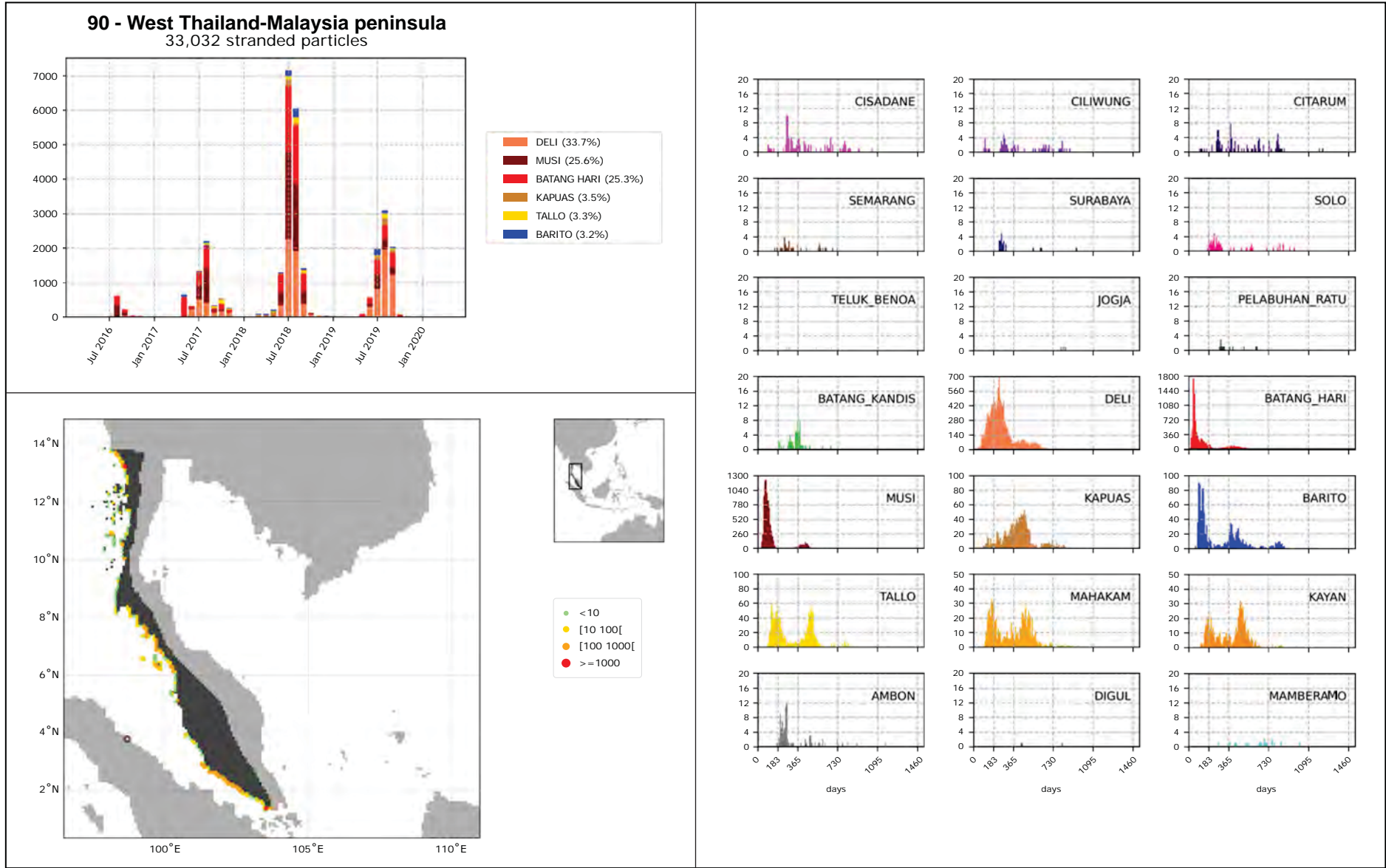


Figure 72: Atlas 90 - West Thailand-Malaysia peninsula

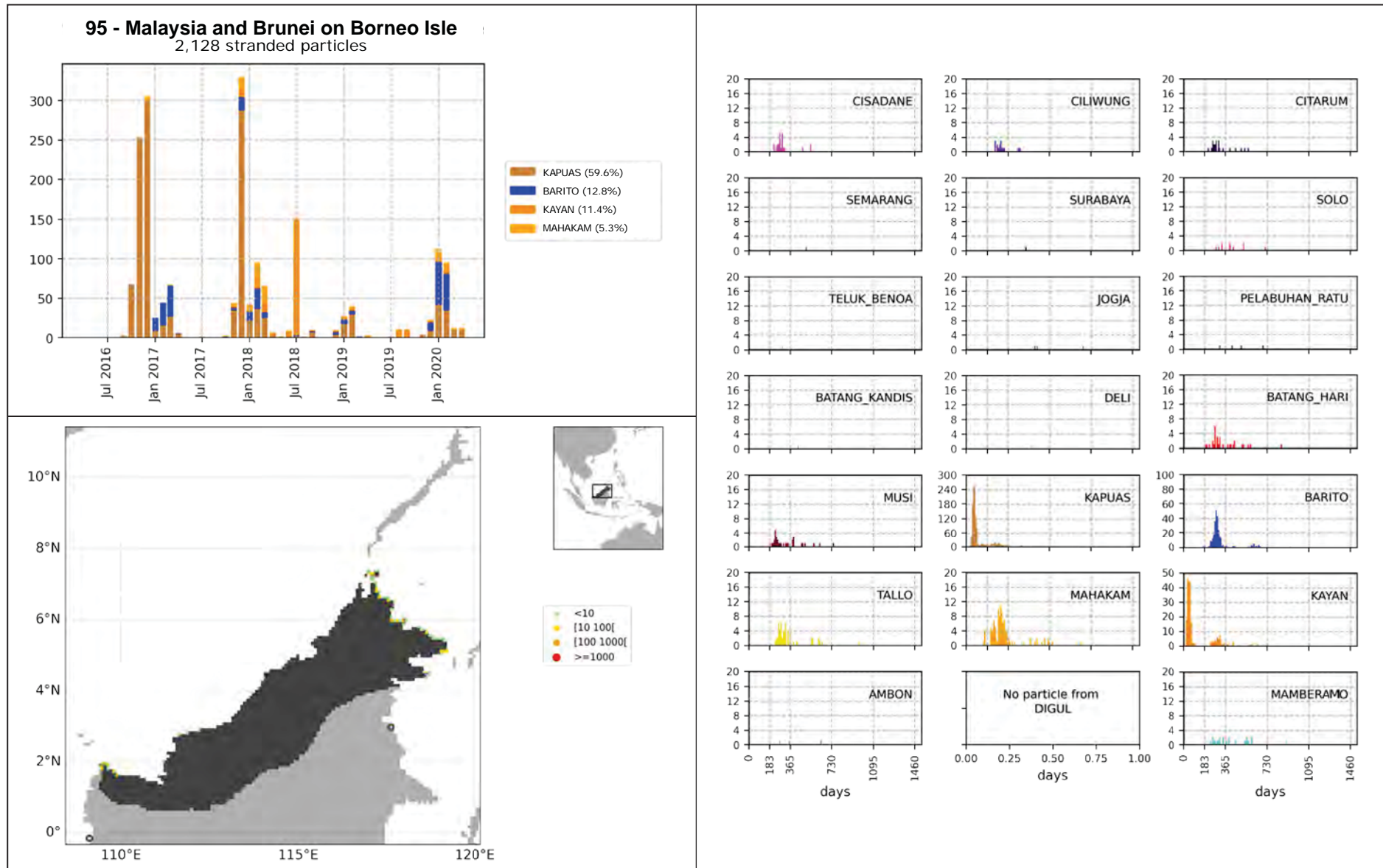


Figure 73: Atlas 95 - Malaysia and Brunei on Borneo Isle

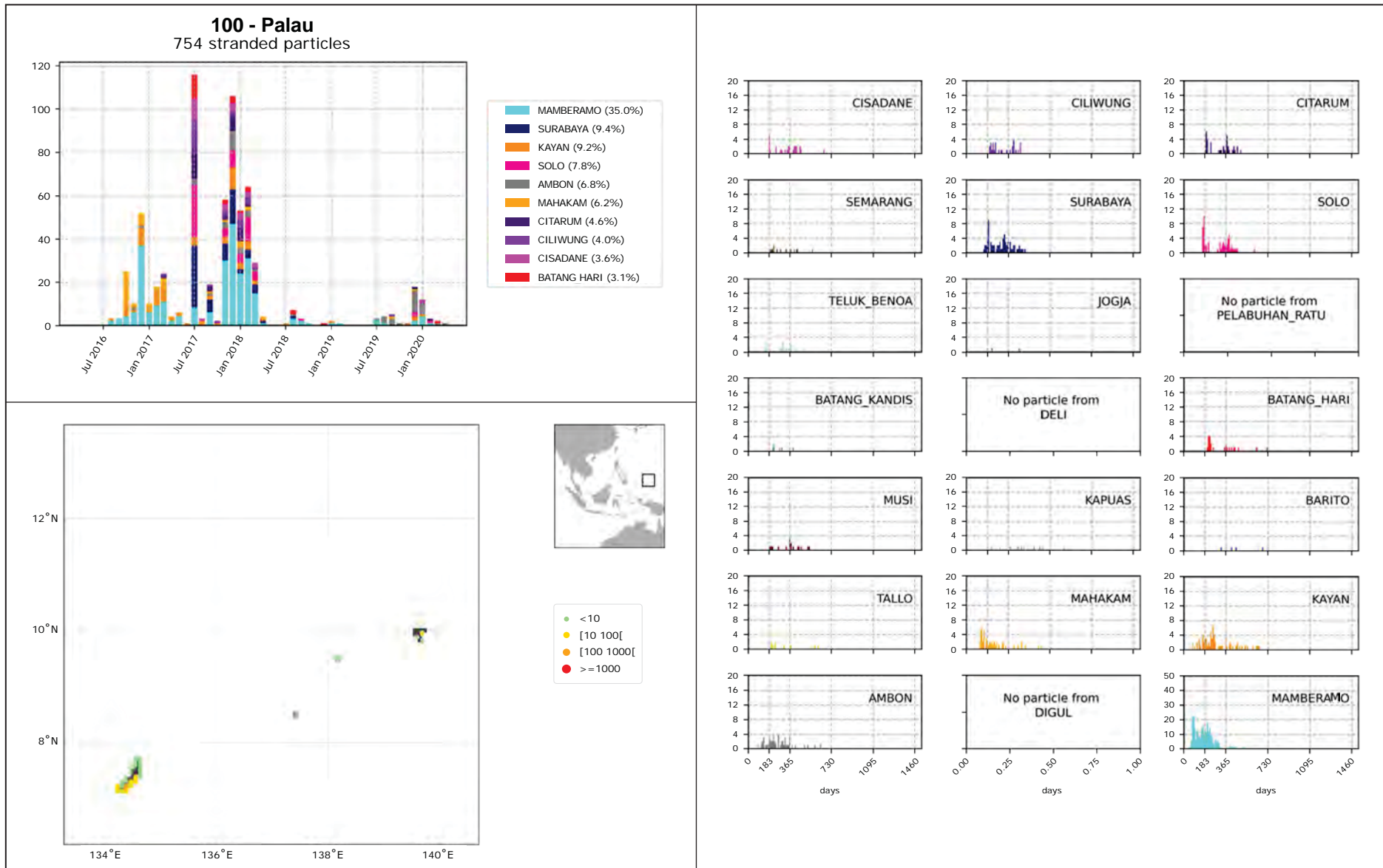


Figure 74: Atlas 100 - Palau



# Conclusion

Numerical particles advection by surface currents including Stokes drift and tides has shown that surface floating marine debris originating from Indonesian rivers tend to strand on Indonesian coasts. These strandings rather occur close in time and space from the riverine sources. However, some variability exists depending on the considered subzone of stranding and some of them can receive remote contributions.

On average, a strong stranding seasonal signal has also been enlightened. It is linked to the monsoon effect on both surface currents and river discharges. These time patterns can be modulated: some subzones can have different seasonality of stranding or no seasonality at all. The strong seasonality of strandings has also been observed by Phelan *et al.* (2020). These authors point out that the local inhabitants observe burst of strandings between January and April in Selayar Island (South Sulawesi) and between December and March in Wakatobi Island (Southeast Sulawesi). In the numerical simulation presented here, the Selayar subzone (zone 146) shows a peak in the number of stranded particles in January and February, consistently with observations of Phelan *et al.* (2020). However, complementary validations should be performed by comparing the simulation trajectories with real drifters trajectories, currently deployed and operated by the Collecte Localisation Satellites (CLS) company.

The physical processes that drive particle dispersion and strandings require further investigation. Surface Stokes drift and tidal surface currents can have a strong influence on the fate of particles. This is the reason why these two processes have been incorporated in the simulation. The addition of the surface Stokes drift to the OGCM surface currents has the strongest impact in terms of regional dispersion and number of strandings. On the other hand, the addition of the tidal currents has a weak impact. Though the surface Stokes drift seems to be the main process impacting particle dispersion and stranding, interactions between tides and the topography as well as interactions between Stokes drift and the mean flow need to be further investigated. Indeed, internal waves generated by tidal interaction with the topography can contribute to local accumulation of surface floating material while the impact of the surface Stokes drift can decrease because of its interaction with the mean flow through the anti-Stokes effect as discussed in van Sebille *et al.* (2020).

Finally, over the last decade, the spatial resolution of operational models has increased from a global  $1/4^\circ$  to  $1/12^\circ$ . Even though this is a great improvement in

numerical modelling, it remains insufficient to solve coastal and strait dynamics, and a finer resolution would be valuable for such a regional study.

© Christophe Maes, IRD



# References

- Andréfouët S. 2020. A census of Indonesia islands. *Second Maluku International Conference on Marine Science and Technology*, Oral presentation, 31<sup>st</sup> October 2020.
- Ardhuin F., Marié L., Rasclé N., Forget P., Roland A. 2009. Observation and estimation of Lagrangian, Stokes, and Eulerian currents induced by wind and waves at the sea surface. *Journal of Physical Oceanography* 39(11): 2820-2838  
doi: 10.1175/2009JPO4169.1
- Blanke B., Raynaud S. 1997. Kinematics of the Pacific Equatorial Undercurrent: an Eulerian and Lagrangian approach from GCM results. *Journal of Physical Oceanography*, 27(6): 1038-1053, 1997.  
doi: 10.1175/1520-0485(1997)027<1038:KOTPEU>2.0.CO;2  
<http://www.univ-brest.fr/lpo/ariane>
- Carrere L., Lyard F., Cancet M., Guillot A. 2015. FES 2014, a new tidal model on the global ocean with enhanced accuracy in shallow seas and in the Arctic region. *EGU General Assembly Conference Abstracts*, 2015.  
<https://ui.adsabs.harvard.edu/abs/2015EGUGA..17.5481C/abstract>
- Center for International Earth Science Information Network. 2018. *Population Density, Revision 11*. Columbia University Gridded Population of the World, Version 4 (GPWv4). Palisades, NY: NASA Socioeconomic Data and Applications Center (SEDAC). Accessed 5 August 2020.  
doi: 10.7927/H49C6VHW
- Couvelard X., Lemarié F., Samson G., Redelsperger J.-L., Ardhuin F., Benshila R., Madec G. 2020. Development of a two-way-coupled ocean wave model: assessment on a global NEMO(v3.6)-WW3(v6.02) coupled configuration. *Geoscientific Model Development* 13: 3067-3090.  
doi: 10.5194/gmd-13-3067-2020
- Cresswell G.R. 2000. Coastal currents of northern Papua New Guinea, and the Sepik River outflow. *Marine and Freshwater Research* 51: 553-564  
doi: 10.1071/MF99135
- Critchell K., Lambrechts J. 2016. Modelling accumulation of marine plastics in the coastal zone; what are the dominant physical processes? *Estuarine, Coastal and Shelf Science* 171: 111-122.  
doi:10.1016/j.ecss.2016.01.036
- Dai A., Qian T., Trenberth K.E., Milliman J.D. 2009. Changes in Continental Freshwater Discharge from 1948 to 2004. *Journal of Climate* 22(10): 2773-2792  
doi: 10.1175/2008JCLI2592.1
- Dobler D., Huck T., Maes C., Grima N., Blanke B., Martinez E., Ardhuin F. 2019. Large impact of Stokes drift on the fate of surface floating debris in the South Indian Basin. *Marine Pollution Bulletin* 148: 202-209.  
doi: 10.1016/j.marpolbul.2019.07.057
- Germanov E.S., Marshall A.D., Gede Hendrawan I., Admiraal R., Rohner C.A., Argeswara J., Wulandari R., Himawan M.R., Loneragan N.R. 2019. Microplastics on the Menu: Plastics Pollute Indonesian Manta Ray and Whale Shark Feeding Grounds. *Frontiers in Marine Science*, 6: 679.  
doi: 10.3389/fmars.2019.00679
- GloFAS. 2019. *River discharge and related historical data from the Global Flood Awareness System (GloFAS) provided by the Copernicus Emergency Management Service*.  
doi: 10-24381/cds.a4fdd6b9
- Gordon A.L., Huber B.A., Metzger E.J., Dwi Susanto R., Hurlburt H.E., Rameyo Adi T. 2012. South China Sea throughflow impact on the Indonesian throughflow. *Geophysical Research Letters* 39: L11602.  
doi:10.1029/2012GL052021
- Harrigan S., Zsoter I.E., Alferi L., Prudhomme C., Salamon P., Wetterhall F., Christopher Barnard C., Cloke H., Pappenberger F. 2020. GloFAS-ERA5 operational global river discharge reanalysis 1979-present. *Earth System Science Data Discussions*.  
doi: 10.5194/essd-2019-232
- Jambeck J.R., Geyer R., Wilcox C., Siegler T.R., Perryman M., Andrady A., Narayan R., Law K.L. 2015. Plastic waste inputs from land into the ocean. *Science* 347(6223):768-771.  
doi: 10.1126/science.1260352
- Jang Y.C., Hong S., Lee J., Lee M.J., Shim W.J. 2014. Estimation of lost tourism revenue in Geoje Island from the 2011 marine debris pollution event in South Korea. *Marine Pollution Bulletin* 81: 49-54.  
doi:10.1016/j.marpolbul.2014.02.021

- Lebreton L., van der Zwet J., Damsteeg J.W., Slat B., Andrady A., Reisser J. 2017. River plastic emissions to the world's oceans. *Nature Communications* 8(1): 15611. doi: 10.1038/ncomms15611
- Lebreton L., Egger M., Slat B. 2019. A global mass budget for positively buoyant macroplastic debris in the ocean. *Scientific Reports* 9(1):12922. doi: 10.1038/s41598-019-49413-5.
- Maes C., Blanke B. 2015. Tracking the origins of plastic debris across the Coral Sea: A case study from the Ouvéa Island, New Caledonia. *Marine Pollution Bulletin* 97(1): 160-168. doi: 10.1016/j.marpolbul.2015.06.022
- Maes C., Grima N., Blanke B., Martinez E., Paviet-Salomon T., Huck T. 2018. A Surface "Superconvergence" Pathway Connecting the South Indian Ocean to the Subtropical South Pacific Gyre. *Geophysical Research Letters* 45(4): 1915-1922. doi: 10.1002/2017GL076366
- Martinez E., Maamaatuaiahutapu K., Taillandier V. 2009. Floating marine debris surface drift: Convergence and accumulation toward the South Pacific subtropical gyre. *Marine Pollution Bulletin* 58(9):1347-1355. doi: 10.1016/j.marpolbul.2009.04.022
- Maximenko N., Hafner J., Niiler P. 2012. Pathways of marine debris derived from trajectories of Lagrangian drifters. *Marine Pollution Bulletin*, 65(1): 51-62. doi: 10.1016/j.marpolbul.2011.04.016
- Ministry of Environment and Forestry. 2020. *National Plastic Waste Reduction Strategic Actions for Indonesia, Republic of Indonesia*. <https://www.unenvironment.org/etc/resources/policy-and-strategy/national-plastic-waste-reduction-strategic-actions-indonesia>.
- Phelan A., Ross H., Setianto N.A., Fielding K., Pradipta L. 2020. Ocean plastic crisis – Mental models of plastic pollution from remote Indonesian coastal communities. *PLoS ONE* 15:e0236149. doi: 10.1371/journal.pone.0236149
- Plastics Europe. *Plastics, the facts 2019*. [https://www.plasticseurope.org/application/files/9715/7129/9584/FINAL\\_web\\_version\\_Plastics\\_the\\_facts2019\\_14102019.pdf](https://www.plasticseurope.org/application/files/9715/7129/9584/FINAL_web_version_Plastics_the_facts2019_14102019.pdf).
- Pres. Decree No. 83/2018. Peraturan Presiden Republik Indonesia Nomor 83 Tahun 2018.2018. <https://sipuu.setkab.go.id/PUUdoc/175608/PerpresNomor83Tahun2018.pdf>.
- Pres. Decree No. 97/2017. Peraturan Presiden Republik Indonesia Nomor 97 Tahun 2017. 2017. <https://sipuu.setkab.go.id/PUUdoc/175342/PerpresNomor97Tahun2017-BatangTubuh.pdf>.
- Ryan P.G., Pichegru L., Perold V., Moloney C.L. 2020. Monitoring Marine Plastics - Will we know if we are making a difference? *South Africa Journal of Science* 116 (5/6): 7678. doi: 10.17159/sajs.2020/7678
- Todd R.E., Chavez F., Clayton S., Cravatte S., Goes M., et al. 2019. Global Perspectives on Observing Ocean Boundary Current Systems. *Frontiers in Marine Science* 6: #423. doi:10.3389/fmars.2019.00423
- Tranchant B., Refray G., Greiner E., Dwiyooga Nugroho E., Koch-Larrouy A., Gaspar P. 2016. Evaluation of an operational ocean model configuration at 1/12° spatial resolution for the Indonesian seas (NEMO2.3/INDO12) – Part I: Ocean physics. *Geoscientific Model Development* 9: 1037-1064. doi: 10.5194/gmd-9-1037-2016
- UNEP Marine Plastic Debris and Microplastics. 2016. Global Lessons and Research to Inspire Action and Guide Policy Change. *United Nations Environment Programme*. URL <http://hdl.handle.net/20.500.11822/7720>
- van der Mheen M., van Sebille E., Pattiaratchi C. 2020. Beaching patterns of plastic debris along the Indian Ocean rim. *Ocean Science Discussions*. doi: 10.5194/os-2020-50
- van Sebille E., England M.H., Froyland G. 2012. Origin, dynamics and evolution of ocean garbage patches from observed surface drifters. *Environmental Research Letters*, 7(4):044040. doi: 10.1088/1748-9326/7/4/044040
- van Sebille E., Griffes S.M., Abernathey R., Thomas P.Adams T.P., Berlof P. et al. 2018. Lagrangian ocean analysis: Fundamentals and practices. *Ocean Modelling* 121: 49-75. doi: <https://doi.org/10.1016/j>

- van Sebille E., Aliani S., Law K.L., Maximenko N., Alsina J.M. et al. 2020. The physical oceanography of the transport of floating marine debris. *Environmental Research Letters*, 15(2): 023003.  
doi: 10.1088/1748-9326/ab6d7d
- Williamson P., Smythe-Wright D., Burkill P. 2016. *Future of the Ocean and its Seas: a non-governmental scientific perspective on seven marine research issues of G7 interest*. ICSU-IAPSO-IUGG-SCOR, Paris.  
<http://www.iugg.org/policy/ReportFutureOceanG72016.pdf>.
- Wyrtki K. 1961. *Physical Oceanography of the Southeast Asian Waters*. Scripps Institution of Oceanography, NAGA REPORT, 2.
- Yan Y., Ling Z., Chen C. 2015. Winter coastal upwelling of northwest Borneo in the South China Sea. *Acta Oceanologica Sinica* 34(1): 3-10.  
doi: 10.1007/s13131-015-0590-2

© John Van Lent, Making Maluku Free Waste





# Floating marine debris along Indonesian coasts

## An atlas of strandings based on Lagrangian modelling

### Abstract

The book *Floating Marine Debris along Indonesian Coasts. An Atlas of Strandings based on Lagrangian Modelling* was conceived within the framework of a collaborative research project conducted jointly by the Indonesian Ministry of Marine Affairs and Fisheries (KKP), Collecte Localisation Satellite (CLS), and the French National Research Institute for Sustainable Development (IRD), and funded, since early 2020, by the Agence Française de Développement (AFD). The project aims to sustain the monitoring and modelling of marine debris in the Indonesian seas and beyond. The final goal is to strengthen Indonesian agencies in their efforts to raise public awareness about marine pollution by plastics, and to implement adapted mitigation strategies. Due to their high durability and relatively low-cost production, plastics constitute by far the predominant fraction of solid waste products, a substantial proportion of which is eventually discharged into the oceans. Emissions and circulation of plastic and marine debris follow complex pathways that vary locally according to waste management, population density and hydrology, but the majority of litter runs off from rivers. A major priority is to understand the sources of floating plastic debris and their eventual beaching locations and to identify potential connectivity patterns at the regional and basin ocean scales. A Lagrangian assessment of the debris dispersion originating from 21 major rivers in Indonesia was carried out as a means to identify the concentration at sea, as well as the geographic and temporal distribution of stranding along Indonesian coastlines based on a state-of-art ocean modelling. The present atlas detailing the results of this assessment at the regional scales should be viewed as a first effort to establish the river connectivity implied in the marine dispersion of surface plastic debris in Indonesia.

© IRD, 2021



ISBN 979-10-699-7188-2



### Abstrak

Penyusunan buku *Floating Marine Debris along Indonesian Coasts: An Atlas of Strandings based on Lagrangian Modelling* terlaksana atas kerja bersama dalam kerangka riset kolaboratif antara Kementerian Kelautan dan Perikanan (KKP) — Indonesia, Collecte Localisation Satellite (CLS) dan Lembaga Penelitian Perancis untuk Pembangunan (IRD), melalui pendanaan oleh Agence Française de Développement (AFD) sejak awal tahun 2020. Penelitian ini bertujuan untuk membantu pemantauan dan pemodelan sampah laut dari perairan laut Indonesia sampai melewati negara Indonesia. Tujuan akhirnya adalah untuk memperkuat kapasitas lembaga-lembaga terkait di Indonesia dalam upaya meningkatkan kesadaran publik tentang dampak pencemaran laut oleh sampah plastik, dan menerapkan strategi mitigasi yang paling sesuai. Upaya ini dipandang sangat krusial untuk dilakukan, mengingat sampai saat ini plastik merupakan bagian utama dari produk limbah padat yang memiliki daya tahan yang tinggi dan biaya produksi yang murah namun sayangnya sebagian besar produk tersebut bersifat sekali pakai kemudian dibuang dan pada akhirnya menjadi sampah di lautan. Pembuangan dan sirkulasi sampah plastik di laut memiliki alur yang kompleks dan bervariasi berdasarkan pengaruh dari beberapa faktor seperti pola pengelolaan sampah di daratan, kepadatan penduduk dan siklus hidrologi, dimana secara umum mayoritas sampah tersebut terbawa hingga ke lautan melalui sungai-sungai. Hal yang menjadi prioritas utama adalah memahami sumber sampah laut dan lokasi terdamparnya sampah tersebut serta untuk mengidentifikasi korelasinya pada skala regional dan antar samudera. Dalam penelitian ini, pemantauan sebaran sampah di perairan laut Indonesia yang bersumber dari 21 sungai besar adalah dengan menggunakan pendekatan model Lagrangian sebagai cara untuk mengetahui sebaran sampah di laut melalui pergerakannya dan prakiraan lokasi terdamparnya sampah di area garis pantai Indonesia. Buku Atlas ini menggambarkan secara detail evaluasi penyebaran sampah laut dalam skala regional, yang dapat dipandang sebagai langkah awal untuk mempelajari peran sungai terhadap penyebaran sampah plastik di laut Indonesia.

